HYDRONAUTICS, incorporated
research in hydrodynamics

Research, consulting, and advanced engineering in the fields of NAVAL and INDUSTRIAL HYDRODYNAMICS. Offices and Laboratory in the Washington, D. C., area: Pindell School Road, Howard County, Laurel, Md.

HYDRONAUTICS, INCORPORATED

TECHNICAL REPORT 7703-1

AD A061723

ON THE CHANGES IN LIFT OF HYDROFOILS DUE TO SURFACE INJECTIONS OF POLYMER ADDITIVES

By

M. Sinnarwalla

T. R. Sundaram

February 1978

DDC FILE COPY

Prepared for

Office of Naval Research
Department of the Navy

under

Contract No. N00014-77-C-0070

DISCLAIMER NOTICE

THIS DOCUMENT IS BEST QUALITY PRACTICABLE. THE COPY FURNISHED TO DDC CONTAINED A SIGNIFICANT NUMBER OF PAGES WHICH DO NOT REPRODUCE LEGIBLY.

UNCLASSIFIED

SECURITY CLASSIFICATION OF THIS PAGE (When Data Entered)

REPORT DOCUMENTATION PAGE		READ INSTRUCTIONS BEFORE COMPLETING FORM
1. REPORT NUMBER Technical Report 7703-1	2. GOVT ACCESSION NO.	3. RECIPIENT'S CATALOG NUMBER
4. TITLE (and Subtitle) On the Changes in Lift of Hydrofoils Due to Surface Injections of Polymer Additives		5. TYPE OF REPORT & PERIOD COVERED Technical Report 6. PERFORMING ORG. REPORT NUMBER TR 7703-1
7. AUTHOR(s) Abbas M. Sinnarwalla and T. R. Sundaram		8. CONTRACT OR GRANT NUMBER(s) N00014-77-C-0070
9. PERFORMING ORGANIZATION NAME AND ADDRESS HYDRONAUTICS, Incorporated 7210 Pindell School Road Laurel, Maryland 20810		10. PROGRAM ELEMENT, PROJECT, TASK AREA & WORK UNIT NUMBERS NR 062-325
11. CONTROLLING OFFICE NAME AND ADDRESS Office of Naval Research (Code 438) Department of Navy Arlington, Virginia 22217		12. REPORT DATE February 1978 13. NUMBER OF PAGES 116
14. MONITORING AGENCY NAME & ADDRESS(if different from Controlling Office)		15. SECURITY CLASS. (of this report) Unclassified 15a. DECLASSIFICATION DOWNGRADING SCHEDULE

16. DISTRIBUTION STATEMENT (of this Report)

Approved for public release; distribution unlimited.

17. DISTRIBUTION STATEMENT (of the abstract entered in Block 20, if different from Report)

18. SUPPLEMENTARY NOTES

19. KEY WORDS (Continue on reverse side if necessary and identify by block number)

Polymer Additives	Pressure Distributions
Lift Effects	Boundary Layer
Drag Effects	Hydrofoil

20. ABSTRACT (Continue on reverse side if necessary and identify by block number)

Existing data on the effects on lift of symmetric hydrofoils due to the injection of polymer solutions on to their surfaces show that the lift can either decrease or increase depending on the polymer, injection velocity, location of injection, side of injection and angle of attack. A unified, albeit semiempirical, approach is suggested in the present report for correlating and explaining the apparently contradictory data. It is proposed

DD FORM 1 JAN 73 1473 EDITION OF 1 NOV 65 IS OBSOLETE

UNCLASSIFIED

SECURITY CLASSIFICATION OF THIS PAGE (When Data Entered)

78 11 03 101

that the observed lift changes may be due to the influence of the injections on the boundary-layer displacement effect that is known to reduce the circulation around hydrofoils.

Four separate boundary-layer effects due to injection are identified and discussed, namely those due to changes in the effective angle of attack, the effective camber, the circulation (in addition to the changes in circulation associated with the previous two effects), and the thickness distribution. Classical methods of airfoil theory are utilized to calculate the "effective" hydrofoil shape that would have produced the observed pressure distributions. This effective shape is utilized to identify the different boundary layer effects, and these, in turn, are identical with the changes likely to be produced by polymer injections.

No explicit treatment of the exact nature of the interaction between the injected polymer flow and the boundary layer or the external pressure gradient is given, since this is outside the scope of the present study. However, it is argued that this interaction must necessarily be dependent on the visco-elastic properties of the polymer. For example, it is shown that when the observed changes in the lift force are normalized with respect to the local velocity at the location of the injection slit, the data for different polymers, different injection velocities and different angles of attack can all be correlated in terms of the single nondimensional parameter $V_i \tau / c$ where V_i is the injection velocity, τ is the polymer relaxation time and c is the hydrofoil chord. A similar correlation is also given for the changes in drag due to injection.

TABLE OF CONTENTS

		Page
FOREWORD		viii
I.	INTRODUCTION	1
II.	FEATURES OF THE EXPERIMENTAL RESULTS AND OBJECTIVES OF THE STUDY	3
III.	PLAUSIBLE MECHANISMS FOR LIFT CHANGES	9
IV.	SEMI-EMPIRICAL CORRELATIONS FOR THE OBSERVED EFFECTS	15
	IV.1 Pressure Distribution and Lift Effects	15
	IV.2 Correlations of Lift and Drag Data	38
V.	CONCLUDING REMARKS	41
REFERENCES		44

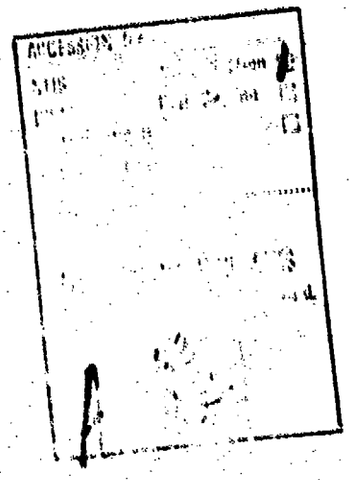

LIFT OF FIGURES

Figure 1 - Lift and Drag Coefficients of the Hydrofoil in Water Without Injection

Figure 2 - Comparison Between Measured ΔC_p Values and the Results of a Theoretical Calculation

Figure 3 - Effect of 10% Chord Injection of Water and Polymers on the Drag Coefficient of the Hydrofoil

Figure 4 - Effect of 30% Chord Injection of Water and Polymers on the Drag Coefficient of the Hydrofoil

Figure 5 - Effect of 10% Chord Injection of Water and Polymers on the Lift Coefficient of the Hydrofoil

Figure 6 - Effect of 30% Chord Injection of Water and Polymers on the Lift Coefficient of the Hydrofoil

Figure 7 - Difference in Pressure Coefficient, ΔC_p Versus Chord Distance, x / c

Figure 8 - Difference in Pressure Coefficient, ΔC_p Versus Chord Distance, x / c

Figure 9 - Comparison Between Measured and Calculated Pressure Distributions

Figure 10 - Comparison Between Measured and Calculated Pressure Coefficients on the Upper and Lower Surfaces

Figure 11a - Basic Pressure Distributions for Foil Angles of -3.5° and 5°

Figure 11b - Basic Pressure Distributions for Foil Angles of 0° and 3.5°

Figure 12 - Comparison of Measured Changes in Pressure with Those Calculated for a Symmetric Hydrofoil

Figure 13 - Boundary-Layer Displacement Effect on a Symmetric Hydrofoil

Figure 14 - Effect of Polymer Injection on Boundary-Layer Displacement

Figure 15 - Types of Boundary-Layer Interaction

Figure 16 - Calculated Camber Distributions

Figure 17 - Lift Change Versus $V_i\tau/c$

Figure 18 - Lift Change Versus $V_i\tau/c$

Figure 19 - Drag Change Versus $V_i\tau/c$

Figure 20 - Change in Drag Coefficient Components Due to Polyox Injection at V_i/V_∞ = .1 Rate

LIST OF SYMBOLS

c	Hydrofoil Chord
C_D	Drag Coefficient
C_{D_p}	Pressure Drag Component
C_{D_f}	Friction Drag Component
C_L	Lift Coefficient
C_{L_k}	Lift Coefficient Corresponding to Kutta-Joukowski value of the circulation
C_p	Pressure Coefficient
h	See Equation [2]
k	Reduction in circulation due to boundary layers; see Equation [1]
I_1	Integral defined by Equation [7]
I_3	Integral defined by Equation [3]
I_4	Integral defined by Equation [5]
V	Local Velocity on hydrofoil surface
V_i	Injection Velocity
V_u	Velocity on upper surface of hydrofoil
V_ℓ	Velocity on lower surface of hydrofoil
V_∞	Free-Stream Velocity
x	Coordinate in the direction of hydrofoil chord
x'	Dummy Variable
z	Coordinate normal to hydrofoil chord
z_c	Coordinate of hydrofoil camber line
z_s	Hydrofoil thickness distribution about camber line

α	Angle of attack
α_{eff}	Effective angle of attack
Γ	Circulation
Γ_k	Circulation corresponding to Kutta-Joukowski Condition
δ^*	Boundary layer displacement thickness
δ_c^*	Displacement effect on camber line
δ_s^*	Displacement effect on thickness distribution
τ	Polymer relaxation time

ABSTRACT

Existing data on the effects on lift of symmetric hydrofoils due to the injection of polymer solutions on to their surfaces show that the lift can either decrease or increase depending on the polymer, injection velocity, location of injection, side of injection and angle of attack. A unified, albeit semiempirical, approach is suggested in the present report for correlating and explaining the apparently contradictory data. It is proposed that the observed lift changes may be due to the influence of the injections on the boundary-layer displacement effect that is known to reduce the circulation around hydrofoils.

Four separate boundary-layer effects due to injection are identified and discussed, namely those due to changes in the effective angle of attack, the effective camber, the circulation (in addition to the changes in circulation associated with the previous two effects), and the thickness distribution. Classical methods of airfoil theory are utilized to calculate the "effective" hydrofoil shape that would have produced the observed pressure distributions. This effective shape is utilized to identify the different boundary layer effects, and these, in turn, are identical with the changes likely to be produced by polymer injections.

No explicit treatment of the exact nature of the interaction between the injected polymer flow and the boundary layer or the external pressure gradient is given, since this is outside the scope of the present study. However, it is argued that this interaction must necessarily be dependent on the viscoelastic properties of the polymer. For example, it is shown that when the observed changes in the lift force are normalized with respect to the local velocity at the location of the injection slit, the data for different polymers, different injection velocities and different angles of attack can all be correlated in terms of the single nondimensional parameter $V_i\tau/c$ where V_i is the injection velocity, τ is the polymer relaxation time and c is the hydrofoil chord. A similar correlation is also given for the changes in drag due to injection.

FOREWORD

The present report summarizes the work that has been carried out over the last four years at HYDRONAUTICS, Incorporated, under the support of the Office of Naval Research, on the lift and drag effects that arise due to the injection of polymer additives on to the surface of hydrofoils. The work has been primarily experimental and an effort is made herein to offer a unified, albeit semiempirical, interpretation to the considerable body of data that has been acquired.

Much of the early work on lift and drag effects were carried out under the general direction of Mr. Marshall P. Tulin, and a number of the correlations given in Section IV are based on theoretical concepts originated by him. Most of the pioneering efforts at HYDRONAUTICS, Incorporated on lift effects on hydrofoils were carried out by Dr. Daniel H. Fruman.

Technical monitoring for the program was provided by Messrs. Stanley Doroff and Ralph Cooper of the Office of Naval Research.

I. INTRODUCTION

It is well known that when dilute polymer additives are present in the external flows over two-dimensional hydrofoils they produce changes in both the drag and lift characteristics of hydrofoils. However, while the drag reduction achieved is generally accepted as being due to a thickening of the viscous sublayer adjacent to the wall, the reasons for the lift changes are far from clear. Indeed the available experimental data are themselves quite ambiguous and contradictory as to the exact nature of the lift effect.

Since Wu's early finding on the possibility of a reduction of (pump) impeller thrust in additive solutions[1], related studies with propellers and hydrofoils have been reported by Kowalski[2], Wolff and Cahn[3], Lehman and Suesawaum[4], Sarpkaya[5], Fruman, Sundaram and Daugard[6], Fruman, Tulin and Liu[7], and Simmarwalla and Sundaram[8]. From direct measurements, Kowalski[2] found that polymer additives decreased the thrust and increased the torque of a propeller resulting in a decreased efficiency. On the other hand, for a hydrofoil with polymer ejection, Wolff and Cahn[3] found a lift reduction, whereas Lehman and Suesawaum[4] reported that lift either increases or decreases depending upon whether the polymer is ejected from the suction side or from the pressure side.

Since 1963, HYDRONAUTICS, Incorporated has been carrying out a research program, under the sponsorship of the Office of Naval Research, on various aspects of the effects of polymer additives on fluid flows. During the last four years, the efforts have centered around investigations of the changes in lift and drag that occur on hydrofoils when polymer additives are injected tangentially into the flow from various locations on the foil surface. Up to date the investigations have been predominantly

experimental, with the tests having been conducted on 10- and 20-cm chord, symmetric hydrofoils in the HYDRONAUTICS High Speed Channel. Measurements have included drag and lift forces, as well as pressure distributions with and without injections. The experimental studies have yielded a large body of valuable data which can assist in the understanding of the effects of polymer additives on external flows. The objective of the research described in the present report is to utilize this body of data, as well as other data that is available in the literature, to attempt to develop a theoretical framework which can be used to analyze and interpret the observed effects.

In order to set the objectives of the present report in a proper perspective, a brief discussion of the experimental observations, with emphasis on the most recent results, is first given in Section II, followed by a detailed description of objectives. A discussion of the various physical mechanisms that have been postulated in the literature to explain the observed lift effects are discussed in Section III in the light of the most recent experimental data. The mechanism that is considered to be the most plausible, as well as the reasons for considering it to be so, are also described in Section III. A semi-empirical analysis is then given in Section IV and is utilized to correlate the data. Finally, some concluding remarks are given in Section V.

II. FEATURES OF THE EXPERIMENTAL RESULTS AND OBJECTIVES OF THE STUDY

Most of the experimental studies conducted at HYDRONAUTICS, Incorporated on the lift effects of polymer additives were carried out with a 10-cm chord NACA 63$_4$-020, two-dimensional hydrofoil placed in the HYDRONAUTICS' High Speed Channel (HSC). In the early tests, the forces on the model were measured, by the use of block gauges, for the cases with and without injection of Polyox WSR301 as well as water (so as to provide a "baseline" condition for assessing the effects of the polymer alone). These early studies[6,7] indicated that, under certain conditions, polymer injection not only leads to a drag decrease but also to a lift increase, so that significant increases in the lift/drag ratio could be realized. In general, it was found that a lift increase accompanied a drag decrease when the polymer injection was on the suction side of the hydrofoil, and that both drag and lift decreased when the polymer injection was on the pressure side of the hydrofoil.

In an attempt to understand the phenomenology responsible for the observed lift behavior, tests[7] were undertaken to measure the pressure distributions on the hydrofoil for the cases with and without polymer injection. These preliminary tests indicated that polymer injection on one surface (suction or pressure) of the hydrofoil changes the pressure distribution on both surfaces, though the effect is more pronounced on the surface on which the injection is made. It was also found that the pressure distributions were consistent with the lift forces measured by the block gauges; that is, the forces obtained by integrating the measured pressure distribution were the same, within accepted experimental error, as those measured by the block gauges.

Based on these experimental results, Fruman, Tulin and Liu[7] concluded that the observed lift increases could not be explained in terms of changes in the boundary-layer-separation point, since the pressure distributions revealed that injection did not significantly alter the pressure distributions in the trailing-edge region. These authors argued that the observed lift effect may not be related directly to the drag-reduction phenomena. There were also indications from the trends in the data* that the observed lift effect may be strongly dependent on the viscoelastic behavior of the polymer. One direct method of examining whether viscoelastic effects are responsible for the observed lift changes is to conduct tests with different polymers of differing viscoelastic behavior under otherwise identical experimental conditions; the results of such tests are described in Reference 8 for three different polymers, namely, Polyox, Polyacrylamide and Jaguar. Since these results formed the basis for the analyses given in the present report, they are described briefly below.

As mentioned earlier, all of the tests were conducted with a 10-cm chord symmetric hydrofoil and were performed in the HYDRONAUTICS High Speed Channel (HSC) modified to obtain a two-dimensional flow. The hydrofoil has two .00127-cm wide injection slits, one located at 10% chord and the other (on the opposite side) at 30% chord. Each surface of the foil has ten pressure taps between 18 to 86 percent chord length. The drag and lift curves for the basic hydrofoil (without any injection) are shown in Figure 1. The slight assymmetry in the hydrofoil caused by the presence of the 10- and 30-percent chord slits on opposite sides of the foil is responsible for the slight assymmetry noted in the lift behavior.

*These aspects will be discussed in more detail in Section III.

Figure 2 shows a comparison between the measured pressure distribution and the results of a calculation using potential theory[9]. While there is general agreement between the measured and calculated pressure distributions, one feature that is noteworthy is the relatively large discrepancy between the two distributions near the trailing edge of the hydrofoil.

Lift, drag and pressure measurements were performed on the hydrofoil under the following test conditions:

a. Injected Fluids:
   1. Water
   2. 200 ppm Polyox WSR 301 (Union Carbide)
   3. 350 ppm Polyacrylamide (Polyscience - Cat. #2806)
   4. 1500 ppm Jaguar WPB (Stein, Hall & Co., Control #23-0548).

b. Injection Velocity Ratios: V_j/V_∞: 0.1 and 0.3, (V_∞ = 11 meters/sec).

c. Angles of Attack; α: 0°, 2.5° (or 3.25°) and 5°.

d. Injection Sides: Suction (upper) and pressure (lower).

e. Injection Positions: 10% and 30% chord.

In all, tests were conducted for eighty different combinations of test conditions. A summary of the test results follows*:

Drag (Figures 3 and 4)

Water injection results in a drag increase, or at most, a slight drag reduction; on the other hand, polymer injection always results in a drag reduction.

Lift (Figures 5 and 6)

Water injection always seems to produce a lift force in a direction opposite to the injection side, the magnitude of this

*All of the experimental data are given in tabular form in Appendix B.

lift change being relatively larger for V_j/V_∞ = .3 and 10% chord injection cases. Polymer injection produces a lift force in either the same direction as that of the injection or opposite to it, depending upon the polymer (compare Jaguar and Polyox at 0° angle of attack and 30% chord injection, Figure 6), the rate of injection (compare 0.1 and 0.3 rates of injection for Polyox at 0° angle of attack, Figure 5), the location of injection (compare 10 and 30% chord locations for Polyox, pressure-side injection at 0.1 rate, Figures 5 and 6), and the angle of attack (compare 0° and 2.5° with 5° angle of attack for the suction-side injection of Polyox at V_j/V_∞ = .3 rate, Figure 5).

Pressure Distribution

The pressure distribution data were taken for all of the different test conditions. Typical pressure distribution curves are shown in Figures 7 and 8. The change in the chordwise pressure distribution due to suction-side injections of Polyox and Jaguar at a foil angle of 2.5° is plotted in Figure 7. The hydrofoil has pressure taps only between 18 and 86% of its chord length; nevertheless, the general trend is good enough to make the following observations.

1. Polyox injection at V_j/V_∞ = 0.1 results in a pressure decrease on most of the suction side and in a pressure increase on the pressure side; hence, one would expect a lift increase. On the other hand, Polyox injection at V_j/V_∞ = 0.3 results in a pressure increase on most of the suction side and in a pressure decrease on the pressure side; hence, one would expect a lift decrease. These observations are consistent with the results given in Figure 5.

2. Jaguar injection at V_j/V_∞ = 0.1 as well as at 0.3 rate results in a pressure decrease on the suction side and in a

pressure increase on the pressure side; hence, a lift increase is expected in both cases. However, the magnitudes of this pressure change on both sides are comparatively larger for $V_j/V_\infty = 0.3$; hence, a relatively larger increase in the lift is expected for that case. Again these observations are very consistent with the results given in Figure 5.

The occurrence of a sharp negative pressure peak in the relative pressure distribution on the side of injection (Figures 7 and 8a) is a characteristic feature of most of the cases considered. Water injection in some cases gives rise to a positive pressure peak; see Figure 8b. The magnitude and the chordwise extent of this peak have an important bearing on the net lift change due to injection.

Even from the brief description given above, it can be seen that the lift behavior is quite complex, with the lift change due to injection being positive or negative for different combinations of conditions involving the injected polymer, the injection velocity, the chordwise location and side of the injection, and so on. Also, quite evidently the exact nature of the changes in the pressure distribution holds the key to the observed differences in lift changes for various combinations of conditions, as illustrated in Figures 7 and 8. It is clear that any theoretical explanation for the lift changes will have to account not only for the rather striking changes in the pressure distribution due to polymer injection, but also for the changes due to water injection. The development of a comprehensive theory to encompass all of the factors involved is undoubtedly quite a complex task, and this is not the objective of the present study. Rather, the objective here is to develop a semi-empirical, phenomenological approach useful for correlating the observed features of the data, appealing where necessary to dimensional reasoning.

In the next section, the various mechanisms that have been proposed in the literature as explanations for the observed lift effects are considered, with emphasis on the one we consider most plausible based on the trends in the data described herein.

III. PLAUSIBLE MECHANISMS FOR LIFT CHANGES

As mentioned earlier, based on their observations, Fruman, Tulin and Liu[7] examined several possible explanations for the observed behavior. A change in boundary-layer separation behavior was discounted as a feasible explanation, since the measured pressure distributions do not display any evidence of this (the major pressure changes occur somewhat aft of the slit rather than near the trailing edge). These authors then considered boundary-layer thinning on the side on which the injection is made as a possible explanation. The decreased boundary-layer thickness at the trailing edge of the hydrofoil can be directly related to the drag reduction, since the change in the momentum flux in the wake must equal the change in drag. In turn, the reduced thickness of the boundary layer at the trailing edge on the side on which the injection is made can be related to a change in the effective angle of attack. It is relevant to note that, according to the above explanation, injection on the pressure side will lead to a decrease in the trailing-edge boundary-layer thickness on this side and a consequent <u>decrease</u> in the effective angle of attack, whereas injection on the suction side will lead to the opposite effect—a result which is consistent with observed lift behavior in most (but not all) of the cases.

Fruman, Tulin and Liu calculated the reduction in trailing-edge boundary-layer thickness using the measured drag reduction and calculated the change in lift corresponding to the change in the effective angle of attack by using the measured lift-curve slope. They found that in all but a few cases, the measured lift changes were considerably larger than those that can be predicted using the mechanism described above. As will be seen later, a change in the effective angle of attack due to boundary-layer thinning at the trailing edge is only a <u>part</u> of the total effect on the boundary layer of the polymer injection.

Fruman, Tulin and Liu[7] then considered viscoelastic effects as possible explanations for the observed changes. They pointed out that when the observed lift forces are plotted against the logarithm of the free stream velocity, a straight-line behavior results in a manner analogous to the behavior noted in pitot-tube measurements in flows containing polymer additives. Such a plot also indicates that there is a threshold velocity below which the lift effect does not appear, the actual value of this threshold velocity being dependent on the test conditions. However, when the results are plotted in terms of the local velocity at the injection slit, a single threshold velocity results. These observations lend credence to the concept that viscoelastic effects may be responsible for the observed lift effects. Moreover, the fact that under otherwise identical experimental conditions different polymers lead to significantly different lift changes, also lends credence to the concept that viscoelastic effects are responsible, at least in part, for the observed effects.

The anamolous lift effect was also noted by Sarpkaya[5] in his tests on two-dimensional hydrofoils immersed in dilute homogeneous solutions of polyethelene oxide, and he concluded that the lift-to-drag ratio of the hydrofoils may either increase or decrease depending on their stall characteristics. Sarpkaya theorized that the observed effect may be due to the different influences of the polymer on the boundary-layer characteristics on the top and bottom surfaces of the hydrofoil and the consequent change in the circulation defect (that is, the difference between the actual circulation and that predicted by the Kutta condition) known to exist in real flows.

The hypothesis that the observed effects may be due to boundary-layer interaction becomes quite plausible when one compares the actual measured pressure distributions under undisturbed

conditions (that is, in the absence of injection) with theoretical computations based on thin-airfoil theory; see Figure 2. It can be seen that there are significant differences between the calculated and measured distributions, especially near the trailing edge of the hydrofoil; these differences are typical of such comparisons, are well known in the literature (see References 10-13, for example), and are attributed to boundary-layer effects. The potential-flow streamlines around the hydrofoil are displaced outward not only due to the thickness distribution of the hydrofoil, but also due to the boundary layer on the foil surface. Hence, better results would be obtained if, in the computations instead of using the actual hydrofoil shape, an altered shape in which the boundary-layer displacement thickness is added to the shape is used.

In general, the boundary layer on the upper surface of the hydrofoil will grow faster than that on the lower surface because of the adverse pressure gradient existing on the top surface from the minimum-pressure point onward. Therefore, the effective hydrofoil shape (that is, the actual shape plus the displacement thickness) will have a slightly turned up trailing edge at a relatively small positive angle of attack. The differences between the computational results and the measurement near the trailing edge of the foil are directly attributable to the effect mentioned above and, indeed, excellent agreement between the two results are obtained if boundary-layer displacement effects are included in the computation[11,12].

The relevance of the above remarks in the present context is that, as can be seen from Figure 2, the boundary-layer displacement effects can have a significant effect on the pressure distributions, these effects being considerably larger than the observed lift effects caused by polymer injections. Thus, even small changes in the

dynamic evolution of the boundary layer on the surface on which the injection is made can be expected to produce changes in the pressure distributions of the type observed in the experiments.

One other important feature of the relative pressure distributions which also indicates* that the observed effect may be due to boundary-layer interaction is the relatively sharp decrease in the pressure coefficient some distance aft of the injection position. This relatively sharp negative peak in the pressure distribution is a characteristic feature of most of the cases considered, and always occurs on the same side on which the injection is made (see Figures 7 and 8). As already noted, and as can be seen from Figures 7 and 8, the magnitude and chordwise extent of this peak have an important bearing on the magnitude as well as the direction of the net lift change that results due to the polymer injection.

In many cases, as in the case of Polyox injection illustrated in Figure 7, there are positive pressure regions before and following the negative pressure peaks. Also, the pressure distribution is affected everywhere on the foil surface regardless of the side or location at which injection is made. Moreover, the actual location at which injection is made seems to have little or no influence on the location of the pressure peak, the latter apparently being influenced more by the basic undisturbed pressure distribution on the hydrofoil.

It is important to note that water injection also leads to peaks in the pressure distribution, as illustrated in Figure 8b. This figure shows the changes in the pressure distributions resulting from water injection at an angle of attack of 0° for lower side injection at 30% chord. For the corresponding case of Polyox injection, there is a negative peak on the bottom-side pressure distribution (the side on which the injection is made). However,

*This statement will be discussed in more quantitative terms in Section IV.

for the case of water injection, while there is a small negative peak for the smaller rate of injection, the pressure peak becomes positive for the larger rate of injection.

The observed features of the pressure distributions described above are compatible with the hypothesis that the lift changes are produced by boundary-layer displacement effects. The interaction between the injected flow and the boundary layer can be expected to depend as much on the undisturbed pressure distribution on the hydrofoil as it does on the location of the injection. For example, clearly portions of the boundary layer in the favorable and adverse pressure-gradient regions in the hydrofoil may respond differently to the perturbations caused by the injections.

Fruman, Tulin and Liu[7] have suggested that the lift effect of polymer injection may be due to the fact that the polymer stream enters the flow around the hydrofoil in the form of a "swollen jet" due to the viscoelastic behavior of polymer solution. While it is plausible to suppose that the observed peaks in the pressure distribution may be due to these "swollen jets", it seems unlikely that the observed effect is a purely viscoelastic one, since water injection also leads to peaks in the pressure distributions.

In any case, the important point to note here is that the local changes in the displacement thickness of the boundary layer due to its interaction with the injected flow will lead to local changes in the effective camber of the hydrofoil. In turn, the effect of the latter changes will be to cause localized changes in the pressure distribution near the locations of maximum interaction as well as to cause more general changes in the pressure distribution over the entire hydrofoil surface due to changes in the circulation. This is exactly what is seen in the data.

As mentioned earlier, based on his experiments on hydrofoils immersed in dilute, homogeneous polymer solutions, Sarpkaya[5] has suggested that the observed lift increases may be due to the restoration, by polymer-induced changes, of some of the circulation reduction created by boundary-layer displacement effects. The present results on the effects of the polymer when it is injected at the hydrofoil surface also seems to suggest that the observed lift changes may be due to a boundary-layer displacement effect caused by the injection, especially in view of the differences between the actual measured pressure distributions under undisturbed conditions (that is, in the absence of injection) and theoretical computations based on potential-flow theory[9]; see Figure 2. However, the observed effect is also evidently a function of the characteristic relaxation time, τ, of the polymer, or, more appropriately, the nondimensional parameter $V_i\tau/\ell$, where V_i is the injection velocity and ℓ is a characteristic hydrofoil dimension. The data also show that the boundary-layer displacement effect must also be a function of the side, location and velocity of the polymer injection.

The hypothesis given above can be verified directly, since the measured pressure distributions can be analyzed using classical airfoil theory, and the "effective" hydrofoil shape that will produce the observed pressure distributions can be calculated. This effective hydrofoil shape can then be viewed in terms of a change in the evolution of the boundary layer around the actual hydrofoil. By these means, correlations can be sought between the observed effects and the test variables in terms of information that exist in the literature on the behavior of boundary layers under favorable and adverse pressure gradients, and under the influence of injections and various surface perturbations. This is the approach that is utilized in the next section.

IV. SEMI-EMPIRICAL CORRELATIONS FOR THE OBSERVED EFFECTS

IV.1 Pressure Distribution and Lift Effects

It was suggested in the previous section that the observed lift effects are due to a change, caused by the injection of water or a polymer at the surface of the hydrofoil, in the boundary-layer-displacement phenomenon which causes the observed lift in real flows to be less than that predicted by potential theory. In essence, the faster growth of the boundary layer on the suction side of the hydrofoil compared to that on the pressure side leads to an effective hydrofoil shape which has a slightly turned-up trailing edge. In turn, this leads to a reduction in effective camber and hence also in circulation and in lift.

It is well known[14,9] that reasonable agreement can be obtained between measured pressure distributions on a hydrofoil and the predictions of potential theory, except near the trailing edge, when the measured values of the lift coefficient, rather than the theoretical values, are used to normalize the pressure coefficients. This is the basis for the comparison shown in Figure 2. Somewhat better agreement between the measured and calculated pressure distributions can be obtained by recognizing that the smaller-than-potential lift that is measured must necessarily imply that the actual circulation around the hydrofoil is smaller than that predicted by the Kutta condition. Hence, the distribution of vortices used to represent the hydrofoil must correspond to the reduced circulation rather than to that predicted by the Kutta condition.

Let

$$\Gamma = \Gamma_k (1 - k) \qquad [1]^*$$

*Equation [1] is equivalent to $C_l = C_{l_k} (1 - k)$ where C_l and C_{l_k} are respectively, the measured and predicted values of the lift coefficient.

and

$$h = 1 - \tfrac{1}{2} k \quad , \qquad [2]$$

where Γ and Γ_K are, respectively, the actual value of the circulation and that predicted by the Kutta condition.

It can be shown[15,16,12] that, for a symmetric hydrofoil, the induced velocity distribution due to the modified vorticity distribution is given by,

$$V = \pm \frac{V_\infty \alpha}{\sqrt{1+(dz/dx)^2}} \left[\frac{h-x}{\sqrt{x(1-x)}} \left\{ 1 + I_3(x) - kI_4(x) \right\} \right] \quad , \qquad [3]^*$$

where V_∞ is the free-stream velocity, α is the angle of attack and the integrals I_3 and I_4 are given by,

$$I_3(x_0) = \frac{1}{\pi} \int_0^1 \left[\frac{dz}{dx} - \frac{2z}{1-(1-2x)^2} \right] \frac{dx}{x_0 - x} \quad , \qquad [4]$$

and

$$I_4(x_0) = \frac{1}{2\pi} \int_0^1 \frac{z\, dx}{x(h-x)(x_0-x)} \quad . \qquad [5]$$

In the above equations $z = z(x)$ represents the thickness distribution of the hydrofoil and all the lengths have been normalized through division by the hydrofoil chord, c. In Equation [3] the positive sign applies to the upper surface of the hydrofoil while the negative sign applies to the lower side.

In Equation [3], the parameter $\sqrt{1+(dz/dx)^2}$ represents the ratio between the (predicted) velocity on the chordline and the actual velocity on the foil surface; its use avoids, for a round-nosed hydrofoil, the occurrence of an infinite suction velocity at the leading edge[15-17]. Since Equation [3]

*This equation is found by representing the hydrofoil surface by appropriate distribution of vortices and sources (see Appendix A).

violates the Kutta condition, it predicts an infinite velocity at the trailing edge; however, this can be eliminated if, as suggested by Preston[10] and Spence[13], the velocities at the edges of the boundary layer along normals to the upper and lower surfaces at the trailing edge are used, along with a judicious fairing procedure, instead of the velocity at the trailing edge itself.

Equation [3] represents the velocity distribution due to the effect of angle of attack, and, for a symmetric hydrofoil, the velocity due to thickness distribution has to be added to this to obtain the total velocity distribution. The latter velocity distribution can be written as

$$V = \frac{V_\infty (1+I_1)}{\sqrt{1+(dz/dx)^2}} \qquad [6]$$

where

$$I_1(x_0) = \frac{1}{\pi} \int_0^1 \frac{(dz/dx)\, dx}{x_0 - x} dx \quad . \qquad [7]$$

The velocity due to thickness distribution is also tabulated in Reference 9 for a number of NACA foil shapes in general, and for the specific hydrofoil under consideration here in particular.

Equations [3] and [6] can be used, along with the simple relation,

$$C_p = 1 - \left(\frac{V}{V_\infty}\right)^2 \quad , \qquad [8]$$

to calculate the pressure coefficient, C_p, on either side of a symmetric hydrofoil at a specified angle of attack and at a arbitrary value of the circulation (that is, at a value

of the circulation that does not necessarily correspond to that given by the idealized Kutta-Joukowski condition). The calculated pressure distributions for the specific hydrofoil shape utilized in the present study are shown in Figures 9 and 10 for an angle of attack of 5° and for a value of the circulation which corresponds to the measured value of the lift coefficient. In the approximate calculation, the integrals given in Equations [4] and [5] were not calculated; rather, the expression within the flower brackets in Equation [3] was equated to unity since this is sufficiently accurate for the present purpose*. Also, the tabular values given in Reference 9, rather than Equation [6], were used to calculate the induced velocity due to the thickness effect.

A comparison between the measured and calculated values of the differences in the pressure coefficients on the upper and lower surfaces of the hydrofoil is shown in Figure 9, while the pressure coefficients themselves are shown in Figure 10. Values corresponding to the Kutta-Joukowski value of the circulation are also shown in these figures for purposes of comparison. It can be seen that the calculations for the reduced-circulation case give very good agreement with the measurements, including in the region of the trailing edge, which is noteworthy in view of a quite approximate method of calculation.

The main point to be derived from the comparisons shown in Figures 9 and 10 is that while the considerably smaller lift that is measured in the tests (in the absence of injection) may be caused, in part, by a lack of two-dimensionality in the flow or by wall interference effects, boundary-layer displacement effects may also be of importance. Hence, it is plausible that even if polymer injection causes only small changes in the boundary-layer thickness, the observed magnitudes of lift and pressure changes can result.

---

*This approximation is equivalent to making the thin-airfoil assumption when determining the vortex distribution on the chordline; see Appendix A.

Estimates of the types of changes that will occur in the pressure distributions on a symmetric hydrofoil due to the observed lift changes caused by injection can be made using Equation [3]. Again, as before, making the approximation that the terms within the flower brackets in Equation [3] are equal to unity, this equation and Equations [1], [2] and [8] yield an expression for the change, ΔC_p, in the pressure coefficient due to a change, ΔC_L, in the lift coefficient, as

$$\Delta C_p = \mp \frac{(V/V_\infty)}{\sqrt{1+(dz/dx)^2} \cdot \sqrt{x(1-x)}} \cdot \frac{\Delta C_L}{2\pi} \quad , \qquad [9]$$

where, now, the negative sign applies to the top surface and the positive sign to the lower surface.

In Equation [9], V represents the velocity on the upper or lower surfaces of the hydrofoil in the absence of injection and can be computed using the measured pressure distribution in the absence of injection; these basic pressure distributions for the four angles of attack considered in the present study are shown in Figure 11.

Comparisons between the measured changes in pressure distributions due to injection and those calculated using Equation [9] are shown in Figure 12 for two cases. The first case shown is that for Jaguar injection on the suction side of the hydrofoil at ten percent chord and at thirty percent of free-stream velocity, with the angle of attack being 2.5°; as can be seen from Figure 5, this case leads to a substantial lift increase. The second case shown is that for water injection, this case leads to a lift decrease.

It can be seen from Figure 12 that there is a very good general agreement between the calculated and measured distributions, except for the presence in the latter of the pressure peaks already discussed. It should be noted that in each of the comparisons shown three separate sets of measurements are involved, namely, the changes in the lift force, the basic pressure distribution and the change in the pressure distribution due to injection. Thus, the good agreement displayed in Figure 12 is evidence of the self-consistency of the experimental data. The fact that the pressure distributions predicted by potential theory using a change in circulation alone go a long way in predicting the observed changes in pressure distributions, appears to support the present method of approach of viewing the lift and pressure changes in terms of changes in the "effective" shape of the hydrofoil.

On the other hand, when the observed lift changes are viewed merely as due to a change in the effective angle of attack of the hydrofoil, the predicted pressure changes are not in good agreement with those observed. This can be seen by letting h and k in Equation [3] equal to unity and zero, respectively, so as to obtain the velocity distribution corresponding to the ideal value of the condition around the hydrofoil. Then, the change in the velocity distribution due to a change, say in the angle of attack, can be written as,

$$\Delta V = \pm \frac{V_\infty}{\sqrt{1 + (dz/dx)^2}} \sqrt{\frac{1-x}{x}} \cdot \Delta\alpha \quad , \qquad [10]$$

where the same approximation as that involved in Equation [9] has been made.

Using Equations [8] and [10], the change in pressure coefficients can then be written as,

$$\Delta C_p = \pm \frac{(V/V_\infty)}{\sqrt{1 + (dz/dx)^2}} \sqrt{\frac{1-x}{x}} \cdot \frac{\Delta C_L}{(\partial C_L/\partial \alpha)_m} , \qquad [11]$$

where $(\partial C_L/\partial \alpha)_m$ is the measured lift curve slope in the absence of injection. Equation [11] is also shown plotted in Figure 12 (in dotted lines); it can be seen that even the qualitative behavior of the measured and predicted distributions are different. It should be noted that both Equations [9] and [11] correspond to the same change in circulation around the hydrofoil, which, in turn, is deduced from the measured value of the lift change. However, these two equations account for the changes in circulation in terms of different distribution of vortices around the hydrofoil chord; the physical significance of the differences between the two cases will be discussed presently.

As already noted, the single expression given in Equation [9] does remarkably well in predicting many of the observed features of the pressure distributions. However, since it only accounts for the changes in the pressure distributions due to a change in circulation for a symmetric hydrofoil, the equation fails, not surprisingly, to predict the observed peak in the pressure distribution on the side on which the injection is made. This pressure peak is evidently associated with an unsymmetric change in the effective shape of the hydrofoil and can be predicted only by explicitly accounting for camber effects. Note that boundary-layer-displacement effects were not accounted for explicitly in Equation [9], though the changes in circulation were assumed to be induced by changes in boundary-layer thickness.

As mentioned earlier, several authors have included the effects of boundary-layer displacement on lift explicitly. Specifically, Preston[10,11] has resolved the displacement effect

into symmetric and antisymmetric parts and has treated each separately. Preston's "change of shape" method is of considerable value in visualizing the effects of surface injections. However, before considering this method in detail it is relevant to briefly discuss an alternate technique developed by Spence[13], since it provides some insight into the manner in which boundary-layer development influences the outside potential flow. In this method the boundary-layer displacement effect is represented at the outset by an unsymmetric source distribution and the circulation is determined by utilizing the condition that equal amounts of vorticity, though of opposite signs, must pass into the wake from the boundary layer on the upper and lower surfaces of the hydrofoil.

The calculational steps in Spence's method involves the transformation, by the use of conformal mapping, of the hydrofoil into a circle; as such, the final results in this method involve complex coordinates. In particular, two of the key parameters that appear in the final results (Equation 45 of Reference 13) are λ_1 and λ_2 which are, respectively, the distances in the complex plane between the trailing edge and the edges of the boundary layers on the upper and lower surfaces. While the result itself is too involved to consider here, it is relevant to cite Spence's observations on the results.

"This equation provides a theoretical explanation of certain qualitative boundary-layer effects on lift which are well recognized experimentally. For an airfoil of finite trailing edge angle, τ, the effect of thickening the upper boundary layer, keeping the lower constant, would be to increase λ_1. The effect would thus be ----- to decrease the circulation and lift, as expected. The converse effect should occur if λ_1 were decreased (e.g., by increasing the amount of laminar flow on the

upper surface*). The effect of increasing and decreasing λ_2, which represents the lower boundary layer thickness are not clear from the equation, and would appear to depend on actual rather than relative thicknesses. It is expected that the larger the trailing-edge angle, the more marked will be such changes in lift obtainable via trailing-edge thickness."

While the exact nature of the interaction between the injected polymer flow and the boundary layer is not known, it is clear that many of the observations of Spence quoted above may be relevant in the context of the present study. For example, if the effect of polymer injection on the upper surface is imagined as producing a more laminar (that is, thinner) boundary-layer behavior on that surface, then the result of the injection would be to yield a lift increase. This is what is observed in many cases of polymer injection studied herein, especially when the effects of polymer injection are viewed relative to that of water injection. However, it should be noted that the injected flow will also interact with the external pressure gradient, and that the effect of the strong, adverse pressure gradient present downstream of the point of injection (see Fig. 11) may be to increase the boundary layer thickness. The net effect will then be governed by the balance between these two counteracting influences.

Water injection on the upper surface presumably leads to a thickening of the boundary layer, since a reduction in lift always accompanies such injection. Also, since water injection on the upper surface causes a drag increase, it is difficult to attribute the observed results to any leading-edge effects such as those associated with boundary-layer control through the use of leading-edge slats or blowing[17].

* Emphasis supplied; not in the original citation.

Spence's results also show that the effects on lift of changes in the upper and lower boundary layer thicknesses are considerably different. Specifically, changes in the lower surface boundary layer can produce either an increase or decrease in lift depending on the actual values of the boundary layer thicknesses on the upper and lower surfaces (that is, on section shape, angle of attack, Reynolds number, etc.) and on the trailing-edge angle. The experimental results are qualitatively consistent with this observation, since the changes in lift due to lower surface injection display considerably fewer trends as compared to effects of upper side injection.

As mentioned earlier, Spence's results are not in a form from which quantitative estimates can be obtained readily; for this purpose we appeal to the technique developed by Preston[10,11].

Consider a symmetric, two-dimensional hydrofoil at an angle of attack α to the free stream as shown in Figure 13(a). Due to the more adverse pressure gradients on the upper surface of the hydrofoil, the boundary-layer displacement thickness on that surface will increase at a more rapid rate than that on the lower surface. The effect of boundary-layer displacement on the external potential flow can be calculated by adding the displacement thickness to the effective cross-sectional shape of the hydrofoil. If δ_u^* and δ_ℓ^* represent the displacement thicknesses of the upper and lower surfaces, the displacement effect can be resolved into two parts, one symmetric and the other antisymmetric, namely,

$$\delta_s^* = \tfrac{1}{2}\,(\delta_u^* + \delta_\ell^*);\quad \delta_c^* = \tfrac{1}{2}\,(\delta_u^* - \delta_\ell^*)\quad , \qquad [12]$$

where δ_c^* represents the change in the effective camber of the hydrofoil and δ_s^* the change in its thickness distribution.

---

* In this and the following figures the boundary-layer-displacement effects are shown highly exaggerated for the sake of clarity.

It is appropriate to first consider the effective camber distribution alone, since its influence on the lift is much more profound than that of the thickness distribution. The effective centerline of the hydrofoil is obtained by adding δ_c^* to its geometric centerline, and the effective cross-sectional shape of the hydrofoil can be represented as in Figure 13(b). As can be seen from the figure, the displacement effect will produce not only a reduction in the effective angle of attack by an amount equal to,

$$\alpha_1 = \left(\frac{\delta_c^*}{c} \right)_{\text{trailing edge}} , \qquad [13]$$

but also a negative camber about the effective chord, LT'. Both of these effects will tend to reduce the lift produced by the hydrofoil.

If the value of the circulation about the effective hydrofoil shape were governed by the Kutta-Joukowski hypothesis, then the above two effects will be the only ones present. However, due to the presence of the boundary layer, the circulation around the effective hydrofoil is not given by the Kutta-Joukowski hypothesis[11], but, rather, has to be determined using the condition that equal and opposite amounts of vorticity must pass into the wake from the upper and lower boundary layers. Preston has shown that the above condition is satisfied, to a first approximation, when the velocities at the edges of the boundary layer on the upper and lower surfaces at the trailing edge of the hydrofoil are equal. These velocities themselves can be estimated by using potential theory with an arbitrary value for the circulation in the absence of displacement effects, and the circulation adjusted to make the velocities equal. If necessary, the results can be improved by iteration.

The effect of the symmetric part, δ_s^*, on the pressure distribution can be calculated by adding δ_s^* to the thickness distribution of the hydrofoil and by using Equations [6] and [7].

The effect of boundary-layer displacement on the lift and pressure distributions on a symmetric, two-dimensional hydrofoil is thus seen to consist of four separate parts. The first is associated with a reduction in the effective angle of attack, while the second is associated with the negative camber of the effective hydrofoil shape. The third effect represents the reduction in circulation as compared to that given by the Kutta-Joukowski criterion, and the fourth effect represents the changed thickness distribution. In the comparisons shown in Figures 9 and 10, only the third of the above effects was included (using the measured lift) and the others were neglected.

The influence of polymer or water injection on the lift and pressure distributions can now be viewed in terms of the boundary-layer-displacement effects described above. Consider the injection of polymer or water from a location, 1, on the surface of a symmetric, two-dimensional hydrofoil. The effective chord and centerline of the hydrofoil in the absence of injection (but including boundary-layer effects) are shown in detail in Figure 14. As a first approximation it is appropriate to assume that the injection alters the boundary-layer thickness only on the side on which the injection is made and only downstream from the point of injection*. The effective centerline of the hydrofoil will then be displaced vertically by an amount equal to $\Delta\delta^*/2$, where $\Delta\delta^*$ is the change (assumed positive when there is thickening on the upper surface or a thinning on the lower surface) in the

* For the sake of convenience only a general thinning is shown in Figs. 14 and 15. As mentioned earlier, there can be a thinning or thickening of the boundary layer locally depending on the relative magnitudes of the effects due to the adverse pressure gradient and the polymer.

boundary-layer-displacement thickness due to injection. The effective centerline and chord are shown as solid lines in Figure 14, with T" being the new effective trailing edge of the hydrofoil.

It can be seen from Figure 14 that the injection leads to a change in the effective angle of attack by an amount equal to $-\Delta\delta_t^*/2c$, where $\Delta\delta_t^*$ is the change in boundary-layer-displacement thickness, due to injection, at the trailing edge. It can also be readily shown that the change in camber is given by $\frac{1}{2}(\Delta\delta^* - x\Delta\delta_t^*)$. Since the camber effect depends on the details of the interaction between the boundary layer and the injected flow, it may be either positive or negative locally and change sign with downstream distance depending on the specific nature of the interaction. As already pointed out, the fact that different polymers lead to significantly different results implies that the characteristic interaction length is likely to be dependent on the parameter $V_\infty\tau$, where τ is the polymer relaxation time. It may be expected that the nondimensional ratio $\delta_1^*/V_\infty\tau$, where δ_1^* is the displacement thickness at the location of the injection, will be an important parameter.

Of course, the exact nature of the interaction of the injected polymer solutions with the boundary layer or with the outside flow is unknown, and it is not the objective of the present study to attempt to describe the details of this interaction. It is our objective to merely illustrate that such interactions can be the plausible reasons for the observed changes in the pressure distributions, lift and drag. Even if the injected flow enters the outside flow as a "swollen jet", the computational procedure described herein can be utilized provided that the displacement effect of this jet is known.

It should be noted that the circulation around the modified centerline LT" will not be that specified by the Kutta-Joukowski hypothesis; nor will it be merely the circulation in the absence of injection (that is, for the centerline LT') corrected for the effects of the changed angle of attack and camber. The new value of the circulation can, and should be, uniquely determined by using the condition that the velocities at the edge of the (changed) top and bottom boundary layers at the trailing edge must be the same.

Finally, the effect of the injection on the thickness distribution can be obtained by subtracting $\Delta\delta^*/2$ from the basic distribution when there is a thinning of the boundary layer and by adding it when there is a thickening.

The four separate effects can be summarized as follows:

(i) A change in angle of attack due to a change in the boundary-layer thickness at the trailing edge; given by $\Delta\alpha = -\Delta\delta_t^*/2c$.

(ii) A change in the effective camber of the hydrofoil due to injection.

(iii) A change in circulation due to injection, determined by using the theorem stated by G. I. Taylor that equal and opposite amounts of vorticity must pass into the wake from the top and bottom boundary layers[11,17].

(iv) A change in thickness distribution due to injection.

In passing, it may be noted that in their analysis of boundary-layer effects, Fruman, Tulin and Liu[7] only considered the first of the above four effects, while in the comparison shown in Figure 12 (that is, in Equation [9]), all of the observed lift change was attributed to the third effect.

Before making quantitative estimates of the four separate effects of injection, it is first relevant to consider their qualitative behavior for a specific example, say, that of polymer injection on the upper surface. If the effect of polymer injection is to make the boundary layer downstream of the point of injection behave in a more laminar fashion, then accompanying the drag reduction, there is also a reduction in the boundary-layer-displacement thickness at the trailing edge. Thus, there will be an increase in the effective angle of attack. Of course, the converse is true if polymer injection is made on the lower surface.

As already pointed out, the sign of the camber effect will depend on the detailed nature of the interactions between the injected and boundary-layer flows. In general, if the thinning effect increases monotonically with increasing downstream distance, as depicted in Figure 15(a), then there will be a net positive increase in camber (due to a decrease in the negative camber) as shown. However, if the maximum degree of thinning occurs, at a short distance downstream of the point of injection, as shown in Figure 15(b), the distribution of the change in camber may be negative over a large portion of the hydrofoil, so that the net effect is a reduction in lift. If the maximum degree of thinning occurs at a location close to the trailing edge but ahead of it, as shown in Figure 15(c), then the maximum (negative) change in camber will also occur close to the trailing edge. Since, as is well known (see, for example, Reference 18, page 88), the values of the camber near the trailing edge have a more profound influence on lift than the values elsewhere, the reduction of lift in this case is likely to be substantial.

The change in circulation due to polymer injection, say, at the top surface, can be determined using the condition that the

new value of the circulation should be such that the velocity at the new edge of the top boundary layer at the trailing edge should be the same as that at the (unchanged) edge of the bottom boundary layer at the trailing edge. For a hydrofoil with a finite trailing-edge angle, the trailing edge is a stagnation point, so that near the trailing edge the velocity will increase with increasing distances from it. Thus, if the circulation remained unchanged after injection, the velocity at the edge of the (thinned)top boundary layer will be smaller than that at the bottom; to increase this velocity to equal that at the bottom, the circulation will have to increase. In other words, a thinning of the top boundary layer must necessarily be accompanied by an increase in the effective circulation around the hydrofoil*.

Conversely, a thinning of the lower boundary layer must necessarily be accompanied by a decrease in circulation, since to make the velocity at the new edge of the (thinner) lower boundary layer at the trailing edge equal to that at the (unchanged) upper edge, the circulation must be decreased.

In summary, if the effect of polymer injection on the boundary layer is to thin it downstream of the point of injection, the angle-of-attack effect will increase the lift for upper side injection and reduce it for lower side injection. The camber effect may either increase or decrease the lift depending on the details of the interaction between the injected

*Since the velocity distribution in the region of the trailing edge is dependent on the hydrofoil geometry in general, and the trailing edge angle in particular, these parameters will influence the change in circulation. These features are included in Spence's theory[13].

flow and the boundary layer. The change in lift due to the modified trailing-edge condition (Taylor's theorem) is positive for upper-side injection and negative for lower-side injection. Thus the total change in lift may be either positive or negative depending on the relative magnitude of the different effects, though, in general, upper-side injection can be expected to produce an increase in lift and lower-side injection a reduction in lift.

It is now appropriate to consider some quantitative estimates. Equations [3] and [4] represent the induced velocity distribution for a symmetric hydrofoil with an arbitrary circulation Γ. For a cambered hydrofoil the induced velocity due to thickness distribution is still represented by Equation [4]. However, utilizing the method developed by Weber[15,16] it can be shown* that the induced velocity due to the vortex distribution for a cambered hydrofoil is given by

$$V = \pm \frac{V_\infty}{\sqrt{1 + (dz_s/dx)^2}} \cdot \frac{h - x}{\sqrt{x(1-x)}} \left\{ \alpha_{eff} + \frac{1}{\pi} \int_0^1 \frac{dz_c(x')}{dx'} \cdot \sqrt{\frac{x'}{1-x'}} \, \frac{dx'}{x - x'} \right\} , \qquad [14]$$

where, as before, the positive sign applies to the upper surface and the negative sign to the lower surface. Also, α_{eff} is the angle of attack measured with respect to the effective chord line, LT' , z_c is the height of the effective camber line above the x axis, while z_s is the thickness distribution of the hydrofoil (including the boundary-layer displacement thickness).

*See Appendix A.

Equations [14] and [6] together describe the velocity distribution on the hydrofoil. From these equations, the change, ΔV , in the velocity distribution due to injection can be obtained as,

$$\Delta V = \frac{V_\infty}{\sqrt{1 + (dz_s/dx)^2}} \left[\pm \frac{h - x}{\sqrt{x(1-x)}} \Delta\alpha_{eff} \pm \left\{ \alpha_{eff} + \frac{1}{\pi} \int_0^1 \frac{dz_c}{dx'} \sqrt{\frac{x'}{1-x'}} \frac{dx'}{x-x'} \right\} \frac{\Delta h}{\sqrt{x(1-x)}} \pm \frac{h - x}{\sqrt{x(1-x)}} \right. \quad [15]$$

$$\left. \cdot \frac{1}{\pi} \int_0^1 \frac{d(\Delta z_c)}{dx'} \sqrt{\frac{x'}{1-x'}} \frac{dx'}{x-x'} + \frac{1}{\pi} \int_0^1 \frac{d(\Delta z_s)}{dx'} \frac{dx'}{x-x'} \right] ,$$

where, as before, the positive sign applies to the upper surface and the negative sign to the lower surface. The four terms on the right-hand side represent the effects on the velocity distribution of changes, respectively, in the effective angle of attack, in circulation, in camber and in the thickness distribution. Note that the first three terms are of opposite signs on the two sides of the hydrofoil, while the last term is of the same sign on both sides; thus the last term will not influence the lift change.

Even though Equation [15] appears to be quite complex, the changes in velocity can be calculated fairly readily if the changes in boundary-layer displacement thickness due to injections are known, since simple algebraic methods for evaluating the intergrals appearing in it are available in the literature[15,16,12]. Equation [15] can be simplified by utilizing the expressions given earlier relating the change in boundary

layer thickness to changes in the effective angle of attack, camber and thickness distribution. After some algebra, one obtains,

$$\Delta V = \pm \frac{V_u - V_\ell}{2} \frac{\Delta h}{h-x} + \frac{V_\infty}{\sqrt{1 + (dz_s/dx)^2}} \cdot \frac{1}{2\pi c} \sqrt{\frac{1-x}{x}} \cdot \int_0^1 \left\{ \frac{d\Delta\delta_s^*}{dx'} \sqrt{\frac{x}{1-x}} \pm \frac{d\Delta\delta_c^*}{dx'} \sqrt{\frac{x'}{1-x'}} \right\} \frac{dx'}{x-x'} \quad , \qquad [16]$$

where V_u and V_ℓ represent, respectively, the velocities on the top and bottom surface of the hydrofoil. In the derivation of this equation the approximation $h \approx 1$ has been made in the second term, so as to facilitate physical understanding of the phenomena involved; the approximation will not significantly alter the numerical values of the velocity.

The first term on the right-hand side of Equation [16] represents an antisymmetric effect of boundary-layer displacement, while the second term reflects both symmetric and antisymmetric effects. The first term accounts for the change in circulation due to a changed trailing-edge condition, and produces velocity changes which are equal in magnitude but opposite in sign on the two sides of the hydrofoil. The lift effect represented in this term is essentially the same as that in Equation [9] and, as already noted, ascribing all of the observed lift changes to this effect results in a predicted pressure distribution which is in good agreement with the measured value, except for the presence in the latter of certain peaks located near the point of maximum hydrofoil thickness and on the same side as the one on which the injection is made.

While the first term on the right-hand side of Equation [16] is not of a form which can yield the experimentally observed pressure peaks, the second term is indeed of this form, as can be seen from the following argument. If we assume that, to the first order, injection changes the boundary-layer thickness only on the side on which the injection is made, $\Delta\delta_s^*$ and $\Delta\delta_c^*$ will be equal in magnitude as well as in sign when injection is on the top surface, while they will be equal in magnitude but of opposite sign when injection is on the bottom surface; see Equation [12]. First consider tne case of injection of polymer or water on to the top surface. For this case it can be seen from Equation [16] that the value of the integrand in the second term has a singularity at $x = x'$, while it is bounded at all values of x on the lower surface*. Thus, depending on the specific behavior of $\Delta\delta^*$, it is likely that a pressure peak of the type observed in the experiments can occur on the top surface, but not on the bottom surface. Also, assuming that polymer and water injections produce changes of opposite sign in the displacement thickness (an assumption which is consistent with the observed drag behavior), it can be seen that water injection will produce peaks of sign opposite to those produced by polymer injection.

For bottom side injection, $\Delta\delta_s^*$ and $\Delta\delta_c^*$ are of opposite sign (though of equal magnitude) so that the integrand in Equation [16] is bounded everywhere on the top surface but not on the bottom surface. Hence in this case the pressure peaks can be expected to occur on the lower surface and not on the upper surface. The features noted above are exactly the ones displayed by the experimental data.

*In this and all other singular integrals occurring in this report, it is understood that the Cauchy principal value is the one of concern.

Since the detailed nature of the interaction of the injected flow with the boundary layer is not known, Equations [15] and [16] cannot be used to make quantitative predictions of the velocity changes that will occur due to injection. However, these equations can be used, along with the measured pressure changes, to estimate the shape of the effective hydrofoil which corresponds to the observed changes, as follows:

The change in the effective angle of attack is first calculated using Equation [13] and the momentum relation expressing the change in boundary layer thickness at the trailing edge in terms of the change in skin-friction drag[7]. This last quantity is itself determined by computing the change in the pressure drag from the measured pressure distributions and by subtracting this from the measured changes in the total drag. The first term on the right-hand side of Equation [15] can then be readily calculated.

If the total velocity field around the hydrofoil, including the boundary-layer-displacement effect, were known, then the change in circulation Δh can be calculated using the trailing-edge condition that the velocities at the edges of the top and bottom boundary layer be the same*. Lacking such information, the second term on the right-hand side of Equation [15], which is the same as the first term in Equation [16], can be estimated for various <u>assumed</u> values of Δh. The fourth term on the right-hand side of Equation [15] can be eliminated by taking the <u>difference</u> between the measured velocity changes on the top and bottom surfaces of the hydrofoil. Thus, finally, the third term (which represents the camber change) on the right-hand side of Equation [16] can be expressed in terms of the measured pressure changes. The method of Weber[15,16]

*The method of Spence[13] provides an approximate procedure for carrying out the step. However, even this approximate procedure is too complex to be useful here.

can then be used to calculate the camber, since she has tabulated the influence coefficients necessary for the inversions of the integral.

Figure 16 shows the results of three sample calculations for the cases of Jaguar, Polyacrilamide and Polyox injections on the suction side of the hydrofoil at 10% chord, 2.5° angle of attack and at an injection velocity equal to thirty percent of free-stream velocity. Calculations are shown both for $\Delta h = 0$ and $\Delta h = 0.015$. As expected, the calculations show that significant changes in camber occur only downstream of the point of injection. For both of the assumed values of Δh in Figure 16, Jaguar injection produces the maximum positive camber, while Polyacrilamide and Polyox injections give successively lower values. It is relevant to note that the change in camber is <u>not</u> confined to a small region close to the point of injection, but occurs over the entire downstream region of the hydrofoil. The changes with downstream distance in sign of the camber (especially evident in the cases for $\Delta h = 0.015$) may be due to the competing influences of the adverse pressure gradient and polymer relaxation.

Also shown in Figure 16, for the sake of comparison, are the results for the cases of 30% chord suction-side and 10% chord pressure-side injections of Jaguar at $V_j/V_\infty = .3$ rate and $\alpha = 3.25°$. As expected, the changes in camber for the case of pressure-side injection are negative (corresponding to the observed <u>decrease</u> in lift). It is interesting to note that for the case of thirty-percent-chord injection, substantial changes in camber begin somewhat ahead of the point of injection.

The sample calculations discussed above illustrate that the changes, due to injection, in the camber corresponding to the observed changes in the pressure distribution, lift and drag are

quite complex. Thus, even when the effects of polymer injection are viewed in terms of the changes in the "effective" shape of the hydrofoil, no straightforward phenomenological explanation suggests itself. However, the observed changes in pressure distribution and the corresponding calculated changes in camber are consistent with those that can be expected from a complex interaction of the injected flow with the boundary layer and the external pressure gradient.

IV.2 Correlations of Lift and Drag Data

As already pointed out, the fact that under otherwise identical conditions different polymers lead to different lift and drag effects implies that viscoelastic effects may be responsible, at least in part, for the observed behavior. Based on similar correlations that exist in Pitot tube data for dilute polymer flows, Fruman and Tulin[19] have suggested that the lift and drag effects should be correlatable in terms of a nondimensional parameter formed by dividing the relaxation length $V_i\tau$ by a characteristic geometric length scale in the problem, where V_i is the polymer injection velocity and τ is the relaxation time. Such a correlation is shown in Figure 17, where all of the lift data are shown plotted against the parameter $(V_i\tau/c)$, with c being the hydrofoil chord.

Note that the ordinates in Figure 17 represent the difference in the lift changes between polymer and water injections; this is a logical way of correlating the data since the relaxation time corresponding to water injection is zero and since for small values of the abscissa, the ordinate can be expected to tend to zero.

While there is considerable data scatter in Figure 17, it is nevertheless clear that the correlation is a valid one since all of the different curves shown have essentially the same shape. It is relevant to note that each of the curves given in Figure 17 not only correlates the cases for the different polymer injections, but also the different injection velocities. The correlations also show that, in general, at a fixed value of the abscissa larger hydrofoil angles display larger lift changes, and that the effects are somewhat smaller for the 30% chord injection than for the 10% chord injection.

The data show that for either injection position the maximum lift effects occur when the value of the abscissa is between 0.03 and 0.04, with suction-side injection giving a lift increase and

pressure-side injection a lift decrease. As the value of the abscissa increases beyond this critical value, the absolute magnitude of the lift effect decreases, and the sign of the effect actually reverses beyond a certain value of the abscissa. Thus, the correlation seems to offer an empirical explanation as to why and how the exception to the rule that "suction-side injection increases lift and pressure-side injection reduces lift" arises.

It was mentioned earlier that Fruman, Tulin and Liu[7] were able to successfully correlate the observed changes in lift for different free-stream velocities by plotting the observed lift force against the local velocity at the injection slit. Thus it is logical to attempt to correlate the data in the present case by normalizing the observed lift changes not by the free-stream velocity, but by the local velocity at the location of the injection slit. Such a correlation is shown in Figure 18. Again, while there is considerable data scatter, the trends in the data are readily apparent. It is noteworthy that all of the four curves shown have similar shapes. The feature that, in general, the 30%-chord injection yields smaller lift effects than the 10%-chord injection, may be related to the fact that in the former case less of the hydrofoil surface is affected by the injection. However, a further correlation of the data to account for the the injection position is not readily apparent.

A correlation for the relative drag change due to injection, similar to that shown in Figure 17 for lift, is shown in Figure 19 in terms of the parameter $V_i \tau/c$. The shape of the curves are seen to be the same as those for the lift effect, with the occurrence of the maximum drag reduction coinciding with the maximum lift reduction for pressure-side injection, and the occurrence of the minimum drag reduction (or maximum drag increase) coinciding with the maximum lift increase for suction-side injection.

The changes in drag due to injection can be resolved into two components, namely, those due to changes in the pressure and frictional parts of the total drag of the hydrofoil. The change in the pressure drag can be computed from the measured changes in the pressure distribution and from the known shape of the hydrofoil by taking the component of the local pressure force in the direction of the free stream. The change in the friction drag can then be deduced by subtracting the calculated pressure drag change from the measured change in the total drag.

A resolution of the drag components is shown in Figure 20 for the case of Polyox injection at ten percent of free-stream velocity. It can be seen that for the lower injection velocity the pressure drag actually increases both for suction-side and pressure-side injections at all values of the angle of attack. The decrease in skin-friction drag seems to be nearly the same for injections on either side of the hydrofoil and for all angles of attack. It is interesting to note that the fact that the total drag reduction for suction-side injection at 5° is small (see Figure 3) is because the increase in pressure drag nearly offsets the reduction in skin-friction drag.

For injection at the 30%-chord location, the change in pressure drag is negative at small angles of attack for injection on either side of the foil, though it becomes positive at larger angles of attack. The reduction in skin-friction drag in this case is somewhat smaller than that in the 10%-chord injection case, consistent with the fact that a smaller fraction of the hydrofoil surface area is affected in this case.

Figures 19 and 20 also illustrate that the drag and lift effects are closely related. Indeed, if the pressure drag component alone is correlated with $(V_1\tau/c)$, it is clear that correlations of the type shown in Figures 17 and 18 must result.

V. CONCLUDING REMARKS

As is evident from the discussion given in the previous sections, the effects of polymer injections on lifting surfaces involve fairly complex phenomena. While the actual magnitude of the lift changes are in themselves not large, it is nevertheless necessary to seek a rational explanation for the observed behavior of the lift-drag ratio before the use of polymer additives to enhance the performance of propellers and hydrofoil craft can become a reality.

In the present study, the observed lift effects were viewed as arising from two separate steps of interaction of the injected flow with the flow about the hydrofoil. In the first step the injected flow was assumed to interact with the boundary layer and the external pressure gradient in some (as yet) unspecified manner and change the "effective" shape of the hydrofoil. This step of the interaction is undoubtedly dependent on the viscoelastic characteristics of the injected polymer since under otherwise identical conditions, different polymers give considerably different results; a detailed consideration of this interaction was outside the scope of the present study.

In the second step of the interaction, the changed "effective" hydrofoil shape was assumed to produce changes in the pressure and velocity distributions on the hydrofoil. It was also assumed that the latter changes can be calculated utilizing potential theory without any further considerations of the viscoelastic effects. In terms of the ability to theoretically predict the exact nature of the lift and pressure changes that can occur due to injection, solution of the first step is a necessary prerequisite to the utilization of the second step, and this was outside the scope of the present study. However, the measured pressure distributions

as well as the observed lift and drag changes can be used along with potential theory to calculate the "effective" hydrofoil shape that would produce the type of changes measured. In turn, the effective shape can be examined to see if it is compatible with what can be expected based on plausible hypotheses of interactions between the injected flow and the boundary layer as well as the external pressure gradient, without having to consider the details of the interactions themselves. This is the approach that was utilized in the present study.

Analysis of the types of interactions that can take place between the injected flow and the external flow around the hydrofoil indicates that four different types of changes in the pressure distribution can occur. These are: a change in the effective angle of attack due to a change in the boundary-layer displacement thickness on the side on which the injection is made; a change in the effective camber of the hydrofoil due to a change in the boundary-layer displacement thickness; a change in the circulation due to a change in the trailing-edge condition requiring that the velocities at the edges of the top and bottom boundary layers at the trailing edge must be the same; and, a change in the effective thickness distribution of the hydrofoil.

The qualitative features of the observed pressure distributions as well as the lift and drag changes are compatible with the types of interaction described above. Calculations carried out using potential theory to determine the "effective" shape of the hydrofoil that produces the observed changes are also compatible with the types of interaction described. However, lacking a specific theory for the interactions themselves, the explanation offered herein has to be regarded as tentative only. On the other hand, the following points support the present explanation, and these have to be taken into account in the development of any alternative explanations.

(i) Even though in many cases polymer injection on the suction side of the hydrofoil produces a lift increase and that on the pressure side a lift decrease, this is not always the case. In general, for injection on either side of the hydrofoil the lift can increase or decrease depending on the polymer, the injection velocity, the location of the injection, and the angle of attack.

(ii) Both polymer and water injections produce peaks (of opposite signs) in the pressure distribution on the side on which the injection is made. These peaks do not occur immediately downstream of the injection slit, but occur near the location of the maximum hydrofoil thickness for all cases.

(iii) Pressure distributions in the absence of injection indicate the presence of boundary-layer effect on the circulation around the hydrofoil.

REFERENCES

1. Wu, Jin, "Lift Reduction in Additive Solutions," Journal of Hydronautics, Vol. 3, #5, pp. 198-200, October 1969.

2. Kowalsky, T., "Effect of Polymer Additives on Propeller Performance," J. Hydronautics, Vol. 5, No. 1, January 1971.

3. Wolff, J. H., and Cahn, R. D., "Lifting Surfaces in Polymer Solutions," NSRDC Report 3653, May 1971.

4. Lehman, A. F., and Suessmann, R. T., "An Experimental Study of the Lift and Drag of a Hydrofoil with Polymer Ejection," Report No. 72-94, Oceanics, Incorporated, November 1972.

5. Sarpkaya, T., "On the Performance of Hydrofoils in Dilute Polyox Solutions," Proceedings of the International Conference on Drag Reduction, BHRA Fluid Engineering, Cranfield, England, Paper E1, September 1974.

6. Fruman, D. H., Sundaram, T. R., and Daugard, S. J., "Effect of Drag Reducing Polymer Injection on the Lift and Drag of a Two-Dimensional Hydrofoil," Proceedings of the International Conference on Drag Reduction, BHRA Fluid Engineering, Cranfield, England, Paper E2, September 1974.

7. Fruman, D. H., Tulin, M. P., and Liu, H-L., "Lift, Drag and Pressure Distribution Effects Accompanying Drag-Reducing Polymer Injection on Two-Dimensional Hydrofoil," HYDRONAUTICS, Incorporated Technical Report 7101-5, October 1975.

8. Simmarwalla, A. M., and Sundaram, T. R., "Lift and Drag Effects Due to Polymer Injections on the Surface of Symmetric Hydrofoils," HYDRONAUTICS, Incorporated Technical Report 7003-1, October 1970.

9. Abbott, I. H., von Doenhoff, A. E., and Stivers, L. S., "NACA Wartime Report," ACR Number L5C05, March 1945.

10. Preston, J. H., "The Approximate Calculation of the Lift of Symmetrical Aerofoils Taking Account of the Boundary Layer, with Application to Control Problems," R. & M. No. 1996, Aeronautical Research Council, London, 1943.

11. Preston, J. H., "The Calculation of Lift Taking Account of Boundary Layer," R. & M. No. 2725, Aeronautical Research Council, London, 1946.

12. Sundaram, T. R., "The Calculation of the Pressure Distribution Over the Surface of a Two-Dimensional Wing Taking Account of the Boundary Layer," Master's Thesis, The Indian Institute of Science, Bangalore, India, 1960.

13. Spence, D. A., "Predictions of the Characteristics of Two-Dimensional Airfoils," J. of Aeronautical Sciences, Vol. 21, No. 9, p. 577, September 1954.

14. Abbot, I. H. and von Doenhoff, A. E., Theory of Wing Sections, Dover Publications, New York, N. Y., 1960.

15. Weber, J., "The Calculation of the Pressure Distribution over the Surface of Two-dimensional and Swept Wings with Symmetrical Aerofoil Sections," R. & M. No. 2918, Aeronautical Research Council, London, 1956.

16. Weber, J., "The Calculation of the Pressure Distribution on the Surface of Thick Cambered Wings and the Design of Wings with Given Pressure Distribution, R. & M. No. 3026, Aeronautical Research Council, London, 1957.

17. Thwaites, B., Incompressible Aerodynamics, Oxford at the Clarendon Press, 1960.

18. Kuethe, A. M., and Schetzer, J. D., Foundation of Aerodynamics, John Wiley and Sons, Inc., New York, N. Y. 1959.

19. Fruman, D. H. and Tulin, M. P., "Effects of Additive Ejection on Lifting Hydrofoils," ASME Paper No. 77-FE-27, 1977.

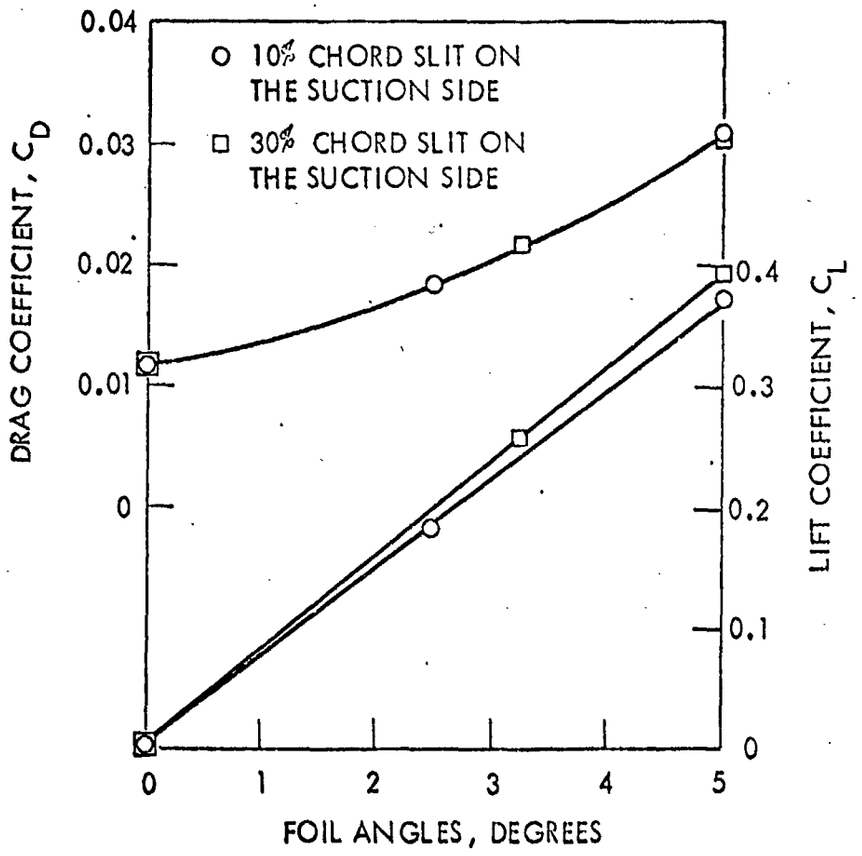

FIGURE 1 - LIFT AND DRAG COEFFICIENTS OF THE HYDROFOIL IN WATER WITHOUT INJECTION

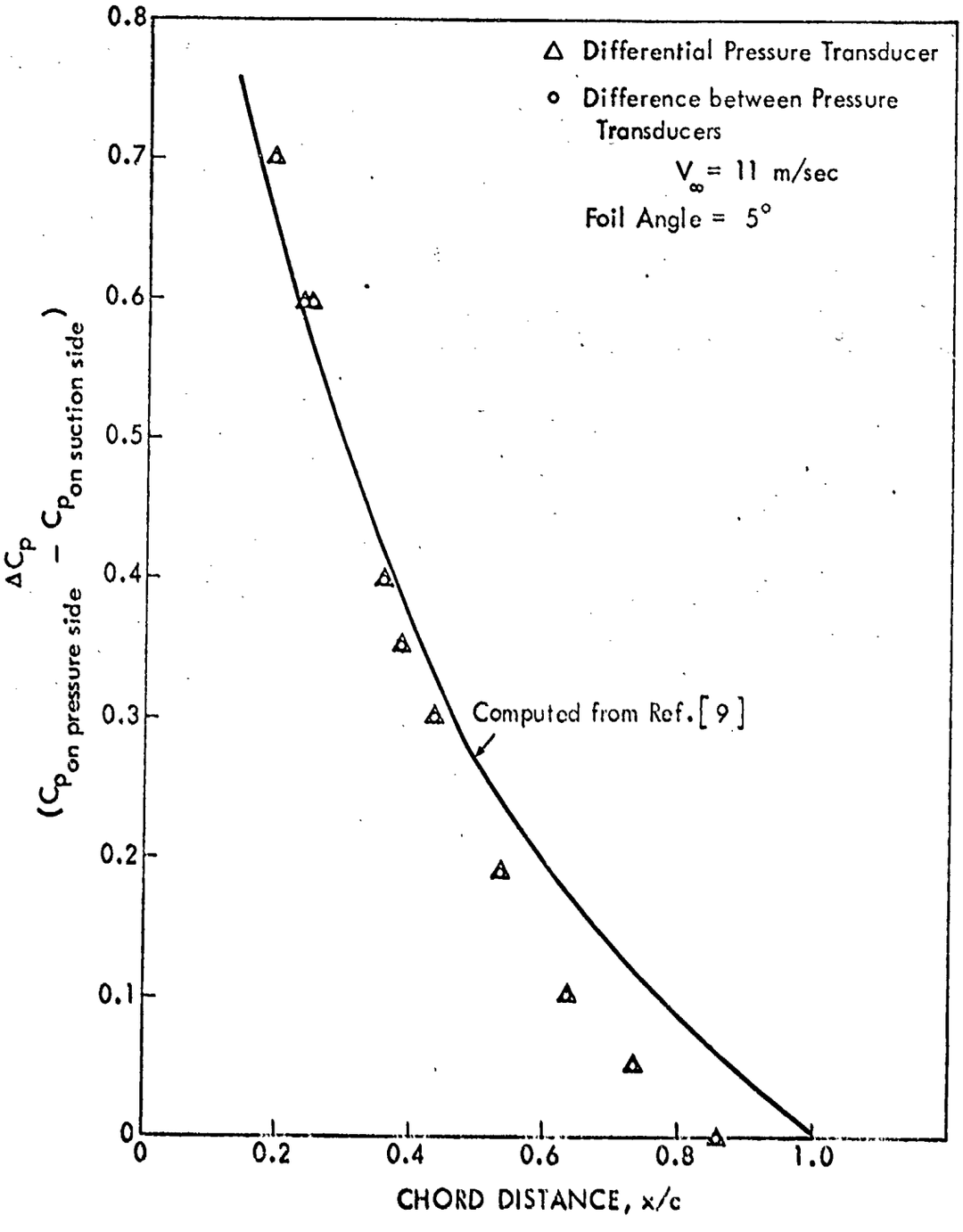

FIGURE 2 - COMPARISON BETWEEN MEASURED ΔCp VALUES AND THE RESULTS OF A THEORETICAL CALCULATION

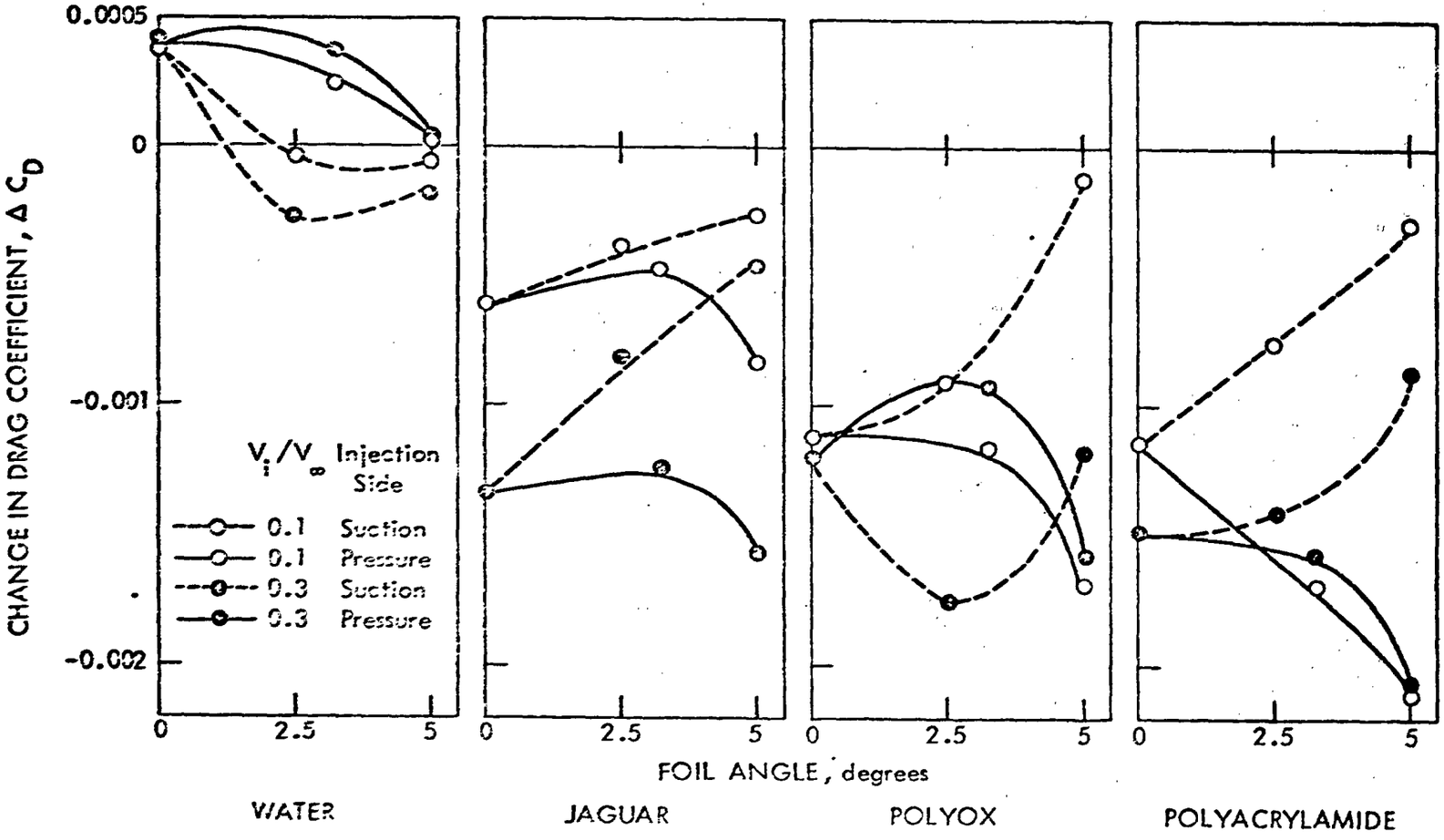

FIGURE 3 - EFFECT OF 10% CHORD INJECTION OF WATER AND POLYMERS ON THE DRAG COEFFICIENT OF THE HYDROFOIL

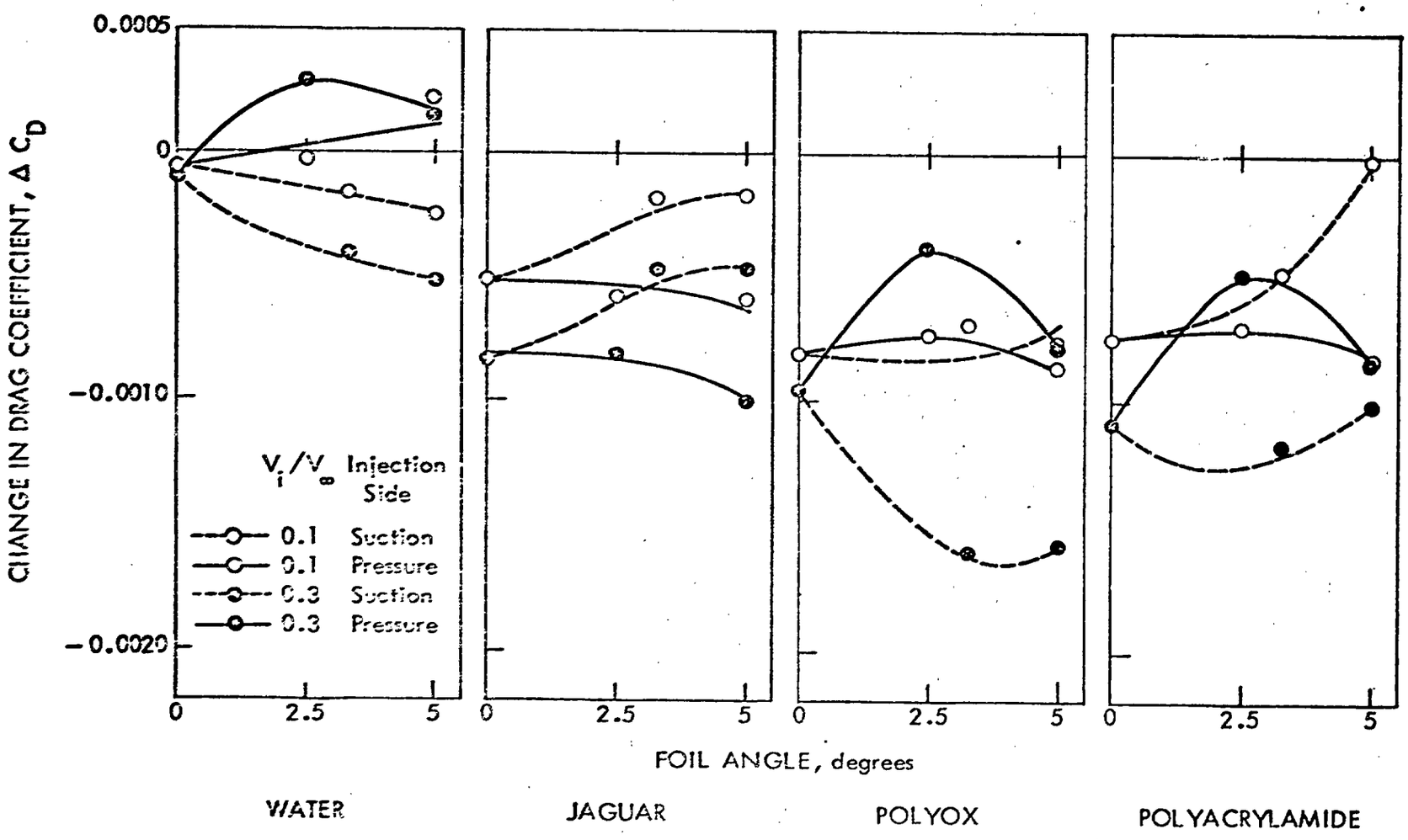

FIGURE 4 - EFFECT OF 30% CHORD INJECTION OF WATER AND POLYMERS ON THE DRAG COEFFICIENT OF THE HYDROFOIL

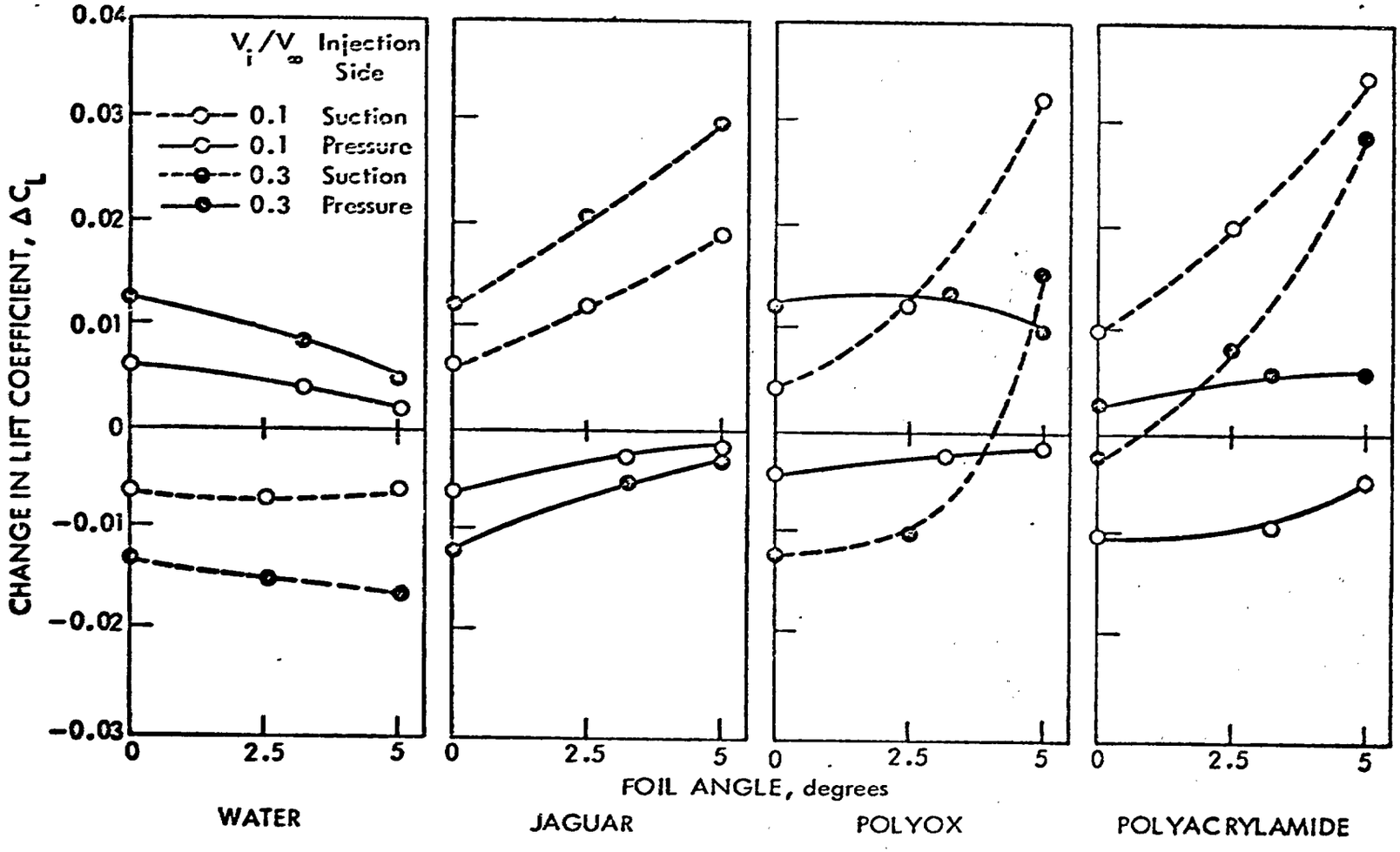

FIGURE 5 - EFFECT OF 10% CHORD INJECTION OF WATER AND POLYMERS ON THE LIFT COEFFICIENT OF THE HYDROFOIL

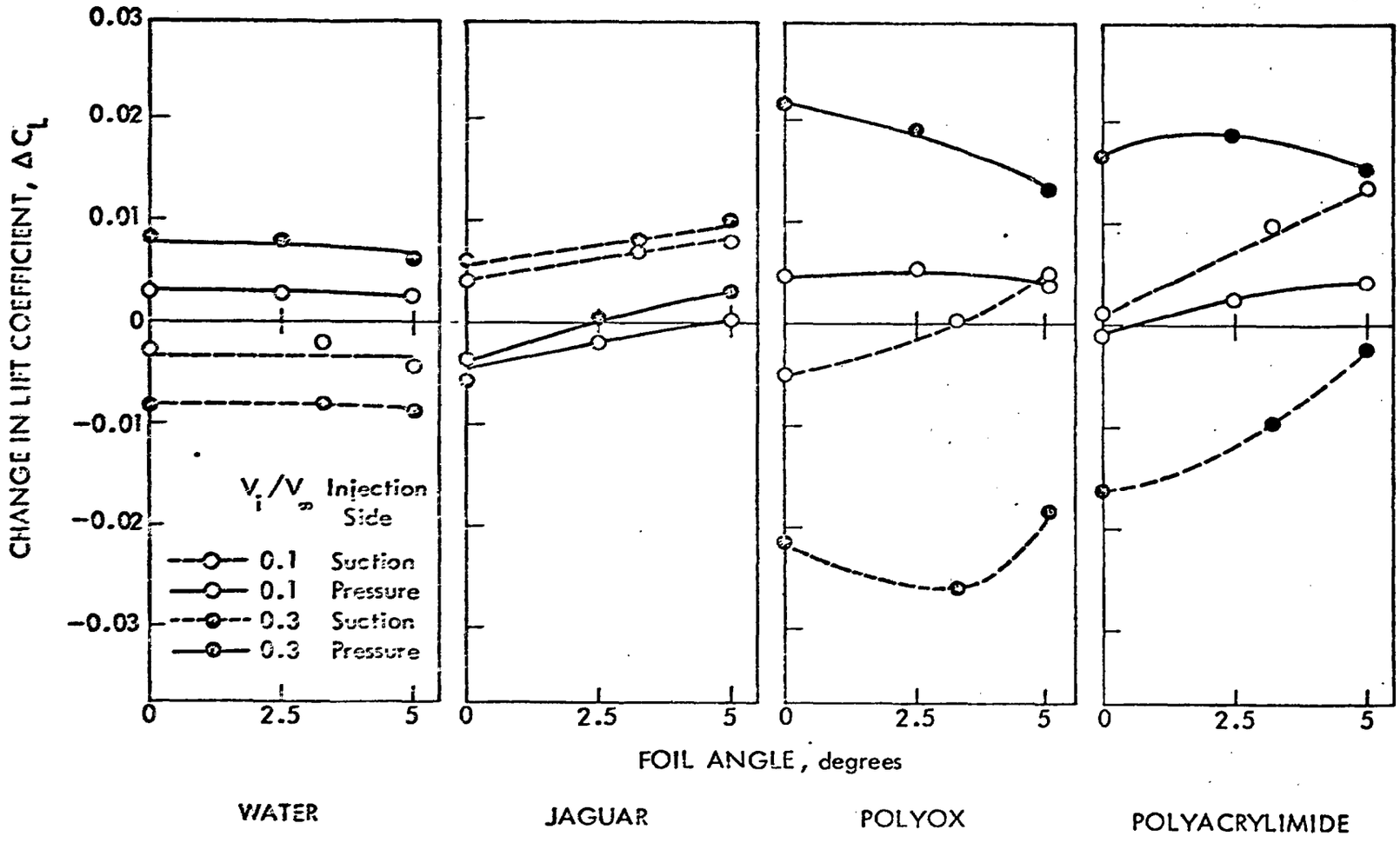

FIGURE 6 - EFFECT OF 30% CHORD INJECTION OF WATER AND POLYMERS ON THE LIFT COEFFICIENT OF THE HYDROFOIL

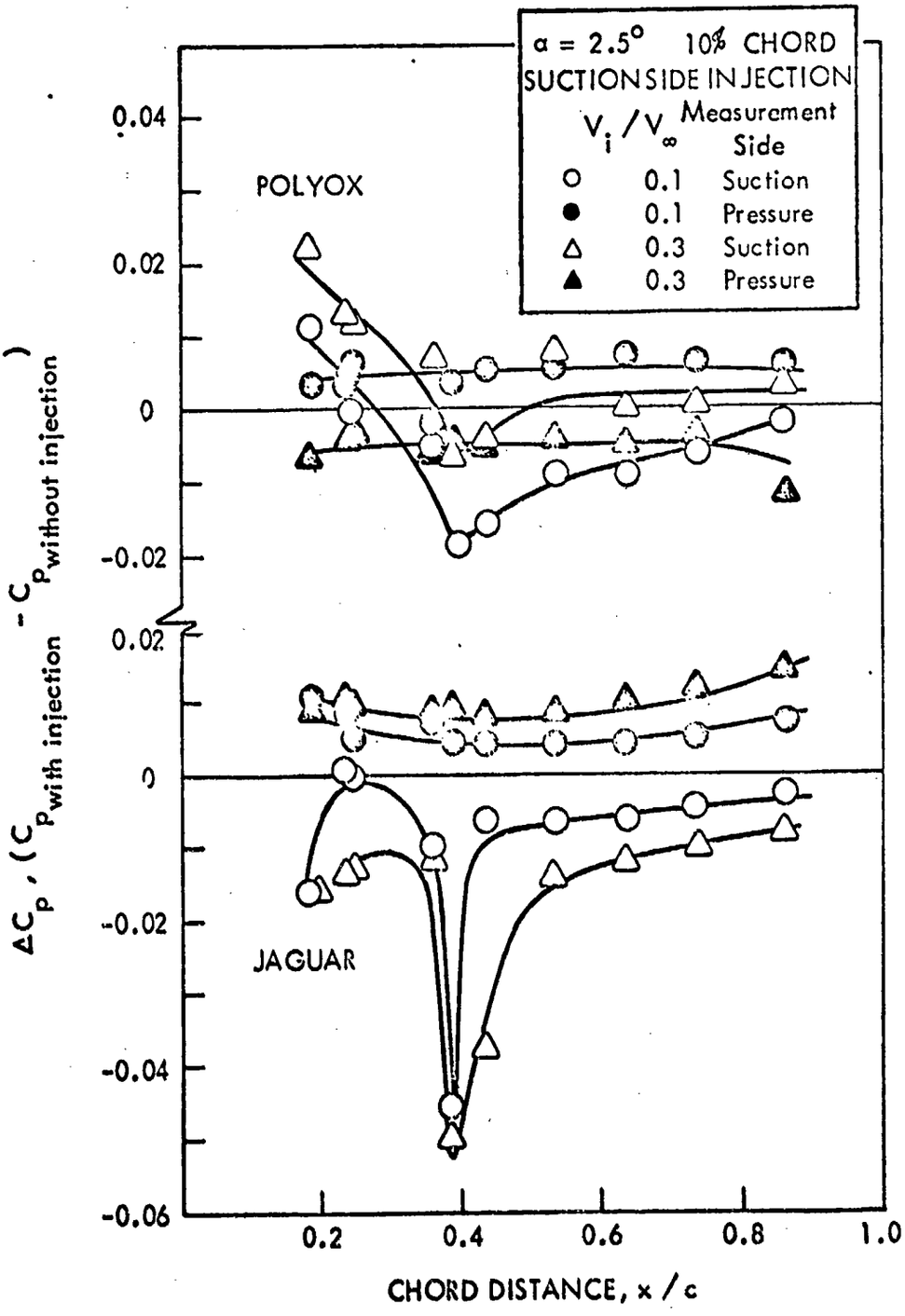

FIGURE 7 - DIFFERENCE IN PRESSURE COEFFICIENT, ΔC_p VERSUS CHORD DISTANCE, x / c

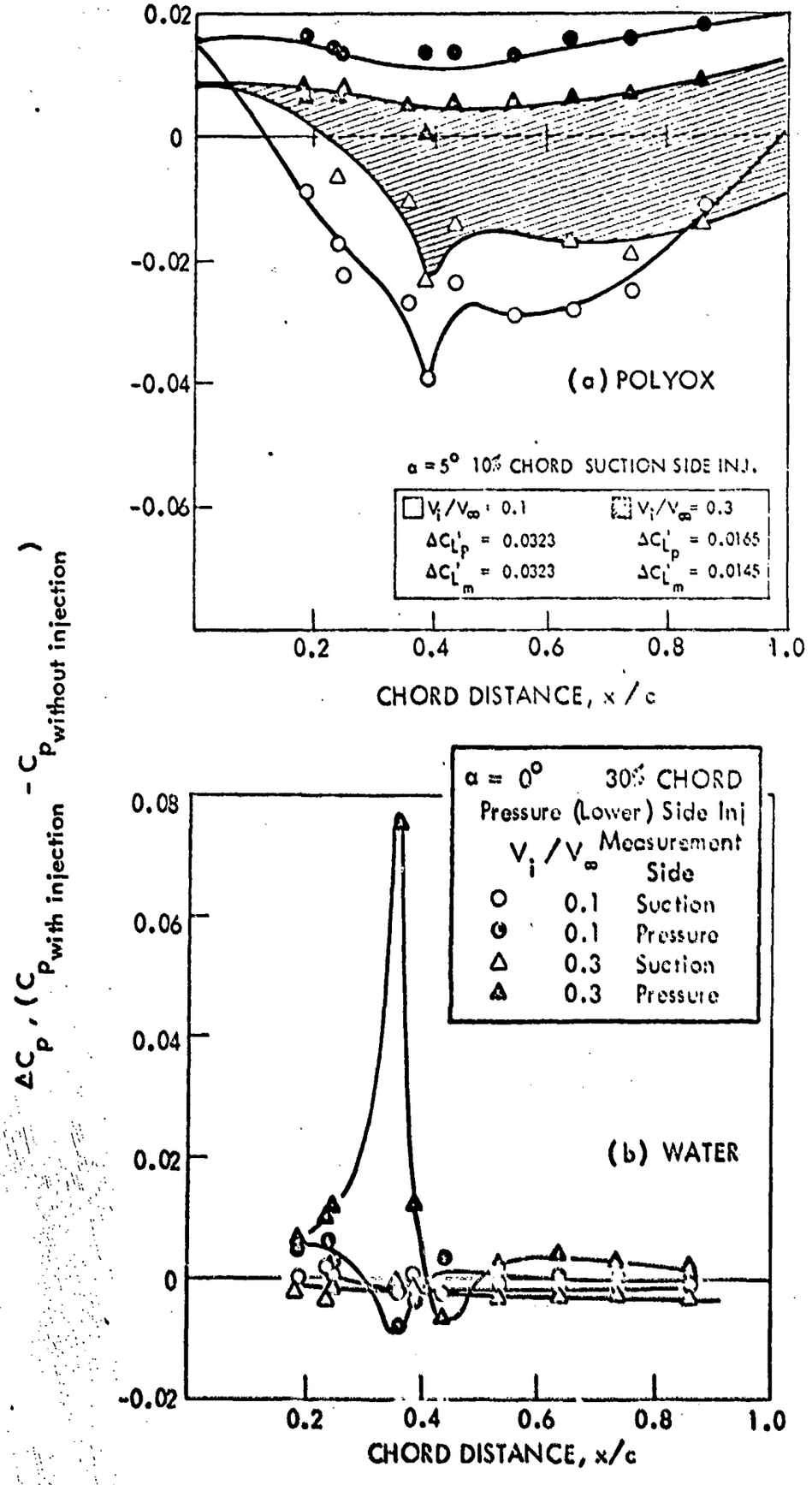

FIGURE 8 - DIFFERENCE IN PRESSURE COEFFICIENT, ΔC_p VERSUS CHORD DISTANCE, x/c

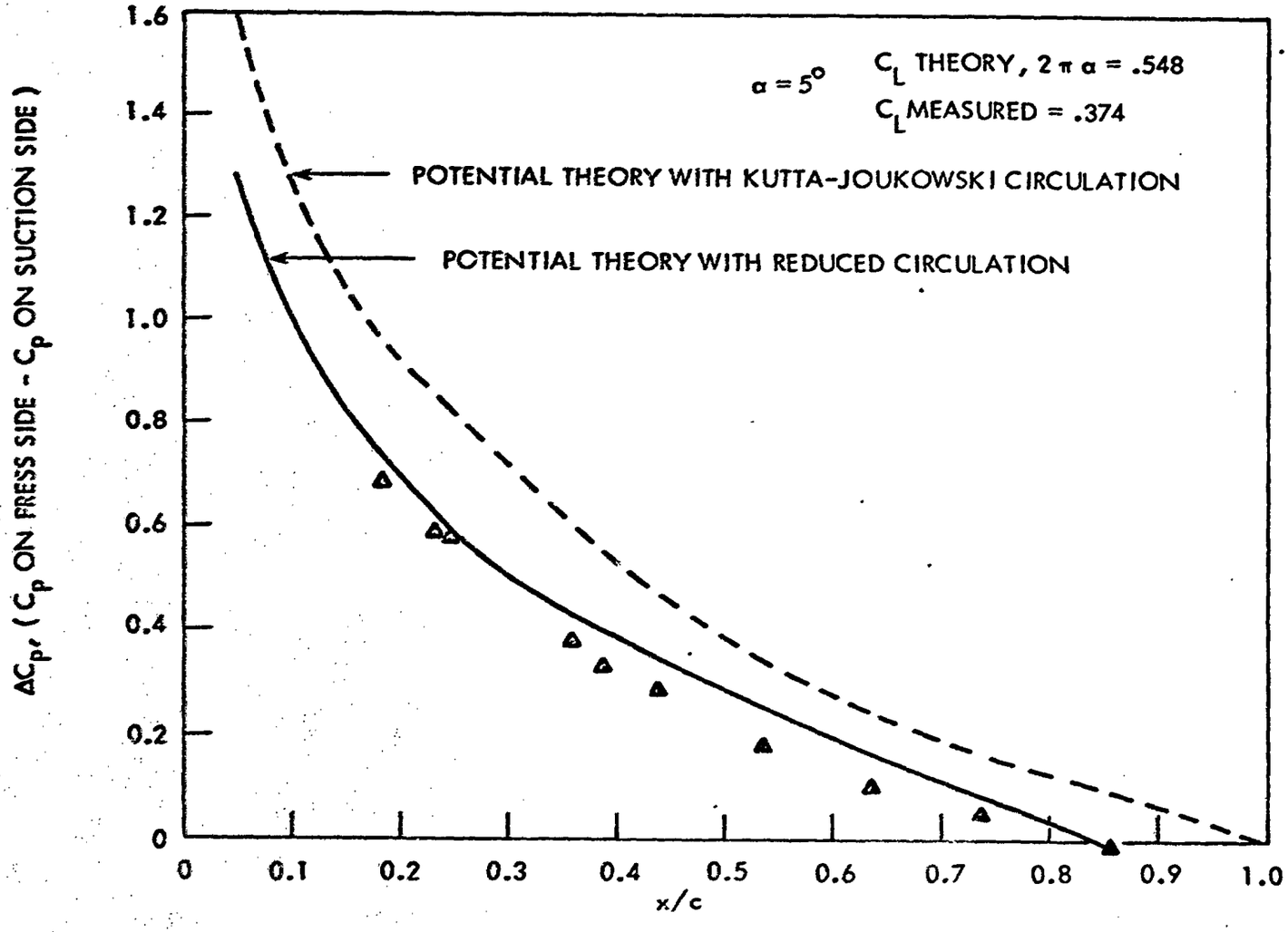

FIGURE 9 - COMPARISON BETWEEN MEASURED AND CALCULATED PRESSURE DISTRIBUTIONS

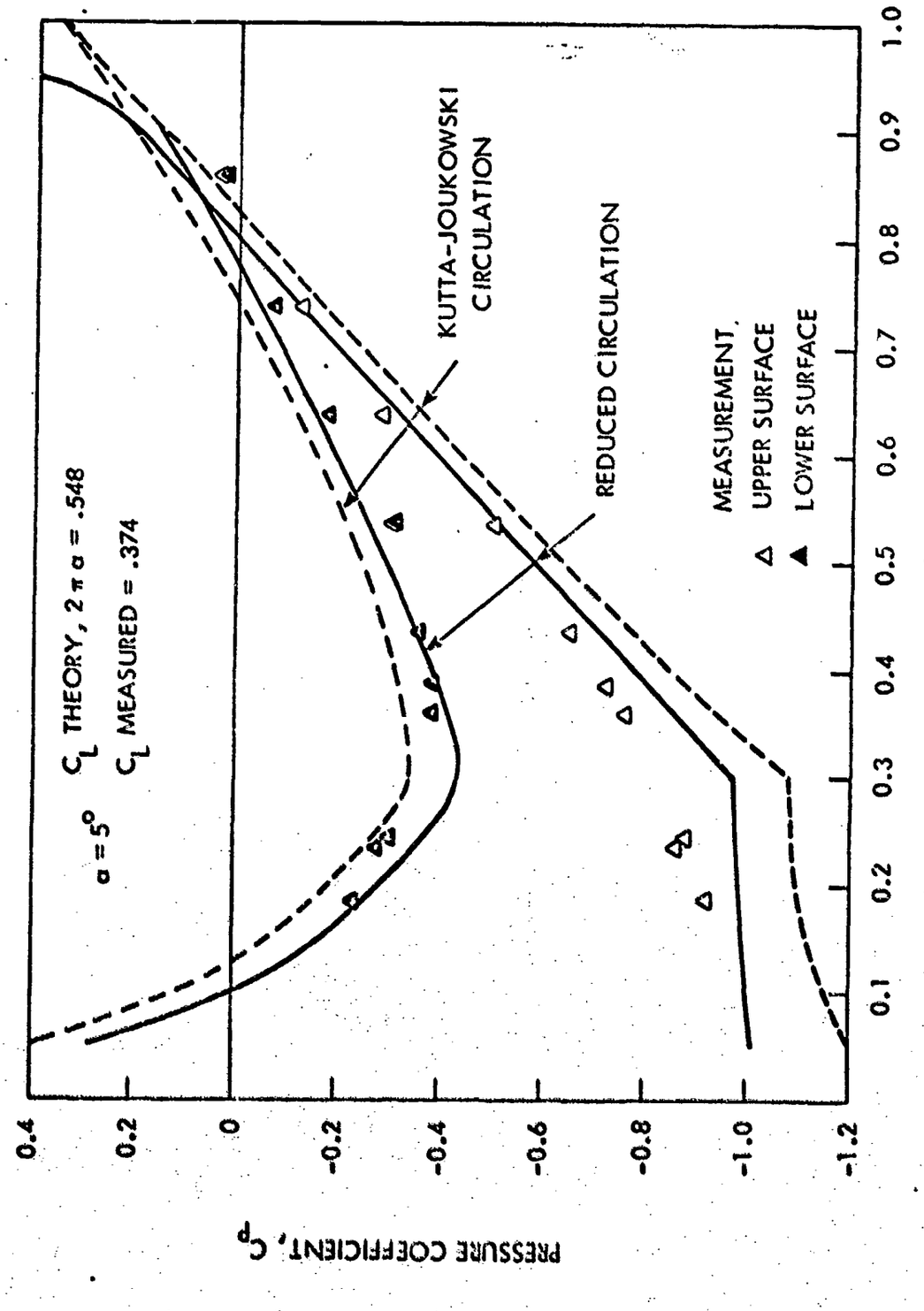

FIGURE 10 - COMPARISION BETWEEN MEASURED AND CALCULATED PRESSURE COEFFICIENTS ON THE UPPER AND LOWER SURFACES

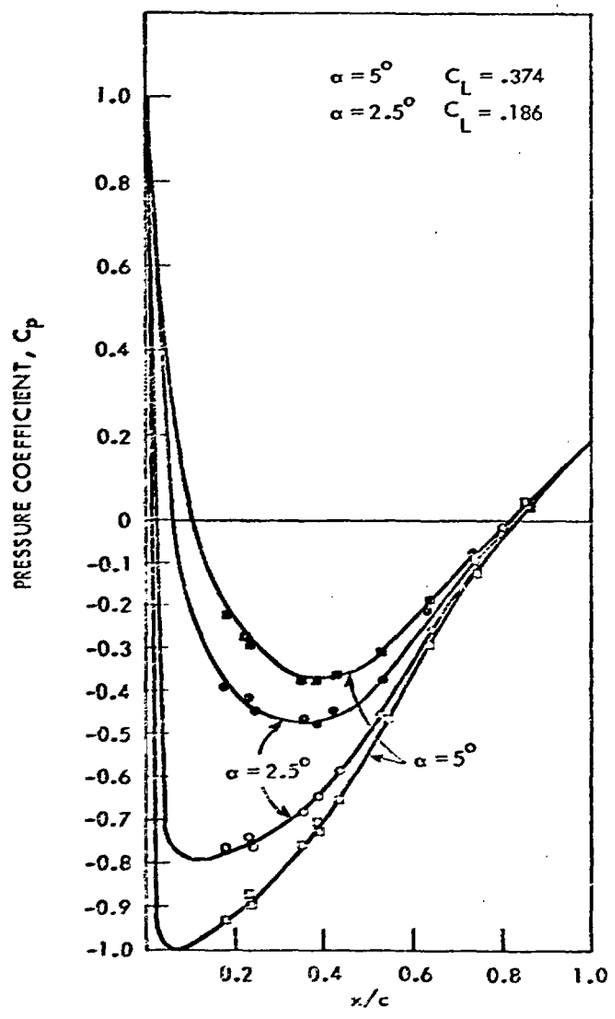

FIGURE 11a - BASIC PRESSURE DISTRIBUTIONS FOR FOIL ANGLES OF 2.5° AND 5°

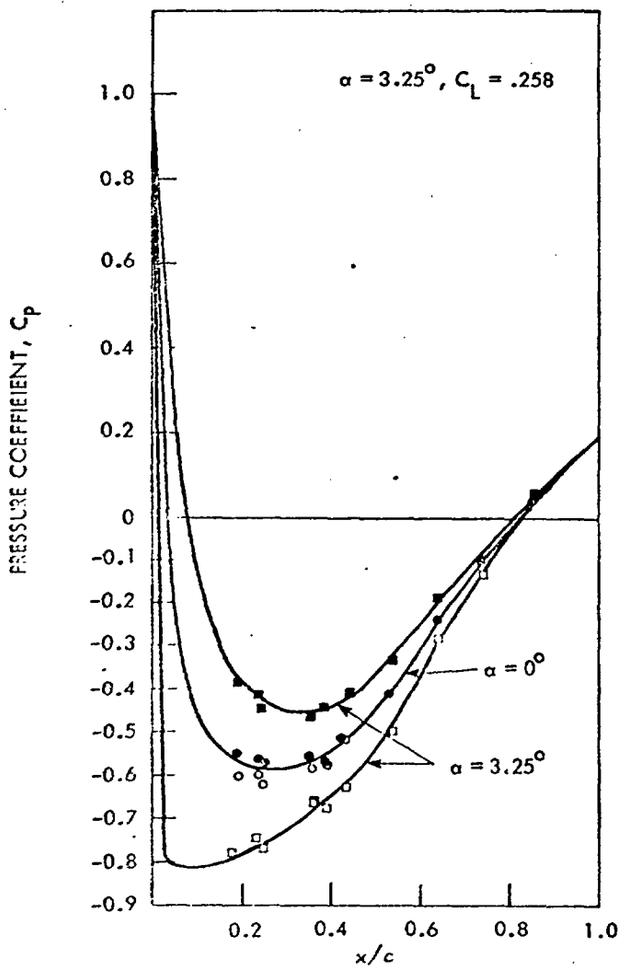

FIGURE 11b - BASIC PRESSURE DISTRIBUTIONS FOR FOIL ANGLES OF 0° AND 3.25°

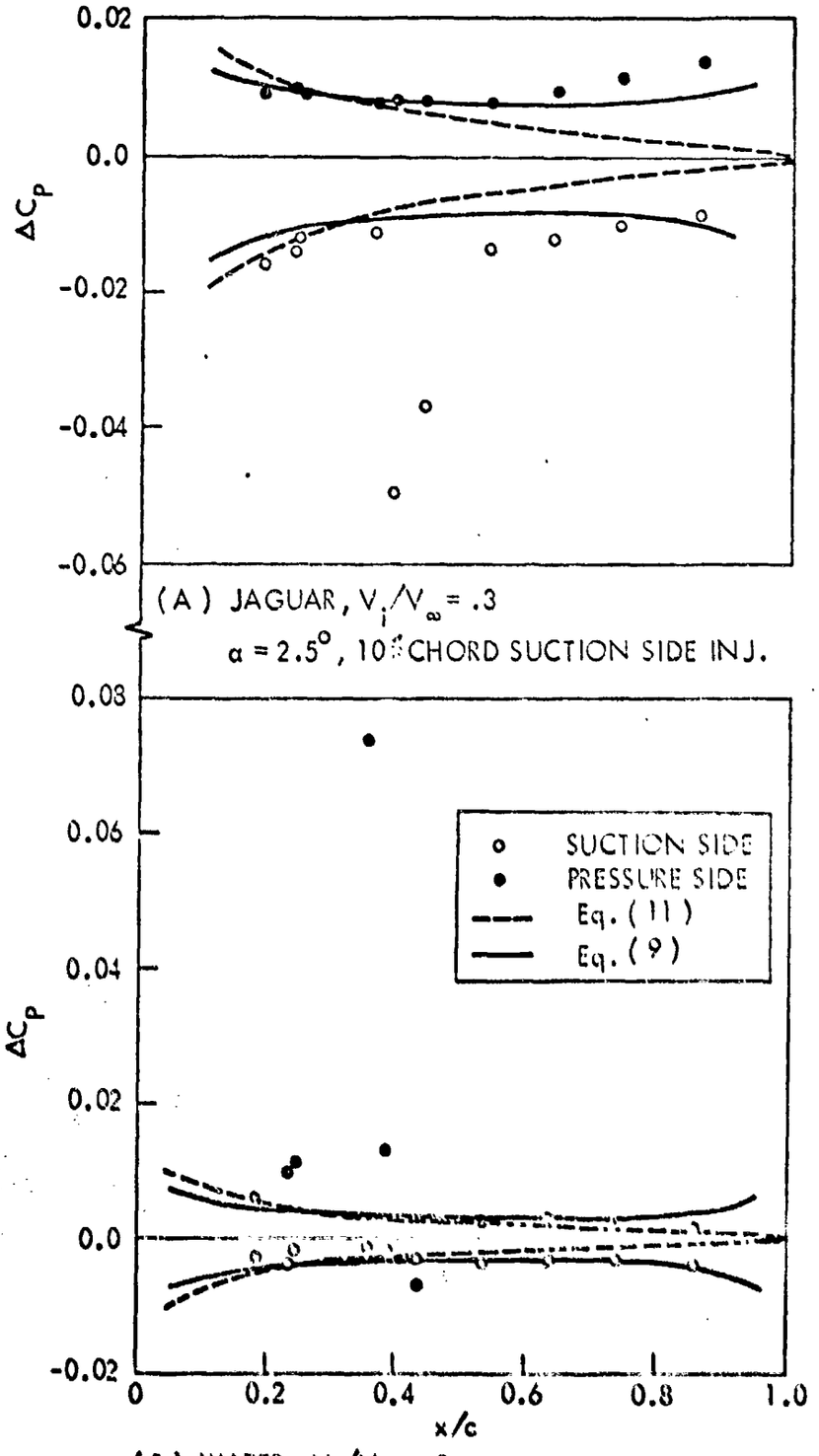

FIGURE 12 - COMPARISON OF MEASURED CHANGES IN PRESSURE WITH THOSE CALCULATED FOR A SYMMETRIC HYDROFOIL

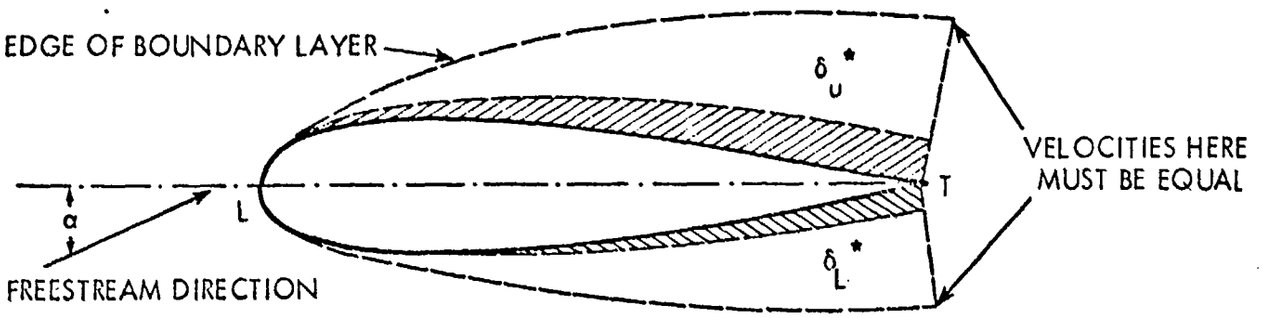

(a) SCHEMATIC OF EFFECT

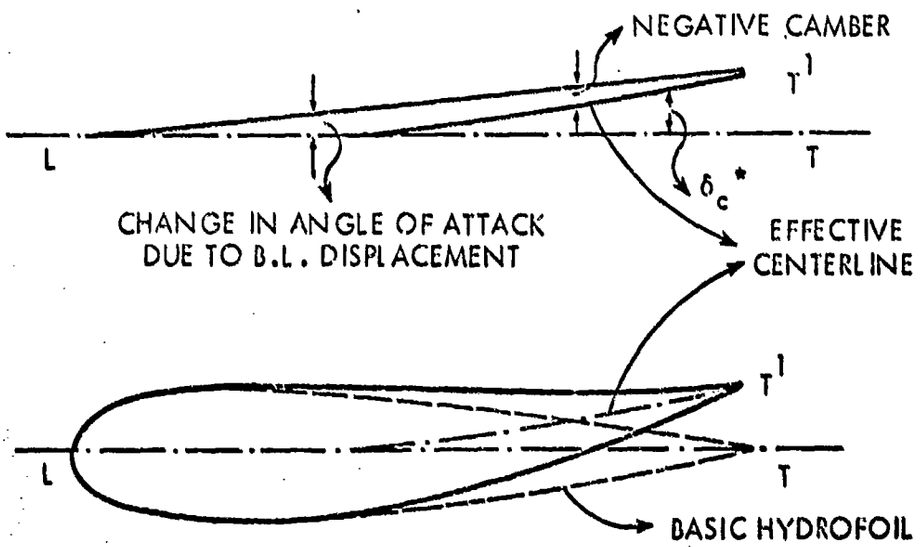

(b) CAMBER EFFECT

FIGURE 13 - BOUNDARY-LAYER DISPLACEMENT EFFECT ON A SYMMETRIC HYDROFOIL

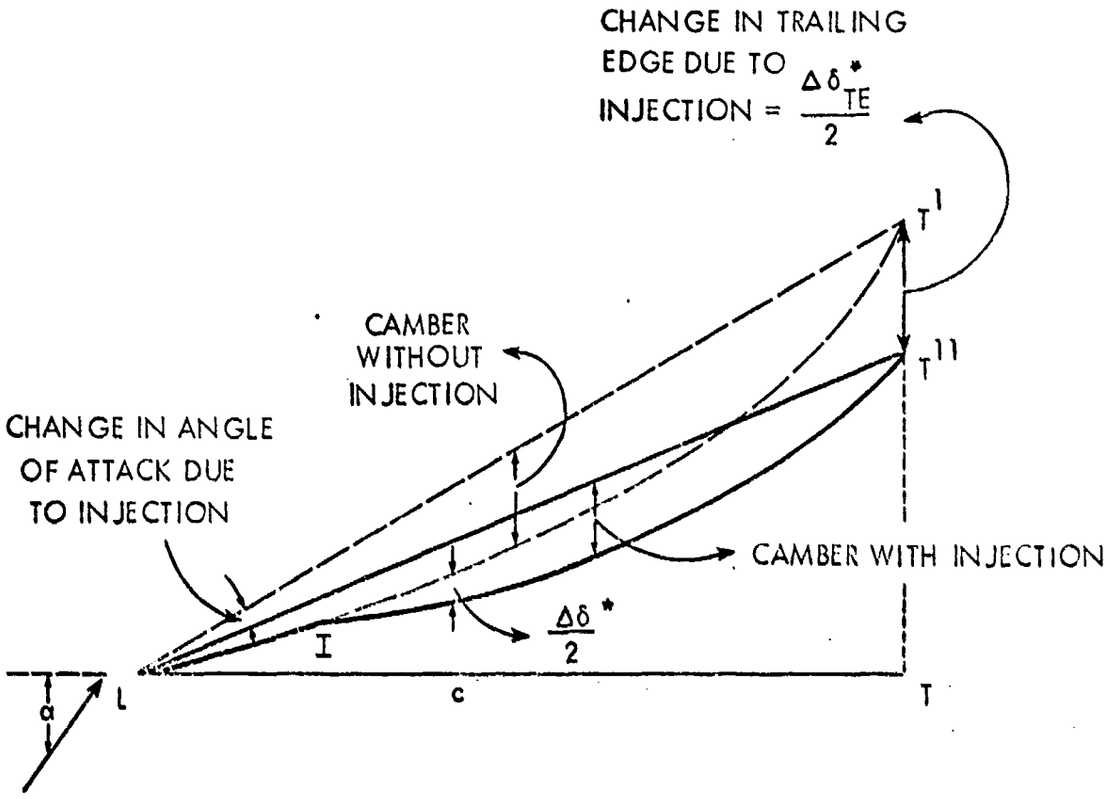

FIGURE 14 - EFFECT OF POLYMER INJECTION ON BOUNDARY LAYER DISPLACEMENT

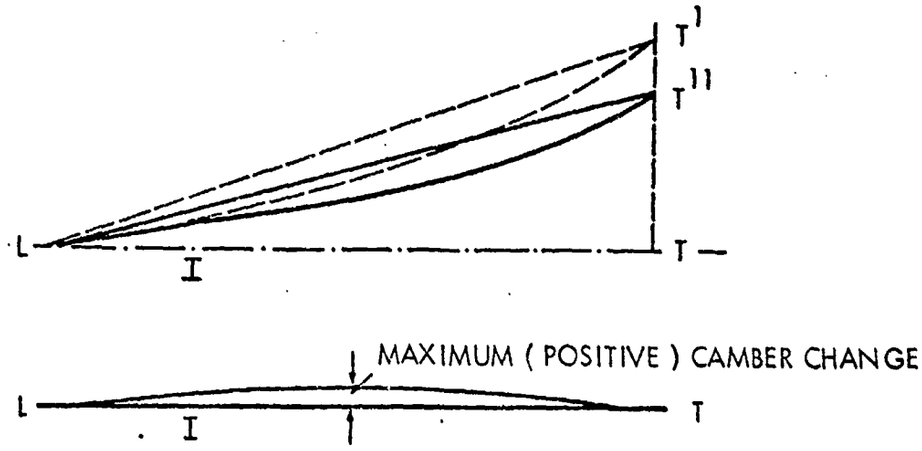

(a) THINNING INCREASES MONOTONICALLY WITH DOWNSTREAM DISTANCE

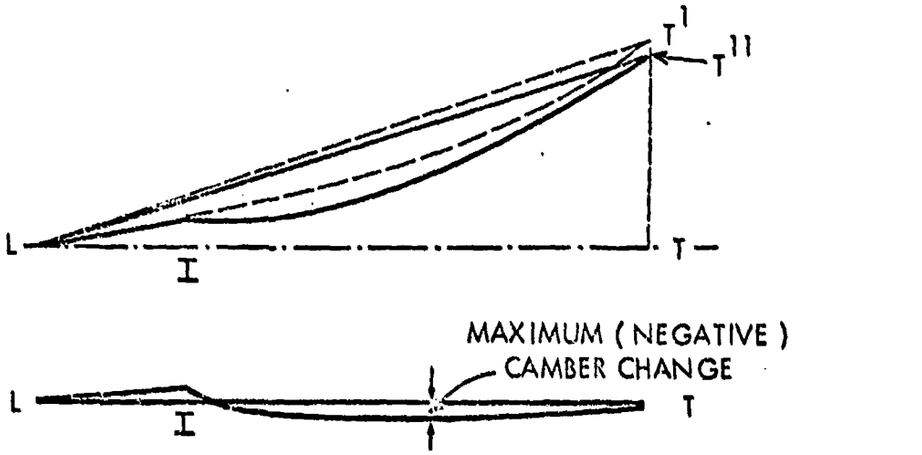

(b) MAXIMUM THINNING OCCURS CLOSE TO POINT OF INJECTION

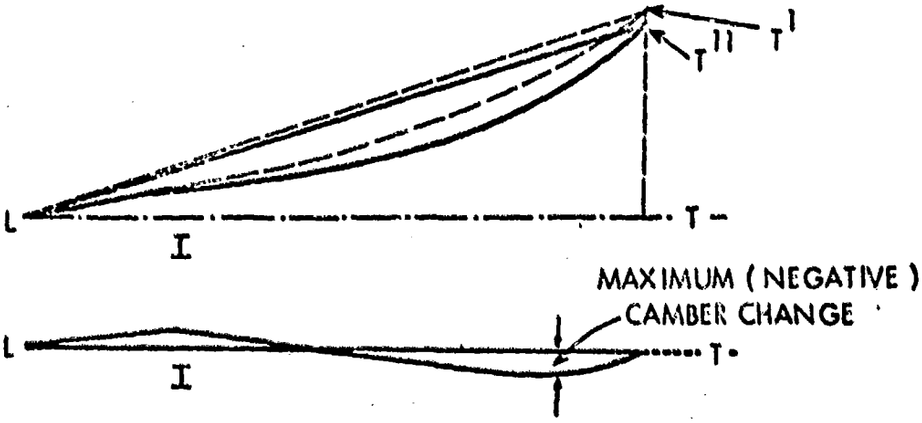

(c) MAXIMUM THINNING OCCURS CLOSE TO, BUT AHEAD OF, TRAILING EDGE

FIGURE 15 - TYPES OF BOUNDARY LAYER INTERACTION

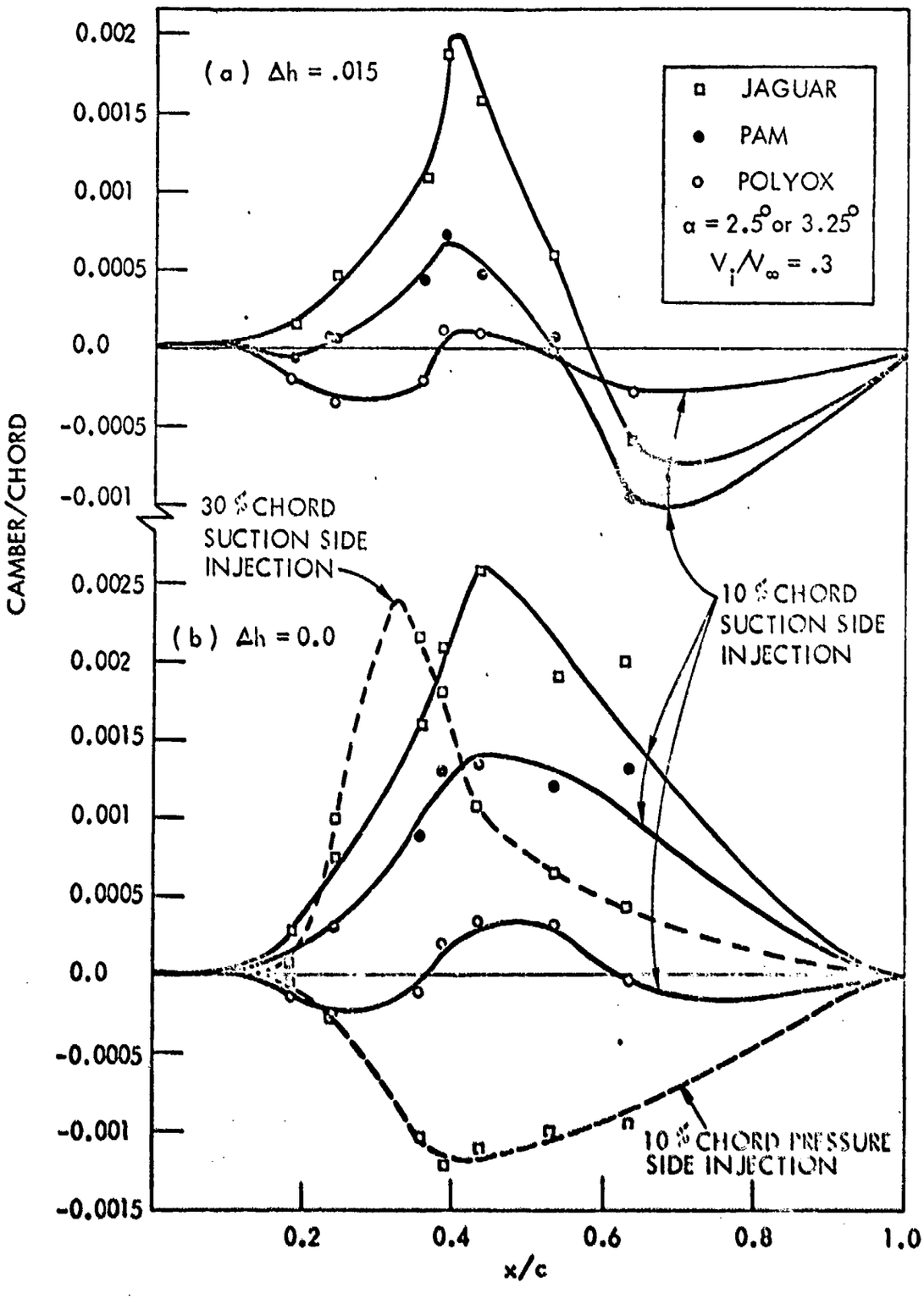

FIGURE 16 - CALCULATED CAMBER DISTRIBUTIONS

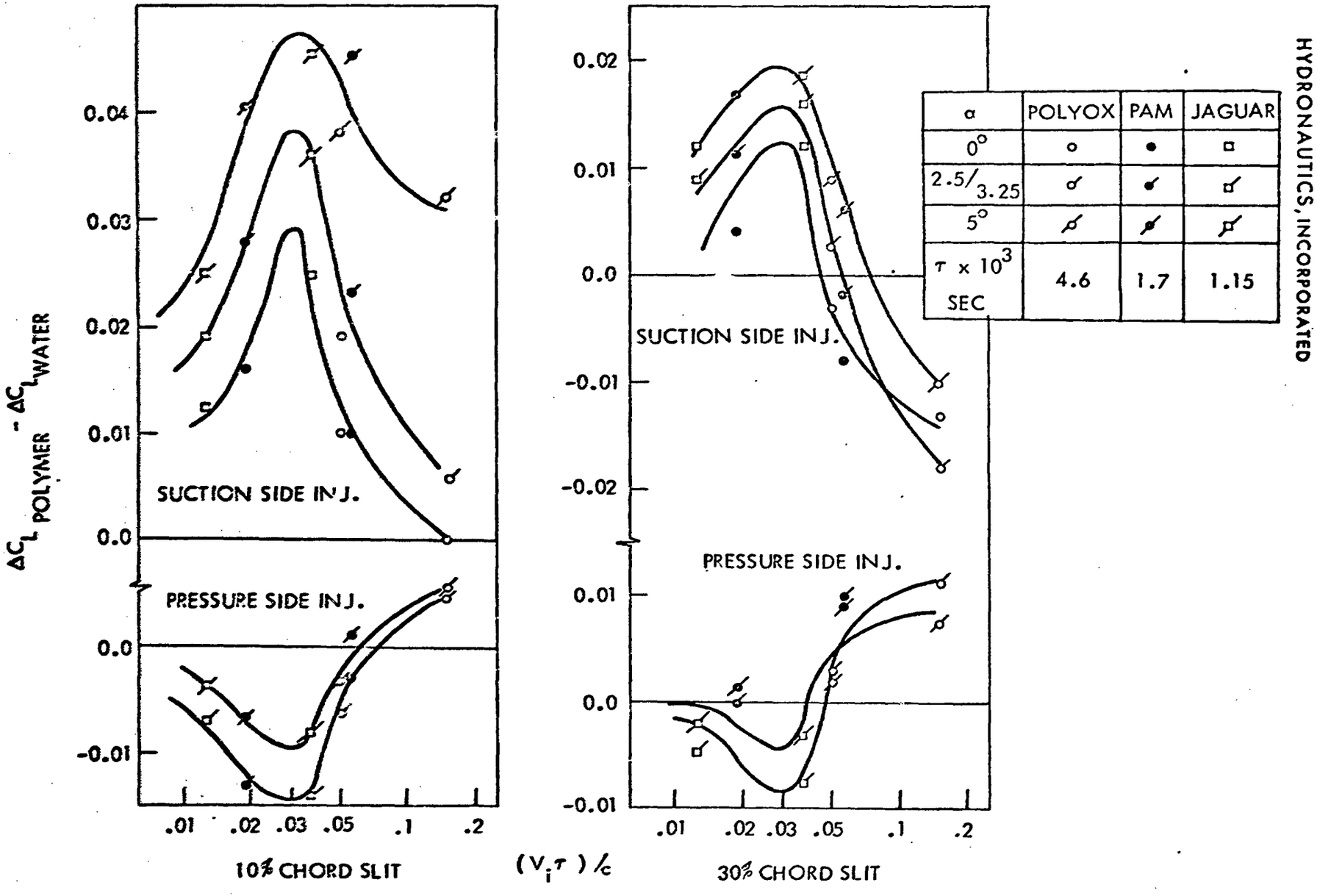

FIGURE 17 - LIFT CHANGE VERSUS $V_i \tau / c$

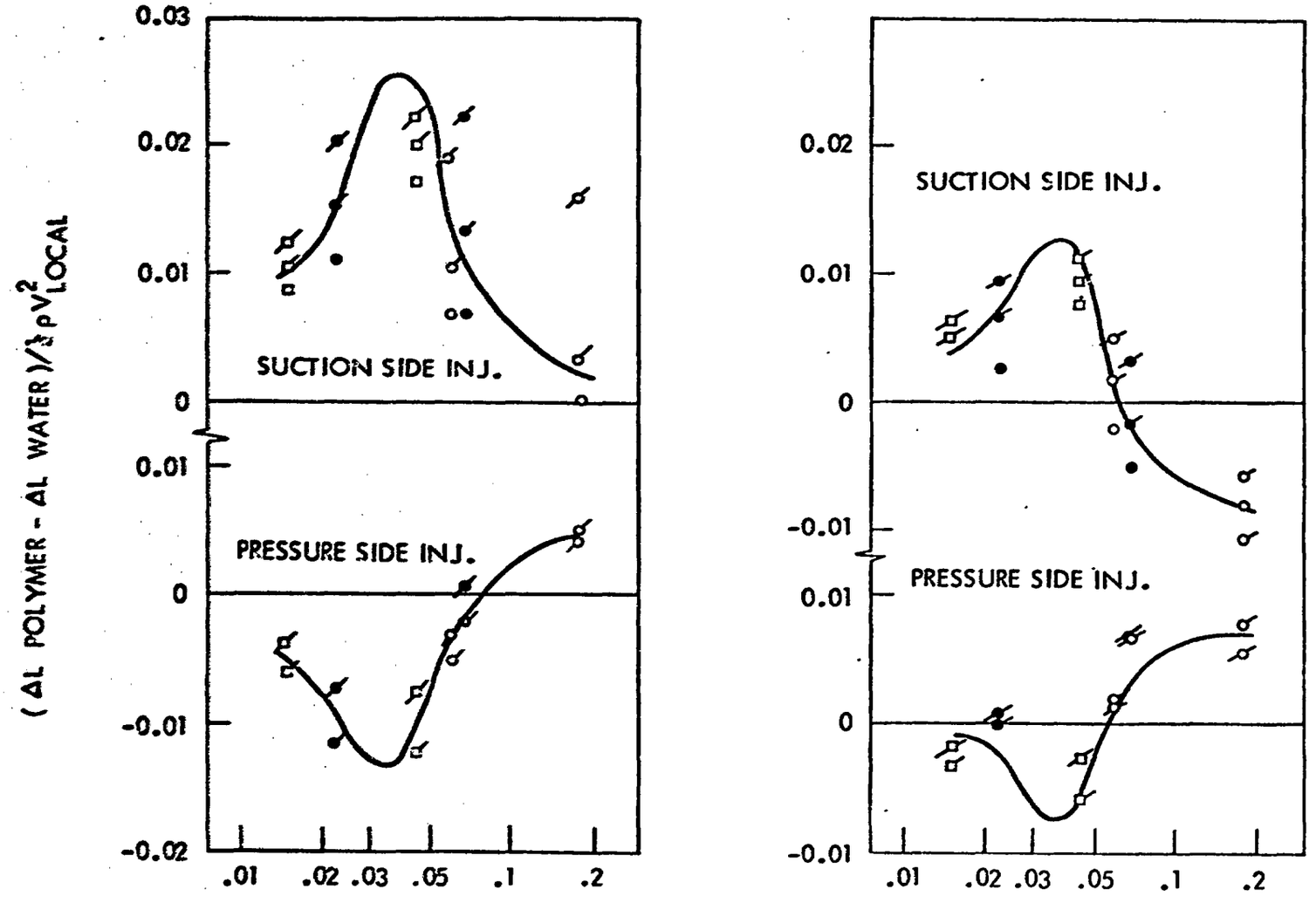

(ΔL POLYMER - ΔL WATER)/½ρV²LOCAL

10 % CHORD SLIT

$(V_i \tau)/c$

30 % CHORD SLIT

FIGURE 18 - LIFT CHANGE VERSUS $V_i \tau / c$

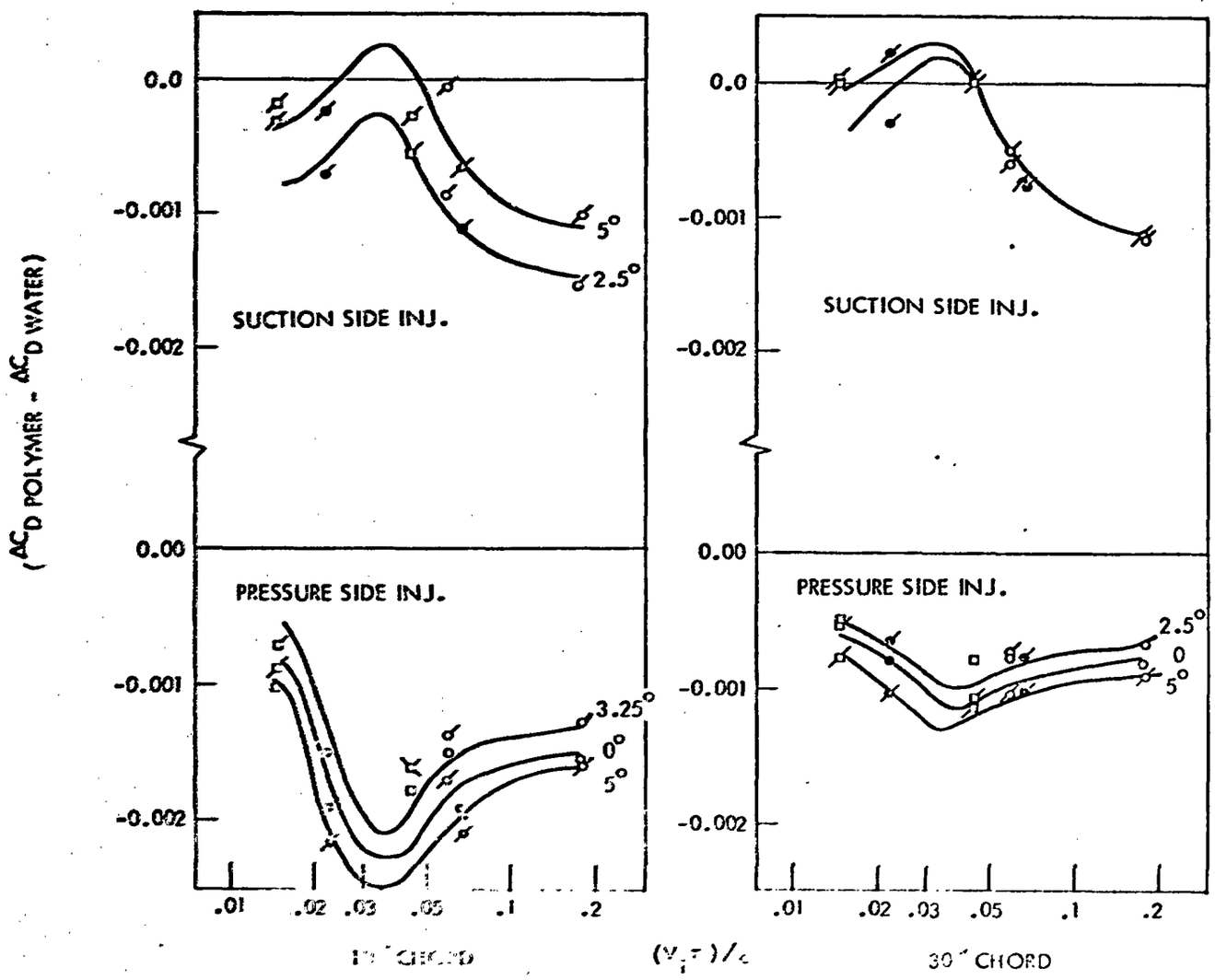

FIGURE 19 - DRAG CHANGE VERSUS $V_i \tau / c$

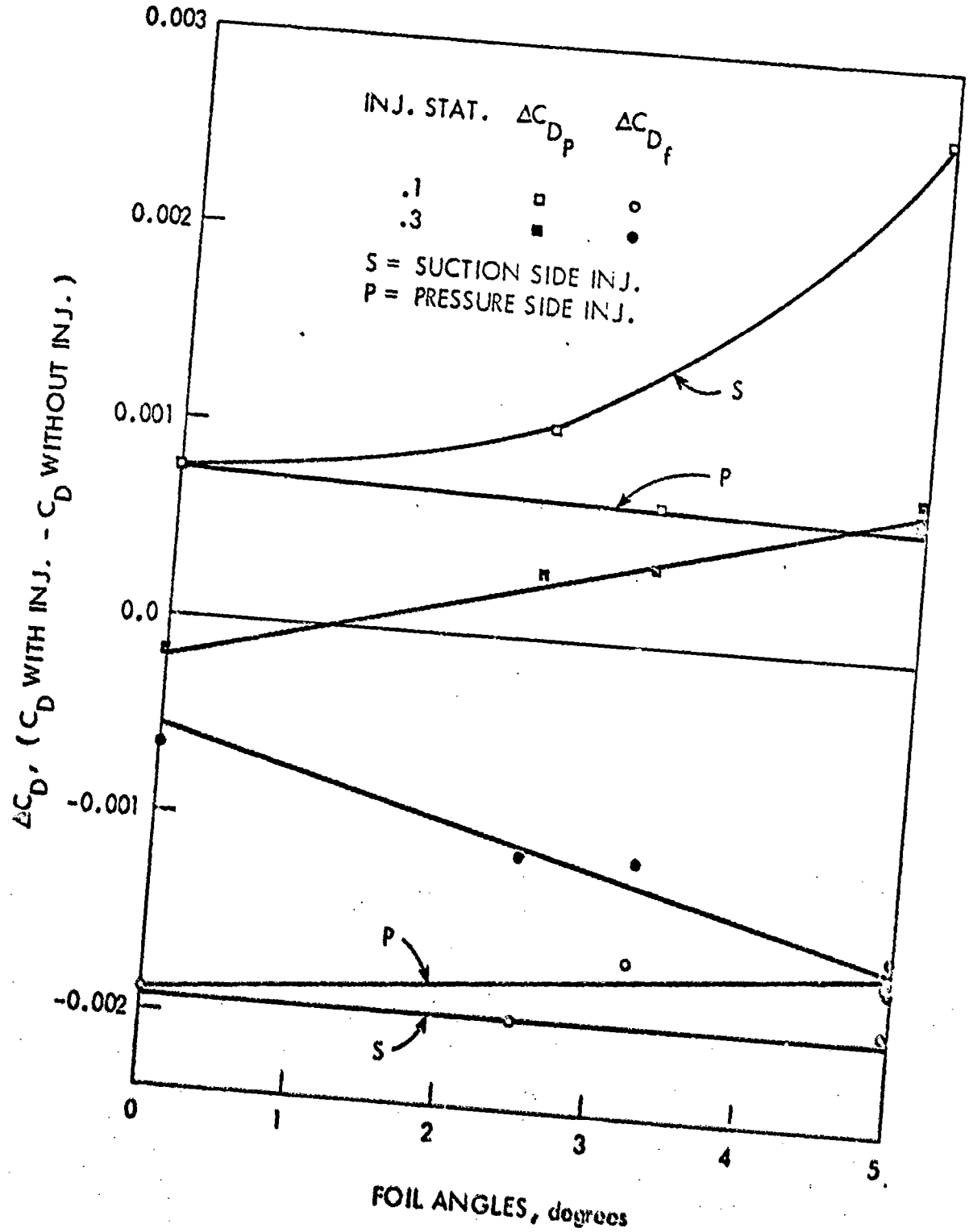

FIGURE 20 - CHANGE IN DRAG COEFFICIENT COMPONENTS DUE TO POLYOX INJECTION AT $V_i / V_\infty = .1$ RATE.

APPENDIX A

VELOCITY DISTRIBUTION INTEGRALS FOR SYMMETRIC AND CAMBERED HYDROFOILS

Weber[15] has deduced an integral relation for the velocity distribution on a flat plate at an angle of attack, α, by using conformal transformation. In particular, she has utilized the transformation

$$\zeta = \zeta_1 + \frac{R^2}{\zeta_1} \qquad [A-1]$$

to transform the flat plate $-\frac{1}{2} \le \zeta \le \frac{1}{2}$ into a circle (for the notation, see Reference 15). The velocity distribution on the flat plate for any arbitrary circulation Γ around it is then expressible in terms of the complex velocity potential, F, as,

$$V_\zeta - iV_\eta = \frac{dF}{d\zeta} = -iV_\infty \alpha \frac{\zeta}{\sqrt{\zeta^2 - \frac{1}{4}}} - i\frac{\Gamma}{2\pi} \frac{1}{\sqrt{\zeta^2 - \frac{1}{4}}} . \qquad [A-2]$$

For the Kutta-Joukowski condition to be satisfied, the trailing edge, given by $\zeta = \frac{1}{2}$, must be a stagnation point, thus requiring that $\Gamma = \Gamma_K = 2\pi V_\infty \alpha$. Then, in the physical coordinate system, Equation [A-2] gives,

$$V = \pm V_\infty \alpha \sqrt{\frac{1 - x}{x}} . \qquad [A-3]$$

For an arbitrary circulation Γ defined by Equations [1] and [2], Equation [A-2] yields,

$$V = \pm V_\infty \alpha \frac{h - x}{\sqrt{x(1 - x)}} . \qquad [A-4]$$

Of course, Equation [A-4] reduces to Equation [A-3] when $h = 1$.

For a cambered hydrofoil, Weber[15] has shown that the velocity distribution is given by,

$$V = \pm \frac{2}{\pi} \cdot V_\infty \alpha \sqrt{\frac{1 - x}{x}} \int_0^1 \frac{dz_c(x')}{dx'} \sqrt{\frac{x'}{1 - x'}} \frac{dx'}{x - x'} , \qquad [A-5]$$

when the circulation is specified by the Kutta-Joukowski condition. When the circulation is specified by Equations [1] and [2], Equation [A-5] becomes,

$$V = \pm \frac{2}{\pi} V_\infty \alpha \frac{h - x}{\sqrt{x(1 - x)}} \int_0^1 \frac{dz_c(x')}{dx'} \sqrt{\frac{x'}{1 - x'}} \frac{dx'}{x - x'} . \quad [A-6]$$

Note that Equations [A-5] and [A-6] reduce, respectively, to Equations [A-3] and [A-4] when $dz_c/dx = - \alpha$.

APPENDIX B

LIFT, DRAG AND PRESSURE MEASUREMENT DATA (DECEMBER 8-19, 1975) ON THE NACA 63_4-020 TWO-DIMENSIONAL HYDROFOIL

VF = free stream velocity (V_∞ used in the text)

CD = drag coefficient

CL = lift coefficient

X/C = chordwise pressure-tap position

CPP = pressure coefficient on the pressure side

CPS = pressure coefficient on the suction side

Ending N means "no-injection" case

Ending W means "with-injection" case

****

TEST CONDS-VF=11 KPS, ALPHA=0.0 DEGREE, VI/VF=0.1, 10 PCT CHORD SUCTN SIDE INJ. OF WATER

****

	VFN	VFW	CDN	CDW	CDW-CDN	CLN	CLW	CLW-CLN
AVG VALUE	11.0095	11.0073	0.0117859	0.0121425	0.0003566	0.0038026	-0.0024455	-0.0062482
STAND DEV	0.0345	0.0376	0.0000370	0.0000539	0.0000692	0.0010570	0.0011938	0.0012211

PRESS TAP	X/C	CPPN	CPPW	CPPW-CPPN	CPSN	CPSW	CPSW-CPSN
1	0.18425	-0.553899	-0.556671	-0.002771	-0.605118	-0.586620	0.018497
2	0.23425	-0.556294	-0.561112	-0.002817	-0.598593	-0.585408	0.013184
3	0.28675	-0.578242	-0.581611	-0.003369	-0.636828	-0.611958	0.024869
4	0.35925	-0.554369	-0.562641	-0.008271	-0.577767	-0.575558	0.002209
5	0.38425	-0.558502	-0.563167	-0.004665	-0.556207	-0.547743	0.008464
6	0.43425	-0.511587	-0.515433	-0.003846	-0.512570	-0.511269	0.001301
7	0.53425	-0.422668	-0.425886	-0.003218	-0.401975	-0.398122	0.003853
8	0.63425	-0.241109	-0.245082	-0.003972	-0.231585	-0.228170	0.003414
9	0.73425	-0.106635	-0.110327	-0.003692	-0.101960	-0.098463	0.003496
10	0.85925	0.029522	0.025438	-0.004083	0.034470	0.037274	0.002803

****

TEST CONDS-VF=11 KPS, ALPHA=0.0 DEGREE, VI/VF=0.3, 10 PCT CHORD SUCTN SIDE INJ. OF WATER

****

	VFN	VFW	CDN	CDW	CDW-CDN	CLN	CLW	CLW-CLN
AVG VALUE	11.0056	11.0049	0.0121268	0.0125288	0.0004019	0.0024173	-0.0105279	-0.0129453
STAND DEV	0.0168	0.0227	0.0000319	0.0000694	0.0000623	0.0005057	0.0011766	0.0010776

PRESS TAP	X/C	CPPN	CPPW	CPPW-CPPN	CPSN	CPSW	CPSW-CPSN
1	0.18425	-0.554439	-0.561994	-0.007554	-0.607114	-0.585952	0.021161
2	0.23425	-0.560996	-0.568177	-0.007180	-0.601184	-0.588697	0.012486
3	0.28675	-0.582049	-0.586014	-0.003965	-0.635835	-0.612910	0.022924
4	0.35925	-0.557328	-0.561232	-0.003903	-0.580197	-0.576050	0.004146
5	0.38425	-0.557416	-0.564167	-0.006751	-0.556056	-0.545119	0.010936
6	0.43425	-0.514137	-0.520226	-0.006089	-0.512997	-0.510434	0.002562
7	0.53425	-0.424395	-0.432026	-0.007630	-0.404435	-0.396764	0.007671
8	0.63425	-0.242140	-0.249232	-0.007092	-0.233323	-0.226656	0.006667
9	0.73425	-0.107252	-0.114549	-0.007297	-0.101256	-0.097860	0.003396
10	0.85925	0.029065	0.021311	-0.007754	0.033918	0.039475	0.005557

****
TEST CONDS-VF=11 MPS, ALPHA=0.0 DEGREE, VJ/VF=0.1, 30 PCT CHORD PRESS SIDE INJ. OF WATER
****

	VFN	VFW	CDN	CDW	CDW-CDN	CLN	CLW	CLW-CLN
AVG VALUE	11.0169	11.0161	0.0118759	0.0118113	-0.0000645	0.0030898	0.0058920	0.0028022
STAND DEV	0.0177	0.0197	0.0000632	0.0000367	0.0000661	0.0007761	0.0016826	0.0020205

PRESS TAP	X/C	CPPN	CPPW	CPPW-CPPN	CPSN	CPSW	CPSW-CPSN
1	0.18425	-0.553302	-0.548721	0.004580	-0.605774	-0.606674	-0.000899
2	0.23425	-0.559637	-0.554365	0.005272	-0.599699	-0.598257	0.001441
3	0.24675	-0.579203	-0.577348	0.001855	-0.635944	-0.636182	-0.000237
4	0.35925	-0.559854	-0.568221	-0.008367	-0.580095	-0.582494	-0.002398
5	0.38425	-0.557947	-0.561946	-0.003999	-0.556923	-0.555790	0.001132
6	0.43425	-0.510749	-0.507657	0.003092	-0.511318	-0.514471	-0.003153
7	0.53425	-0.423404	-0.423494	-0.000090	-0.403[illegible]4	-0.405001	-0.001347
8	0.63425	-0.241997	-0.241615	0.000381	-0.232[illegible]6	-0.234396	-0.001769
9	0.73425	-0.106545	-0.105594	0.000950	-0.101412	-0.103654	-0.002242
10	0.85925	0.029845	0.030304	0.000459	0.034374	0.033249	-0.001125

****
TEST CONDS-VF=11 MPS, ALPHA=0.0 DEGREE, VJ/VF=0.3, 30 PCT CHORD PRESS SIDE INJ. OF WATER
****

	VFN	VFW	CDN	CDW	CDW-CDN	CLN	CLW	CLW-CLN
AVG VALUE	11.0126	11.0176	0.0120394	0.0119118	-0.0001275	0.0030623	0.0114977	0.0084354
STAND DEV	0.0245	0.0334	0.0000611	0.0000571	0.0000572	0.0004463	0.0009703	0.0008307

PRESS TAP	X/C	CPPN	CPPW	CPPW-CPPN	CPSN	CPSW	CPSW-CPSN
1	0.18425	-0.555497	-0.549453	0.006044	-0.610351	-0.612758	-0.002406
2	0.23425	-0.562429	-0.551924	0.010505	-0.599576	-0.603626	-0.004049
3	0.24675	-0.581880	-0.570423	0.011456	-0.639016	-0.640663	-0.001647
4	0.35925	-0.559354	-0.485501	0.073853	-0.579455	-0.581938	-0.002483
5	0.38425	-0.555536	-0.542604	0.012932	-0.556394	-0.558275	-0.001880
6	0.43425	-0.512027	-0.518929	-0.006902	-0.512084	-0.515621	-0.003536
7	0.53425	-0.422717	-0.420576	0.002141	-0.403746	-0.407699	-0.003953
8	0.63425	-0.241410	-0.238021	0.003388	-0.231884	-0.235186	-0.003301
9	0.73425	-0.106307	-0.104179	0.002128	-0.101996	-0.104972	-0.002975
10	0.85925	0.029246	0.030966	0.001720	0.034764	0.030852	-0.003912

10	0.85925	0.029246	0.030966	0.001720	0.034764	0.030852	-0.003912

****

TEST CONDS-VF=11 FPS, ALPHA=2.5 DEGREE, VI/VF=0.1, 10 PCT CHORD SUCTN SIDE INJ. OF WATER

****

	VFN	VFW	CDN	CDW	CDW-CDN	CLN	CLW	CLW-CLN
AVG VALUE	11.0255	11.0275	0.0181631	0.0181130	-0.0000500	0.1828224	0.1759756	-0.0068468
STAND DEV	0.0327	0.0403	0.0000802	0.0001197	0.0000950	0.0007890	0.0010139	0.0007178

PRESS TAP	X/C	CPPN	CPPW	CPPW-CPPN	CPSN	CPSW	CPSW-CPSN
1	0.18425	-0.395599	-0.399109	-0.003510	-0.758082	-0.744413	0.013669
2	0.23425	-0.421165	-0.423768	-0.002603	-0.729029	-0.722518	0.006510
3	0.24675	-0.444372	-0.449250	-0.004878	-0.759599	-0.748574	0.011025
4	0.35925	-0.474503	-0.477332	-0.002828	-0.671490	-0.669626	0.001864
5	0.38425	-0.474359	-0.477608	-0.003249	-0.635858	-0.636218	-0.000359
6	0.43425	-0.439826	-0.442885	-0.003058	-0.586102	-0.582873	0.003228
7	0.53425	-0.370490	-0.373642	-0.003152	-0.448936	-0.443938	0.004998
8	0.63425	-0.210681	-0.213920	-0.003239	-0.258223	-0.253569	0.004654
9	0.73425	-0.092828	-0.097693	-0.004864	-0.116406	-0.112524	0.003882
10	0.85925	0.027622	0.024917	-0.002705	0.036523	0.038537	0.002013

****

TEST CONDS-VF=11 FPS, ALPHA=2.5 DEGREE, VI/VF=0.3, 10 PCT CHORD SUCTN SIDE INJ. OF WATER

****

	VFN	VFW	CDN	CDW	CDW-CDN	CLN	CLW	CLW-CLN
AVG VALUE	11.0178	11.0148	0.0181761	0.0179079	-0.0002681	0.1820098	0.1670243	-0.0149855
STAND DEV	0.0228	0.0266	0.0000956	0.0001019	0.0000807	0.0007795	0.0013297	0.0014716

PRESS TAP	X/C	CPPN	CPPW	CPPW-CPPN	CPSN	CPSW	CPSW-CPSN
1	0.18425	-0.393263	-0.400665	-0.007401	-0.756052	-0.746429	0.009622
2	0.23425	-0.420892	-0.429178	-0.008285	-0.728274	-0.718605	0.009668
3	0.24675	-0.444950	-0.452655	-0.007705	-0.753259	-0.742797	0.010461
4	0.35925	-0.473412	-0.482680	-0.009268	-0.670714	-0.665148	0.005565
5	0.38425	-0.475901	-0.481576	-0.005674	-0.635711	-0.629378	0.006333
6	0.43425	-0.441362	-0.447711	-0.006349	-0.585722	-0.578059	0.007663
7	0.53425	-0.369897	-0.377849	-0.007951	-0.448019	-0.437936	0.010083
8	0.63425	-0.211113	-0.218198	-0.007085	-0.257554	-0.248936	0.008618
9	0.73425	-0.092201	-0.096653	-0.004452	-0.114692	-0.108350	0.006342
10	0.85925	0.028327	0.020092	-0.008235	0.035793	0.040351	0.004557

****
TEST CONDS-VF=11 MPS, ALPHA=2.5 DEGREE, VI/VF=0.1, 30 PCT CHORD PRESS SIDE INJ. OF WATER
****

	VFN	VFW	CDN	CDW	CDW-CDN	CLN	CLW	CLW-CLN
AVG VALUE	11.0109	11.0119	0.0182173	0.0181726	-0.0000447	0.1821694	0.1848948	0.0027254
STAND DEV	0.0146	0.0197	0.0000650	0.0001620	0.0001479	0.0006548	0.0009314	0.0011479

PRESS TAP	X/C	CPPN	CPPW	CPPW-CPPN	CPSN	CPSW	CPSW-CPSN
1	0.18425	-0.393421	-0.387453	0.005967	-0.756962	-0.759134	-0.002201
2	0.23425	-0.423004	-0.418255	0.004748	-0.729135	-0.730102	-0.000967
3	0.24675	-0.444763	-0.440683	0.004079	-0.757634	-0.754944	0.002690
4	0.35925	-0.479347	-0.495431	-0.016084	-0.670823	-0.670001	0.000822
5	0.38425	-0.470999	-0.471684	-0.000685	-0.634926	-0.634688	0.000238
6	0.43425	-0.439367	-0.436004	0.003363	-0.586112	-0.586234	-0.000121
7	0.53425	-0.372782	-0.371836	0.000952	-0.449081	-0.450217	-0.001136
8	0.63425	-0.212156	-0.210683	0.001472	-0.259435	-0.261048	-0.001613
9	0.73425	-0.092306	-0.091396	0.000909	-0.115350	-0.117015	-0.001664
10	0.85925	0.027286	0.026921	-0.000365	0.035847	0.034121	-0.001725

****
TEST CONDS-VF=11 MPS, ALPHA=2.5 DEGREE, VI/VF=0.3, 30 PCT CHORD PRESS SIDE INJ. OF WATER
****

	VFN	VFW	CDN	CDW	CDW-CDN	CLN	CLW	CLW-CLN
AVG VALUE	10.9995	11.0029	0.0182133	0.0184977	0.0002843	0.1817572	0.1897252	0.0079680
STAND DEV	0.0220	0.0304	0.0000577	0.0001391	0.0001595	0.0008717	0.0010016	0.0012589

PRESS TAP	X/C	CPPN	CPPW	CPPW-CPPN	CPSN	CPSW	CPSW-CPSN
1	0.18425	-0.392795	-0.386525	0.006270	-0.756647	-0.759367	-0.002719
2	0.23425	-0.422638	-0.413639	0.008998	-0.731285	-0.734568	-0.003282
3	0.24675	-0.444438	-0.435144	0.009293	-0.754682	-0.760709	-0.006026
4	0.35925	-0.474835	-0.427207	0.047627	-0.670552	-0.674039	-0.003487
5	0.38425	-0.475299	-0.461779	0.013519	-0.633400	-0.634917	-0.001517
6	0.43425	-0.440496	-0.441788	-0.001292	-0.585043	-0.588903	-0.003859
7	0.53425	-0.373491	-0.373040	0.000451	-0.449110	-0.451833	-0.002722
8	0.63425	-0.211533	-0.209508	0.002024	-0.258312	-0.262376	-0.004063
9	0.73425	-0.093324	-0.089943	0.003381	-0.115384	-0.117308	-0.001924
10	0.85925	0.025587	0.027603	0.002015	0.038264	0.032193	-0.006071

****
TEST CONDS-VF=11 MPS, ALPHA=5.0 DEGREE, VI/VF=0.1, 10 PCT CHORD SUCTN SIDE INJ. OF WATER
****

	VFN	VFW	CDN	CDW	CDW-CDN	CLN	CLW	CLW-CLN
AVG VALUE	11.0189	11.0251	0.0308625	0.0307887	-0.0000736	0.3710589	0.3651850	-0.0058738
STAND DEV	0.0268	0.0343	0.0001750	0.0002208	0.0002653	0.0006561	0.0016276	0.0012424

PRESS TAP	X/C	CPPN	CPPW	CPPW-CPPN	CPSN	CPSW	CPSW-CPSN
1	0.18425	-0.226494	-0.229994	-0.003500	-0.912419	-0.909440	0.002979
2	0.23425	-0.276578	-0.279991	-0.003413	-0.862030	-0.857814	0.004215
3	0.24675	-0.301529	-0.303846	-0.002317	-0.882095	-0.879043	0.003051
4	0.35925	-0.379579	-0.382856	-0.003177	-0.756632	-0.753156	0.003476
5	0.38425	-0.380573	-0.387710	-0.007136	-0.706365	-0.703391	0.002973
6	0.43425	-0.363640	-0.362308	0.001332	-0.654123	-0.647251	0.006872
7	0.53425	-0.314953	-0.316163	-0.001210	-0.489102	-0.482737	0.006364
8	0.63425	-0.177542	-0.181038	-0.003495	-0.279206	-0.276274	0.002931
9	0.73425	-0.073202	-0.076073	-0.002871	-0.122148	-0.118545	0.003603
10	0.85925	0.026421	0.023454	-0.002967	0.035682	0.036400	0.000718

****
TEST CONDS-VF=11 MPS, ALPHA=5.0 DEGREE, VI/VF=0.3, 10 PCT CHORD SUCTN SIDE INJ. OF WATER
****

	VFN	VFW	CDN	CDW	CDW-CDN	CLN	CLW	CLW-CLN
AVG VALUE	11.0049	11.0037	0.0309048	0.0307082	-0.0001966	0.3708667	0.3541723	-0.0166944
STAND DEV	0.0209	0.0192	0.0001884	0.0002467	0.0003250	0.0008496	0.0013396	0.0018615

PRESS TAP	X/C	CPPN	CPPW	CPPW-CPPN	CPSN	CPSW	CPSW-CPSN
1	0.18425	-0.227165	-0.232686	-0.005520	-0.913861	-0.910786	0.003075
2	0.23425	-0.274891	-0.282469	-0.007577	-0.860851	-0.855388	0.005463
3	0.24675	-0.301284	-0.309218	-0.007934	-0.884411	-0.877418	0.006993
4	0.35925	-0.380577	-0.384931	-0.004353	-0.758535	-0.747613	0.010922
5	0.38425	-0.383884	-0.392009	-0.008125	-0.720262	-0.710191	0.010070
6	0.43425	-0.363660	-0.367903	-0.004242	-0.654807	-0.645666	0.009140
7	0.53425	-0.311457	-0.319229	-0.007772	-0.489623	-0.475607	0.014016
8	0.63425	-0.176299	-0.184321	-0.008021	-0.279467	-0.268818	0.010649
9	0.73425	-0.073419	-0.081063	-0.007644	-0.123081	-0.115226	0.007855
10	0.85925	0.025347	0.017771	-0.007576	0.033299	0.034338	0.001039

TEST CONDS-VF=11 KPS, ALPHA=5.0 DEGREE, VJ/VF=0.1, 30 PCT CHORD PRESS SIDE INJ. OF WATER

	VFN	VFW	CDN	CDW	CDW-CDN	CLN	CLW	CLW-CLN
AVG VALUE	11.0162	11.0211	0.0309145	0.0311278	0.0002132	0.3708814	0.3734295	0.0025481
STAND DEV	0.0204	0.0280	0.0001166	0.0004183	0.0003575	0.0012070	0.0011988	0.0013600

PRESS TAP	X/C	CPPN	CPPW	CPPW-CPPN	CPSN	CPSW	CPSW-CPSN
1	0.18425	-0.227879	-0.223886	0.003992	-0.916082	-0.917764	-0.001682
2	0.23425	-0.275053	-0.269084	0.005969	-0.858163	-0.853846	0.004316
3	0.24675	-0.302385	-0.298283	0.004102	-0.882083	-0.885972	-0.003889
4	0.35925	-0.380392	-0.403690	-0.023298	-0.759866	-0.761621	-0.001754
5	0.38425	-0.385540	-0.386906	-0.001366	-0.720289	-0.720063	0.000226
6	0.43425	-0.360363	-0.353843	0.006519	-0.652628	-0.653857	-0.001229
7	0.53425	-0.314497	-0.313675	0.000821	-0.488250	-0.489113	-0.000863
8	0.63425	-0.177534	-0.176097	0.001436	-0.280973	-0.283046	-0.002072
9	0.73425	-0.073276	-0.073754	-0.000478	-0.123481	-0.124090	-0.000609
10	0.85925	0.026061	0.025213	-0.000848	0.034501	0.033710	-0.000791

TEST CONDS-VF=11 KPS, ALPHA=5.0 DEGREE, VJ/VF=0.3, 30 PCT CHORD PRESS SIDE INJ. OF WATER

	VFN	VFW	CDN	CDW	CDW-CDN	CLN	CLW	CLW-CLN
AVG VALUE	11.0019	10.9996	0.0309093	0.0310478	0.0001385	0.3711583	0.3771966	0.0060383
STAND DEV	0.0245	0.0302	0.0001510	0.0001720	0.0002652	0.0012633	0.0013396	0.0023370

PRESS TAP	X/C	CPPN	CPPW	CPPW-CPPN	CPSN	CPSW	CPSW-CPSN
1	0.18425	-0.224499	-0.220715	0.003784	-0.917515	-0.916182	0.001333
2	0.23425	-0.273958	-0.265298	0.008660	-0.859461	-0.863904	-0.004442
3	0.24675	-0.299426	-0.291307	0.008118	-0.885156	-0.886683	-0.001526
4	0.35925	-0.376459	-0.328257	0.048201	-0.759273	-0.761091	-0.001817
5	0.38425	-0.381147	-0.368867	0.012280	-0.719170	-0.722141	-0.002971
6	0.43425	-0.362744	-0.358877	0.003867	-0.656945	-0.657954	-0.001009
7	0.53425	-0.314373	-0.314570	-0.000197	-0.488992	-0.491914	-0.002922
8	0.63425	-0.176895	-0.176820	0.000075	-0.281387	-0.283225	-0.001838
9	0.73425	-0.073631	-0.073472	0.000159	-0.123225	-0.125763	-0.002537
10	0.85925	0.025222	0.025022	-0.000199	0.033685	0.030747	-0.002937

****
TEST CONDS-VF=11 FPS, ALPH=3.25 DEGREE, VI/VF=0.1, 10 PCT CHORD PRESS SIDE INJ. OF WATER
****

	VFN	VFW	CDN	CDW	CDW-CDN	CLN	CLW	CLW-CLN
AVG VALUE	11.0216	11.0136	0.0215456	0.0217874	0.0002418	0.2583053	0.2621374	0.0038320
STAND DEV	0.0150	0.0287	0.0000495	0.0000638	0.0000913	0.0012957	0.0012969	0.0018125

PRESS TAP	X/C	CPPN	CPPW	CPPW-CPPN	CPSN	CPSW	CPSW-CPSN
1	0.18425	-0.379475	-0.360479	0.018996	-0.759589	-0.759399	0.000189
2	0.23425	-0.399662	-0.393188	0.006473	-0.734152	-0.736120	-0.001967
3	0.24675	-0.445614	-0.422561	0.023052	-0.756945	-0.756518	0.000426
4	0.35925	-0.443536	-0.442311	0.001225	-0.636865	-0.635533	0.001331
5	0.38425	-0.439901	-0.421894	0.018006	-0.665994	-0.668297	-0.002303
6	0.43425	-0.402603	-0.402382	0.000221	-0.623562	-0.626796	-0.003234
7	0.53425	-0.328422	-0.327714	0.000708	-0.493925	-0.496820	-0.002895
8	0.63425	-0.186124	-0.185715	0.000409	-0.282305	-0.284512	-0.002206
9	0.73425	-0.076841	-0.076162	0.000678	-0.125897	-0.126928	-0.001031
10	0.85925	0.037002	0.037327	0.000325	0.030845	0.029920	-0.000925

****
TEST CONDS-VF=11 FPS, ALPH=3.25 DEGREE, VI/VF=0.3, 10 PCT CHORD PRESS SIDE INJ. OF WATER
****

	VFN	VFW	CDN	CDW	CDW-CDN	CLN	CLW	CLW-CLN
AVG VALUE	11.0072	11.0082	0.0216019	0.0219734	0.0003715	0.2580915	0.2670595	0.0089680
STAND DEV	0.0216	0.0227	0.0000363	0.0000540	0.0000702	0.0009225	0.0015863	0.0019687

PRESS TAP	X/C	CPPN	CPPW	CPPW-CPPN	CPSN	CPSW	CPSW-CPSN
1	0.18425	-0.377134	-0.363566	0.013568	-0.768151	-0.770761	-0.002609
2	0.23425	-0.400547	-0.390125	0.010421	-0.737459	-0.737229	0.000230
3	0.24675	-0.445487	-0.420560	0.024927	-0.755007	-0.762683	-0.007675
4	0.35925	-0.443753	-0.443190	0.000562	-0.639644	-0.639552	0.000091
5	0.38425	-0.430758	-0.419841	0.010917	-0.671435	-0.676204	-0.004769
6	0.43425	-0.402814	-0.402160	0.000654	-0.625386	-0.629724	-0.004337
7	0.53425	-0.328941	-0.325738	0.003202	-0.497148	-0.502704	-0.005556
8	0.63425	-0.186212	-0.183652	0.002559	-0.284641	-0.289459	-0.004817
9	0.73425	-0.076959	-0.074210	0.002748	-0.128066	-0.131224	-0.003157
10	0.85925	0.036816	0.039410	0.002593	0.030056	0.026217	-0.003838

****

TEST CONDS-VF=11 FPS, ALPH=3.25 DEGREE, VI/VF=0.1, 30 PCT CHORD SUCTN SIDE INJ. OF WATER

****

	VFN	VFW	CDN	CDW	CDW-CDN	CLN	CLW	CLW-CLN
AVG VALUE	11.0157	11.0206	0.0215748	0.0214084	-0.0001664	0.2582796	0.2565621	-0.0017175
STAND DEV	0.0102	0.0124	0.0000473	0.0000315	0.0000682	0.0011451	0.0011349	0.0012210

PRESS TAP	X/C	CPPN	CPPW	CPPW-CPPN	CPSN	CPSW	CPSW-CPSN
1	0.18425	-0.377351	-0.379530	-0.002176	-0.767483	-0.764603	0.002879
2	0.23425	-0.400517	-0.400088	0.000428	-0.733364	-0.734255	-0.000890
3	0.24675	-0.445747	-0.448789	-0.003041	-0.754570	-0.754761	-0.000191
4	0.35925	-0.442750	-0.443861	-0.001110	-0.636492	-0.650976	-0.014483
5	0.38425	-0.434479	-0.437280	-0.002801	-0.662877	-0.666818	-0.003940
6	0.43425	-0.402076	-0.403385	-0.001309	-0.622720	-0.623516	-0.000795
7	0.53425	-0.328696	-0.328923	-0.000227	-0.494589	-0.493282	0.001306
8	0.63425	-0.185933	-0.186595	-0.000661	-0.282899	-0.281326	0.001572
9	0.73425	-0.076325	-0.076953	-0.000628	-0.127561	-0.126958	0.000602
10	0.85925	0.036642	0.036188	-0.000453	0.030431	0.030831	0.000400

****

TEST CONDS-VF=11 FPS, ALPH=3.25 DEGREE, VI/VF=0.3, 30 PCT CHORD SUCTN SIDE INJ. OF WATER

****

	VFN	VFW	CDN	CDW	CDW-CDN	CLN	CLW	CLW-CLN
AVG VALUE	11.0165	11.0191	0.0215682	0.0211664	-0.0004017	0.2578636	0.2498020	-0.0080615
STAND DEV	0.0128	0.0140	0.0000370	0.0000434	0.0000461	0.0014523	0.0011472	0.0015952

PRESS TAP	X/C	CPPN	CPPW	CPPW-CPPN	CPSN	CPSW	CPSW-CPSN
1	0.18425	-0.371775	-0.374506	-0.002730	-0.763017	-0.757195	0.005822
2	0.23425	-0.401120	-0.406047	-0.004926	-0.733718	-0.726488	0.007229
3	0.24675	-0.447604	-0.450524	-0.002919	-0.755451	-0.746600	0.008851
4	0.35925	-0.441838	-0.446533	-0.004695	-0.638614	-0.648178	-0.009563
5	0.38425	-0.435959	-0.441525	-0.005566	-0.672471	-0.683752	-0.011281
6	0.43425	-0.401828	-0.405020	-0.003192	-0.624335	-0.626891	-0.002556
7	0.53425	-0.328560	-0.332035	-0.003474	-0.499327	-0.493961	0.005365
8	0.63425	-0.185484	-0.188436	-0.002952	-0.284183	-0.281132	0.003051
9	0.73425	-0.076704	-0.078911	-0.002206	-0.127548	-0.125476	0.002071
10	0.85925	0.037324	0.035597	-0.001726	0.029985	0.031169	0.001184

****

TEST CONDS-VF=11 MPS, ALPHA=5.0 DEGREE, VI/VF=0.1, 10 PCT CHORD PRESS SIDE INJ. OF WATER

****

	VFN	VFW	CDN	CDW	CDW-CDN	CLN	CLW	CLW-CLN
AVG VALUE	11.0259	11.0210	0.0305353	0.0305776	0.0000422	0.3940734	0.3960387	0.0019652
STAND DEV	0.0200	0.0227	0.0000855	0.0002055	0.0002176	0.0014671	0.0018414	0.0017667

PRESS TAP	X/C	CPPN	CPPW	CPPW-CPPN	CPSN	CPSW	CPSW-CPSN
1	0.18425	-0.261379	-0.248631	0.012747	-0.880255	-0.877820	0.002434
2	0.23425	-0.300493	-0.293232	0.007260	-0.816392	-0.815532	0.000860
3	0.24675	-0.343650	-0.326572	0.017078	-0.842213	-0.842080	0.000133
4	0.35925	-0.377705	-0.374507	0.003197	-0.695976	-0.698004	-0.002027
5	0.38425	-0.357544	-0.356476	0.001068	-0.742040	-0.741349	0.000691
6	0.43425	-0.347854	-0.347902	-0.000047	-0.680291	-0.681044	-0.000752
7	0.53425	-0.291421	-0.290422	0.000999	-0.531865	-0.534934	-0.003069
8	0.63425	-0.163368	-0.162822	0.000546	-0.302032	-0.303024	-0.000991
9	0.73425	-0.065405	-0.065266	0.000139	-0.135648	-0.136223	-0.000574
10	0.85925	0.033518	0.032526	-0.000991	0.029877	0.030704	0.000827

****

TEST CONDS-VF=11 MPS, ALPHA=5.0 DEGREE, VI/VF=0.3, 10 PCT CHORD PRESS SIDE INJ. OF WATER

****

	VFN	VFW	CDN	CDW	CDW-CDN	CLN	CLW	CLW-CLN
AVG VALUE	11.0117	11.0107	0.0306639	0.0307003	0.0000364	0.3937870	0.3986368	0.0048497
STAND DEV	0.0190	0.0219	0.0001159	0.0001903	0.0002712	0.0010358	0.0017736	0.0017848

PRESS TAP	X/C	CPPN	CPPW	CPPW-CPPN	CPSN	CPSW	CPSW-CPSN
1	0.18425	-0.259567	-0.253421	0.006146	-0.871766	-0.869740	0.002025
2	0.23425	-0.299640	-0.295189	0.004450	-0.812340	-0.818354	-0.006013
3	0.24675	-0.346759	-0.324121	0.022638	-0.839091	-0.841209	-0.002117
4	0.35925	-0.377147	-0.374267	0.002880	-0.695664	-0.699720	-0.004056
5	0.38425	-0.357984	-0.357769	0.000214	-0.740391	-0.742473	-0.002082
6	0.43425	-0.347798	-0.348024	-0.000225	-0.680414	-0.685365	-0.004951
7	0.53425	-0.291195	-0.288935	0.002259	-0.531184	-0.533752	-0.002567
8	0.63425	-0.163509	-0.162318	0.001191	-0.303106	-0.305791	-0.002684
9	0.73425	-0.064731	-0.063593	0.001138	-0.136093	-0.137958	-0.001865
10	0.85925	0.033599	0.033876	0.000276	0.029911	0.028656	-0.001254

****

TEST CONDS-VF=11 FPS, ALPHA=5.0 DEGREE, VI/VF=0.1, 30 PCT CHORD SUCTN SIDE INJ. OF WATER

****

	VFN	VFW	CDN	CDW	CDW-CDN	CLN	CLW	CLW-CLN
AVG VALUE	11.0198	11.0229	0.0305581	0.0303111	-0.0002469	0.3944065	0.3905922	-0.0038143
STAND DEV	0.0227	0.0238	0.0001297	0.0001894	0.0002016	0.0015674	0.0010196	0.0017523

PRESS TAP	X/C	CPPN	CPPW	CPPW-CPPN	CPSN	CPSW	CPSW-CPSN
1	0.18425	-0.261246	-0.261373	-0.000126	-0.879710	-0.870652	0.009057
2	0.23425	-0.300304	-0.301596	-0.000692	-0.812666	-0.809882	0.002783
3	0.24675	-0.340929	-0.348699	-0.007770	-0.840595	-0.838231	0.002363
4	0.35925	-0.375827	-0.375618	0.000208	-0.694183	-0.710347	-0.016163
5	0.38425	-0.356555	-0.361588	-0.005033	-0.739589	-0.742186	-0.002596
6	0.43425	-0.347996	-0.348683	-0.000687	-0.679699	-0.679800	-0.000101
7	0.53425	-0.290921	-0.292029	-0.001107	-0.531140	-0.530209	0.000930
8	0.63425	-0.163428	-0.164517	-0.001089	-0.303734	-0.303448	0.000285
9	0.73425	-0.064994	-0.066304	-0.001309	-0.137984	-0.136138	0.001845
10	0.85925	0.032871	0.032621	-0.000250	0.028748	0.029879	0.001130

****

TEST CONDS-VF=11 FPS, ALPHA=5.0 DEGREE, VI/VF=0.3, 30 PCT CHORD SUCTN SIDE INJ. OF WATER

****

	VFN	VFW	CDN	CDW	CDW-CDN	CLN	CLW	CLW-CLN
AVG VALUE	11.0220	11.0202	0.0305995	0.0300640	-0.0005354	0.3939756	0.3853235	-0.0086522
STAND DEV	0.0222	0.0197	0.0001597	0.0002167	0.0002882	0.0009799	0.0015268	0.0019592

PRESS TAP	X/C	CPPN	CPPW	CPPW-CPPN	CPSN	CPSW	CPSW-CPSN
1	0.18425	-0.260942	-0.264719	-0.003776	-0.876402	-0.871672	0.004729
2	0.23425	-0.300692	-0.303689	-0.003596	-0.812961	-0.805335	0.007626
3	0.24675	-0.341388	-0.349519	-0.007530	-0.839704	-0.827875	0.011829
4	0.35925	-0.374439	-0.378381	-0.003941	-0.695825	-0.718906	-0.023080
5	0.38425	-0.360845	-0.361128	-0.000283	-0.738141	-0.753023	-0.014881
6	0.43425	-0.348265	-0.350549	-0.002283	-0.679716	-0.681802	-0.002086
7	0.53425	-0.290571	-0.293160	-0.002588	-0.531397	-0.525026	0.006371
8	0.63425	-0.162792	-0.165626	-0.002834	-0.303074	-0.298263	0.004811
9	0.73425	-0.064666	-0.067943	-0.003277	-0.136091	-0.133480	0.002610
10	0.85925	0.034032	0.031011	-0.003021	0.028228	0.030442	0.002214

****
TEST CONDS-VF=11 FPS, ALPHA=0.0 DEGREE, VI/VF=0.1, 10 PCT CHORD SUCTN SIDE INJ. OF POLYOX
****

	VFN	VFW	CDN	CDW	CDW-CDN	CLN	CLW	CLW-CLN
AVG VALUE	11.0242	11.0214	0.0117689	0.0106393	-0.0011296	0.0006325	0.0044053	0.0037727
STAND DEV	0.0099	0.0086	0.0000594	0.0000570	0.0000824	0.0005908	0.0014778	0.0015408

PRESS TAP	X/C	CPPN	CPPW	CPPW-CPPN	CPSN	CPSW	CPSW-CPSN
1	0.18425	-0.560597	-0.558051	0.002546	-0.602965	-0.585692	0.017273
2	0.23425	-0.563131	-0.562616	0.000514	-0.599387	-0.589907	0.009479
3	0.28675	-0.580330	-0.578121	0.002208	-0.625671	-0.616762	0.008908
4	0.35925	-0.564818	-0.567352	-0.002533	-0.588458	-0.599586	-0.011127
5	0.38425	-0.558747	-0.558995	-0.000248	-0.557496	-0.569220	-0.011723
6	0.43425	-0.516749	-0.513229	0.003520	-0.518452	-0.535590	-0.017138
7	0.53425	-0.428902	-0.426889	0.002013	-0.406280	-0.410975	-0.004695
8	0.63425	-0.245905	-0.243749	0.002156	-0.235211	-0.240443	-0.005232
9	0.73425	-0.108830	-0.107618	0.001212	-0.107747	-0.111381	-0.003634
10	0.85925	0.031040	0.031886	0.000845	0.029388	0.028924	-0.000463

****
TEST CONDS-VF=11 FPS, ALPHA=0.0 DEGREE, VI/VF=0.3, 10 PCT CHORD SUCTN SIDE INJ. OF POLYOX
****

	VFN	VFW	CDN	CDW	CDW-CDN	CLN	CLW	CLW-CLN
AVG VALUE	11.0099	11.0098	0.0117888	0.0105900	-0.0011987	0.0013583	-0.0106864	-0.0120448
STAND DEV	0.0186	0.0202	0.0000323	0.0000431	0.0000496	0.0004759	0.0007033	0.0009157

PRESS TAP	X/C	CPPN	CPPW	CPPW-CPPN	CPSN	CPSW	CPSW-CPSN
1	0.18425	-0.558935	-0.561805	-0.002870	-0.600695	-0.578016	0.022679
2	0.23425	-0.558005	-0.564561	-0.006555	-0.595207	-0.581849	0.013358
3	0.28675	-0.577747	-0.584644	-0.006897	-0.622107	-0.605391	0.016716
4	0.35925	-0.550193	-0.555316	-0.005123	-0.588363	-0.578345	0.010018
5	0.38425	-0.550838	-0.555831	-0.004992	-0.555452	-0.562221	-0.006768
6	0.43425	-0.516331	-0.523278	-0.006947	-0.516388	-0.522937	-0.006549
7	0.53425	-0.428584	-0.435365	-0.006781	-0.404994	-0.400201	0.004792
8	0.63425	-0.244199	-0.251522	-0.007322	-0.233137	-0.231316	0.001821
9	0.73425	-0.108503	-0.116756	-0.006255	-0.106096	-0.102876	0.003220
10	0.85925	0.030695	0.018521	-0.012173	0.030981	0.041847	0.010866

****
TEST CONDS-VF=11 KPS, ALPHA=0.0 DEGREE, VI/VF=0.1, 30 PCT CHORD PRESS SIDE INJ. OF POLYOX
****

	VFN	VFW	CDN	CDW	CDW-CDN	CLN	CLW	CLW-CLN
AVG VALUE	11.0080	11.0138	0.0117315	0.0109051	-0.0008264	0.0014771	0.0067074	0.0052302
STAND DEV	0.0276	0.0368	0.0000591	0.0000668	0.0000618	0.0005406	0.0018380	0.0018160

PRESS TAP	X/C	CPPN	CPPW	CPPW-CPPN	CPSN	CPSW	CPSW-CPSN
1	0.18425	-0.559095	-0.558536	0.000559	-0.607065	-0.608908	-0.001842
2	0.23425	-0.562688	-0.561387	0.001301	-0.613793	-0.616820	-0.003027
3	0.28675	-0.579978	-0.575326	0.004652	-0.641224	-0.640599	0.000624
4	0.35925	-0.568163	-0.621750	-0.053587	-0.589740	-0.591311	-0.001571
5	0.38425	-0.559768	-0.604153	-0.044384	-0.567421	-0.570814	-0.003393
6	0.43425	-0.517408	-0.514604	0.002804	-0.519810	-0.523970	-0.004159
7	0.53425	-0.430439	-0.420843	0.009595	-0.408762	-0.411461	-0.002699
8	0.63425	-0.245935	-0.239136	0.006799	-0.235853	-0.240389	-0.004536
9	0.73425	-0.109175	-0.105430	0.003744	-0.108210	-0.111634	-0.003423
10	0.85925	0.029209	0.030150	0.000941	0.027894	0.024303	-0.003590

****
TEST CONDS-VF=11 KPS, ALPHA=0.0 DEGREE, VI/VF=0.3, 30 PCT CHORD PRESS SIDE INJ. OF POLYOX
****

	VFN	VFW	CDN	CDW	CDW-CDN	CLN	CLW	CLW-CLN
AVG VALUE	11.0096	11.0097	0.0116244	0.0106654	-0.0009589	0.0013406	0.0228917	0.0215511
STAND DEV	0.0205	0.0220	0.0000704	0.0000661	0.0001137	0.0003123	0.0006841	0.0006383

PRESS TAP	X/C	CPPN	CPPW	CPPW-CPPN	CPSN	CPSW	CPSW-CPSN
1	0.18425	-0.558738	-0.547456	0.011281	-0.603957	-0.612265	-0.008308
2	0.23425	-0.559101	-0.547077	0.012024	-0.611213	-0.622462	-0.011248
3	0.28675	-0.578097	-0.560359	0.017738	-0.636879	-0.646719	-0.009839
4	0.35925	-0.563584	-0.641601	-0.078017	-0.584947	-0.593675	-0.008727
5	0.38425	-0.551605	-0.559441	-0.007835	-0.559072	-0.570855	-0.011782
6	0.43425	-0.515486	-0.519520	-0.004034	-0.514687	-0.526606	-0.011919
7	0.53425	-0.428204	-0.414504	0.013699	-0.404516	-0.415076	-0.010560
8	0.63425	-0.243799	-0.234621	0.009178	-0.233099	-0.244810	-0.011711
9	0.73425	-0.107265	-0.095834	0.011431	-0.104377	-0.117478	-0.013101
10	0.85925	0.032147	0.041718	0.009571	0.032600	0.016209	-0.016391

****

TEST CONDS-VF=11 FPS, ALPHA=2.5 DEGREE, VI/VF=0.1, 10 PCT CHORD SUCTN SIDE INJ. OF POLYOX

****

	VFN	VFW	CDN	CDW	CDW-CDN	CLN	CLW	CLW-CLN
AVG VALUE	11.0134	11.0133	0.0179885	0.0170871	-0.0009013	0.1863614	0.1988256	0.0124642
STAND DEV	0.0160	0.0197	0.0001186	0.0000957	0.0001605	0.0006497	0.0004603	0.0006857

PRESS TAP	X/C	CPPN	CPPW	CPPW-CPPN	CPSN	CPSW	CPSW-CPSN
1	0.18425	-0.394242	-0.390475	0.003766	-0.761265	-0.749650	0.011615
2	0.23425	-0.420888	-0.416682	0.004206	-0.732332	-0.726762	0.005569
3	0.24675	-0.439752	-0.433202	0.006549	-0.756474	-0.756469	0.000005
4	0.35925	-0.463564	-0.465585	-0.002020	-0.678827	-0.689743	-0.010915
5	0.38425	-0.465396	-0.462641	0.003254	-0.644439	-0.663444	-0.019005
6	0.43425	-0.437497	-0.432628	0.005069	-0.589450	-0.605569	-0.016119
7	0.53425	-0.373904	-0.368196	0.005708	-0.451182	-0.460291	-0.009109
8	0.63425	-0.212518	-0.205605	0.006913	-0.260153	-0.269852	-0.009699
9	0.73425	-0.093869	-0.087765	0.006104	-0.118285	-0.124026	-0.005740
10	0.85925	0.028947	0.034750	0.005803	0.033449	0.030207	-0.003241

****

TEST CONDS-VF=11 FPS, ALPHA=2.5 DEGREE, VI/VF=0.3, 10 PCT CHORD SUCTN SIDE INJ. OF POLYOX

****

	VFN	VFW	CDN	CDW	CDW-CDN	CLN	CLW	CLW-CLN
AVG VALUE	11.0137	11.0152	0.0160191	0.0162587	-0.0017603	0.1869955	0.1769551	-0.0100404
STAND DEV	0.0188	0.0172	0.0000586	0.0001129	0.0001461	0.0006784	0.0010057	0.0007917

PRESS TAP	X/C	CPPN	CPPW	CPPW-CPPN	CPSN	CPSW	CPSW-CPSN
1	0.18425	-0.392002	-0.396894	-0.006891	-0.762217	-0.740486	0.021731
2	0.23425	-0.419054	-0.422262	-0.004207	-0.734399	-0.721400	0.012999
3	0.24675	-0.438909	-0.442362	-0.003453	-0.762092	-0.750624	0.011468
4	0.35925	-0.460554	-0.466343	-0.005789	-0.684179	-0.677026	0.007152
5	0.38425	-0.462041	-0.467269	-0.004628	-0.648057	-0.654600	-0.006563
6	0.43425	-0.437317	-0.442451	-0.005134	-0.594179	-0.598869	-0.004690
7	0.53425	-0.373107	-0.377752	-0.004645	-0.455548	-0.448281	0.007266
8	0.63425	-0.211468	-0.216735	-0.005266	-0.263841	-0.264141	-0.000300
9	0.73425	-0.093290	-0.095790	-0.002500	-0.121060	-0.120344	0.000716
10	0.85925	0.030897	0.019102	-0.011794	0.031579	0.034228	0.002648

TEST CONDS-VF=11 FPS, ALPHA=2.5 DEGREE, VI/VF=0.1, 30 PCT CHORD PRESS SIDE INJ. OF POLYOX

	VFN	VFW	CDN	CDW	CDW-CDN	CLN	CLW	CLW-CLN
AVG VALUE	11.0289	11.0290	0.0180359	0.0173190	-0.0007169	0.1864442	0.1923061	0.0058618
STAND DEV	0.0293	0.0279	0.0000692	0.0001579	0.0001697	0.0006845	0.0014529	0.0014404

PRESS TAP	X/C	CPPN	CPPW	CPPW-CPPN	CPSN	CPSW	CPSW-CPSN
1	0.18425	-0.391886	-0.388248	0.003557	-0.760216	-0.768574	-0.008357
2	0.23425	-0.419287	-0.413321	0.005966	-0.740952	-0.736415	0.004536
3	0.28675	-0.440879	-0.435865	0.003013	-0.759665	-0.764074	-0.004408
4	0.35325	-0.467600	-0.517173	-0.049572	-0.679424	-0.682128	-0.002703
5	0.38425	-0.496630	-0.493166	-0.003535	-0.642928	-0.646693	-0.003765
6	0.43425	-0.436421	-0.435604	0.000816	-0.590274	-0.592797	-0.002522
7	0.53425	-0.374141	-0.371729	0.002412	-0.451197	-0.455598	-0.004401
8	0.63425	-0.211867	-0.210899	0.000967	-0.261233	-0.264726	-0.003493
9	0.73425	-0.094723	-0.100079	-0.005356	-0.118413	-0.122000	-0.003587
10	0.85925	0.032076	0.033440	0.001364	0.033375	0.028695	-0.004679

TEST CONDS-VF=11 FPS, ALPHA=2.5 DEGREE, VI/VF=0.3, 30 PCT CHORD PRESS SIDE INJ. OF POLYOX

	VFN	VFW	CDN	CDW	CDW-CDN	CLN	CLW	CLW-CLN
AVG VALUE	11.0037	10.9980	0.0179715	0.0175835	-0.0003880	0.1863617	0.2060217	0.0196599
STAND DEV	0.0160	0.0302	0.0000692	0.0001089	0.0001268	0.0005811	0.0006735	0.0009714

PRESS TAP	X/C	CPPN	CPPW	CPPW-CPPN	CPSN	CPSW	CPSW-CPSN
1	0.18425	-0.389397	-0.379251	0.009146	-0.764801	-0.774291	-0.009489
2	0.23425	-0.418845	-0.403884	0.014960	-0.743354	-0.751286	-0.007932
3	0.28675	-0.442759	-0.425602	0.017157	-0.764147	-0.771420	-0.007272
4	0.35025	-0.470789	-0.549148	-0.078359	-0.681725	-0.693059	-0.011333
5	0.38425	-0.463274	-0.467793	-0.004518	-0.643712	-0.653878	-0.010166
6	0.43425	-0.436693	-0.442171	-0.005478	-0.590742	-0.599021	-0.008278
7	0.53425	-0.373273	-0.362968	0.010304	-0.453027	-0.463255	-0.010228
8	0.63425	-0.211668	-0.206407	0.005261	-0.261742	-0.271811	-0.010068
9	0.73425	-0.093902	-0.082022	0.011879	-0.119927	-0.132353	-0.012426
10	0.85925	0.030738	0.036766	0.006028	0.031080	0.016959	-0.014121

TEST CONDS-VF=11 MPS, ALPHA=5.0 DEGREE, VI/VF=0.1, 10 PCT CHORD SUCTN SIDE INJ. OF POLYOX

	VFN	VFW	CDN	CDW	CDW-CDN	CLN	CLW	CLW-CLN
AVG VALUE	11.0112	11.0099	0.0302424	0.0301225	-0.0001199	0.3745012	0.4069481	0.0324469
STAND DEV	0.0209	0.0303	0.0001826	0.0001736	0.0002367	0.0009420	0.0015181	0.0020015

PRESS TAP	X/C	CPPN	CPPW	CPPW-CPPN	CPSN	CPSW	CPSW-CPSN
1	0.18425	-0.222790	-0.206490	0.016299	-0.917870	-0.927009	-0.009138
2	0.23425	-0.268637	-0.254941	0.013695	-0.860644	-0.878746	-0.018101
3	0.28675	-0.294491	-0.281042	0.013448	-0.884757	-0.907559	-0.022801
4	0.35925	-0.365471	-0.360589	0.004881	-0.760326	-0.789115	-0.028789
5	0.38425	-0.369427	-0.357221	0.012205	-0.721276	-0.762356	-0.041080
6	0.43425	-0.349022	-0.336197	0.012825	-0.653603	-0.678357	-0.024754
7	0.53425	-0.311227	-0.298453	0.012773	-0.489559	-0.519588	-0.030028
8	0.63425	-0.175598	-0.160382	0.015216	-0.279434	-0.308489	-0.029055
9	0.73425	-0.073837	-0.058316	0.015521	-0.124650	-0.150331	-0.025681
10	0.85925	0.027216	0.044862	0.017645	0.034165	0.022016	-0.012169

TEST CONDS-VF=11 MPS, ALPHA=5.0 DEGREE, VI/VF=0.3, 10 PCT CHORD SUCTN SIDE INJ. OF POLYOX

	VFN	VFW	CDN	CDW	CDW-CDN	CLN	CLW	CLW-CLN
AVG VALUE	11.0071	11.0065	0.0302552	0.0291168	-0.0011384	0.3747288	0.3901750	0.0154462
STAND DEV	0.0150	0.0184	0.0001150	0.0001047	0.0001749	0.0012261	0.0011128	0.0014164

PRESS TAP	X/C	CPPN	CPPW	CPPW-CPPN	CPSN	CPSW	CPSW-CPSN
1	0.18425	-0.220940	-0.215253	0.005686	-0.921466	-0.913702	0.007763
2	0.23425	-0.270210	-0.264082	0.006127	-0.859824	-0.866796	-0.006971
3	0.28675	-0.292824	-0.285539	0.007284	-0.885809	-0.903950	-0.018140
4	0.35925	-0.376012	-0.371388	0.004624	-0.760794	-0.771737	-0.010942
5	0.38425	-0.369818	-0.370567	-0.000748	-0.718809	-0.743481	-0.024672
6	0.43425	-0.349288	-0.344105	0.005182	-0.653970	-0.669155	-0.015185
7	0.53425	-0.311568	-0.306464	0.005103	-0.489844	-0.492558	-0.002714
8	0.63425	-0.174987	-0.169475	0.005512	-0.278984	-0.297102	-0.018117
9	0.73425	-0.073129	-0.066982	0.006145	-0.124841	-0.144778	-0.019937
10	0.85925	0.028385	0.036422	0.008037	0.035091	0.019388	-0.015702

TEST CONDS-VF=11 MPS, ALPHA=5.0 DEGREE, VI/VF=0.1, 30 PCT CHORD PRESS SIDE INJ. OF POLYOX

	VFN	VFW	CDN	CDW	CDW-CDN	CLN	CLW	CLW-CLN
AVG VALUE	10.9938	10.9978	0.0303100	0.0294462	-0.0008638	0.3734401	0.3777253	0.0042852
STAND DEV	0.0140	0.0141	0.0001254	0.0001548	0.0002246	0.0007233	0.0012815	0.0014348

PRESS TAP	X/C	CPPN	CPPW	CPPW-CPPN	CPSN	CPSW	CPSW-CPSN
1	0.18425	-0.221971	-0.215373	0.006498	-0.921293	-0.920595	0.000698
2	0.23425	-0.269177	-0.266713	0.002464	-0.859320	-0.861863	-0.002543
3	0.28675	-0.293004	-0.289315	0.004688	-0.884574	-0.885155	-0.000581
4	0.35925	-0.368995	-0.418223	-0.049228	-0.758365	-0.762336	-0.003970
5	0.38425	-0.371640	-0.396546	-0.024906	-0.720242	-0.722287	-0.002044
6	0.43425	-0.349658	-0.352534	-0.002875	-0.651859	-0.654428	-0.002568
7	0.53425	-0.312191	-0.310116	0.002074	-0.487469	-0.491394	-0.003925
8	0.63425	-0.175292	-0.171487	0.003805	-0.278397	-0.281402	-0.003005
9	0.73425	-0.074800	-0.073826	0.000973	-0.124635	-0.125225	-0.000590
10	0.85925	0.025856	0.025683	-0.000173	0.034791	0.032197	-0.002593

TEST CONDS-VF=11 MPS, ALPHA=5.0 DEGREE, VI/VF=0.3, 30 PCT CHORD PRESS SIDE INJ. OF POLYOX

	VFN	VFW	CDN	CDW	CDW-CDN	CLN	CLW	CLW-CLN
AVG VALUE	11.0236	11.0195	0.0303077	0.0295027	-0.0008050	0.3745250	0.3880372	0.0135122
STAND DEV	0.0141	0.0135	0.0002444	0.0001297	0.0003067	0.0010293	0.0014895	0.0012194

PRESS TAP	X/C	CPPN	CPPW	CPPW-CPPN	CPSN	CPSW	CPSW-CPSN
1	0.18425	-0.219360	-0.214039	0.005320	-0.919659	-0.925433	-0.005773
2	0.23425	-0.268236	-0.259484	0.008752	-0.863235	-0.869122	-0.005886
3	0.28675	-0.292264	-0.279933	0.012330	-0.884773	-0.888524	-0.003750
4	0.35925	-0.375579	-0.433199	-0.057519	-0.759869	-0.765822	-0.005952
5	0.38425	-0.374911	-0.410808	-0.035897	-0.721286	-0.727000	-0.005713
6	0.43425	-0.349992	-0.363972	-0.013980	-0.652405	-0.658442	-0.006036
7	0.53425	-0.311942	-0.306623	0.005319	-0.489798	-0.497562	-0.007764
8	0.63425	-0.174775	-0.167693	0.007082	-0.278850	-0.287297	-0.008446
9	0.73425	-0.073663	-0.069355	0.004308	-0.123649	-0.133716	-0.010066
10	0.85925	0.026590	0.028321	0.001731	0.035463	0.025930	-0.009533

****

TEST CONDS-VF=11 MPS, ALPH=3.25 DEGREE, VI/VF=0.1, 10 PCT CHORD PRESS SIDE INJ. OF POLYOX

****

	VFN	VFW	CDN	CDW	CDW-CDN	CLN	CLW	CLW-CLN
AVG VALUE	11.0130	11.0100	0.0207687	0.0196222	-0.0011464	0.2537046	0.2512176	-0.0024870
STAND DEV	0.0166	0.0131	0.0000443	0.0001102	0.0000894	0.0012408	0.0015016	0.0013542

PRESS TAP	X/C	CPPN	CPPW	CPPW-CPPN	CPSN	CPSW	CPSW-CPSN
1	0.14425	-0.383340	-0.372000	0.011939	-0.763749	-0.766055	-0.002305
2	0.23425	-0.421984	-0.394087	0.027817	-0.733868	-0.732824	0.001044
3	0.24575	-0.450756	-0.425038	0.025717	-0.754082	-0.753180	0.000902
4	0.35925	-0.467682	-0.455236	0.012446	-0.652704	-0.647988	0.004716
5	0.38425	-0.447348	-0.449671	-0.002323	-0.673192	-0.674250	-0.001058
6	0.43425	-0.407421	-0.423906	-0.016484	-0.625759	-0.626806	-0.001047
7	0.53425	-0.332412	-0.340410	-0.007998	-0.499521	-0.498470	0.001051
8	0.63425	-0.198491	-0.195775	-0.002283	-0.284859	-0.284351	0.000508
9	0.73425	-0.090926	-0.088182	-0.007355	-0.130169	-0.128073	0.002096
10	0.85925	0.032173	0.031261	-0.000912	0.027621	0.031375	0.003753

****

TEST CONDS-VF=11 MPS, ALPH=3.25 DEGREE, VI/VF=0.3, 10 PCT CHORD PRESS SIDE INJ. OF POLYOX

****

	VFN	VFW	CDN	CDW	CDW-CDN	CLN	CLW	CLW-CLN
AVG VALUE	11.0158	11.0116	0.0208420	0.0199182	-0.0009237	0.2533769	0.2672190	0.0138421
STAND DEV	0.0229	0.0293	0.0000215	0.0000519	0.0000490	0.0012382	0.0018637	0.0024546

PRESS TAP	X/C	CPPN	CPPW	CPPW-CPPN	CPSN	CPSW	CPSW-CPSN
1	0.14425	-0.321454	-0.357465	0.023968	-0.766420	-0.779692	-0.013271
2	0.23425	-0.420737	-0.386971	0.033765	-0.736064	-0.738487	-0.002422
3	0.24575	-0.449699	-0.419885	0.030814	-0.749961	-0.755321	-0.005360
4	0.35925	-0.463772	-0.446955	0.016816	-0.643896	-0.649255	-0.005358
5	0.38425	-0.440466	-0.437123	0.003343	-0.673531	-0.679686	-0.006154
6	0.43425	-0.406019	-0.415012	-0.008993	-0.624512	-0.633806	-0.009293
7	0.53425	-0.332425	-0.330179	0.002246	-0.499289	-0.508839	-0.009550
8	0.63425	-0.186399	-0.186085	0.002313	-0.286312	-0.293920	-0.007607
9	0.73425	-0.080373	-0.078404	0.001969	-0.132588	-0.139826	-0.007237
10	0.85925	0.033461	0.040060	0.006598	0.025574	0.015275	-0.010299

****

TEST CONDS-VF=11 FPS, ALPH=3.25 DEGREE, WI/WF=0.1, 30 PCT CHORD SUCTN SIDE INJ. OF POLYOX

****

	VFL	VFA	CDL	CDA	CDA-CDL	CLN	CLW	CLW-CLN
AVG VALUE	11.0146	11.0156	0.0076123	0.0231160	-0.0076939	0.2548542	0.2556195	0.0007652
STAND DEV	0.0152	0.0221	0.0000393	0.0000582	0.0000591	0.0014906	0.0015811	0.0016914

PRESS TAP	X/C	CPPL	CPPA	CPPA-CPPL	CPSN	CPSW	CPSW-CPSN
1	0.1[illegible]25	-0.3[illegible]0487	-0.3[illegible]0018	0.000470	-0.765064	-0.767203	-0.002138
2	0.2[illegible]25	-0.4[illegible]0561	-0.4[illegible]7293	0.000268	-0.736672	-0.734770	0.002101
3	0.4[illegible]75	-0.[illegible]07297	-0.[illegible]45372	0.000724	-0.752691	-0.746441	0.006249
4	0.[illegible]725	-0.4[illegible]0423	-0.4[illegible]3287	0.000132	-0.[illegible]0599	-0.726362	-0.075762
5	0.[illegible]25	-0.[illegible]0502	-0.[illegible]3231	-0.000267	-0.673163	-0.695807	-0.022644
6	0.[illegible]25	-0.[illegible]6422	-0.[illegible]7044	-0.000460	-0.424704	-0.431083	-0.006379
7	0.[illegible]25	-0.3[illegible]97	-0.[illegible]52	-0.000155	-0.500220	-0.504131	-0.003911
8	0.[illegible]25	-0.[illegible]50	-0.[illegible]33	-0.000423	-0.286939	-0.288271	-0.001331
9	0.75-25	-0.079271	-0.[illegible]9639	-0.000361	-0.130849	-0.133079	-0.002230
10	0.[illegible]925	0.[illegible]34714	0.[illegible]34715	0.000401	0.026946	0.023815	-0.003131

****

TEST CONDS-VF=11 FPS, ALPH=3.25 DEGREE, WI/WF=0.3, 30 PCT CHORD SUCTN SIDE INJ. OF POLYOX

****

	VFL	VFA	CDL	CDA	CDA-CDL	CLN	CLW	CLW-CLN
AVG VALUE	11.0213	11.0353	0.0076488	0.0192326	-0.0016056	0.2531069	0.2270100	-0.0260969
STAND DEV	0.0140	0.0197	0.0000408	0.0000665	0.0000697	0.0012995	0.0016513	0.0017955

PRESS TAP	X/C	CPPL	CPPA	CPPA-CPPL	CPSN	CPSW	CPSW-CPSN
1	0.1[illegible]25	-0.3[illegible]0498	-0.3[illegible]93229	-0.012535	-0.764208	-0.747296	0.016911
2	0.2[illegible]25	-0.4[illegible]7337	-0.4[illegible]1755	-0.014952	-0.730438	-0.721533	0.008904
3	0.4[illegible]75	-0.4[illegible]9217	-0.[illegible]9[illegible]212	-0.[illegible]09990	-0.749380	-0.730545	0.018834
4	0.[illegible]725	-0.4[illegible]7297	-0.473191	-0.[illegible]33894	-0.647195	-0.747183	-0.099988
5	0.[illegible]25	-0.4[illegible]3721	-0.[illegible]52[illegible]14	-0.[illegible]95494	-0.671652	-0.712424	-0.040791
6	0.[illegible]25	-0.[illegible][illegible]9[illegible]	-0.[illegible]17277	-0.[illegible]13257	-0.623442	-0.623021	0.000600
7	0.[illegible]25	-0.3[illegible]257	-0.[illegible]42137	-0.011780	-0.498419	-0.480475	0.017944
8	0.[illegible]25	-0.[illegible]96791	-0.[illegible]99465	-0.012665	-0.285322	-0.269408	0.015914
9	0.75-25	-0.[illegible]75[illegible]3	-0.[illegible]95329	-0.016465	-0.131255	-0.118369	0.012886
10	0.[illegible]925	-0.[illegible]33764	0.[illegible]17115	-0.016649	0.027051	0.033580	0.006528

****
TEST CONDS-VF=11 KPS, ALPHA=5.0 DEGREE, VI/VF=0.1, 10 PCT CHORD PRESS SIDE INJ. OF POLYOX
****

	VFI	VFA	CDI	CDW	CDW-CDI	CLI	CLW	CLW-CLI
AVG VALUE	11.0103	11.0107	0.0293155	0.0276298	-0.0016857	0.3923050	0.3912163	-0.0010886
STAND DEV	0.0117	0.0127	0.0001251	0.0002362	0.0002639	0.0012995	0.0010066	0.0015159

PRESS TAP	X/C	CPPI	CPPA	CPPW-CPPI	CPSN	CPSW	CPSW-CPSN
1	0.18425	-0.243640	-0.254817	0.008822	-0.877360	-0.874242	0.003118
2	0.23425	-0.319096	-0.290983	0.022102	-0.817876	-0.819152	-0.001275
3	0.28475	-0.350477	-0.323748	0.026729	-0.840383	-0.842062	-0.001679
4	0.33425	-0.394180	-0.385695	0.008492	-0.695702	-0.695547	0.000154
5	0.38425	-0.376494	-0.374354	0.002140	-0.740292	-0.741148	-0.000855
6	0.43425	-0.359609	-0.369479	-0.015498	-0.681608	-0.681133	0.000474
7	0.53425	-0.295246	-0.303761	-0.008515	-0.534382	-0.532979	0.001403
8	0.63425	-0.166047	-0.173374	-0.007326	-0.303777	-0.303498	0.000279
9	0.73425	-0.070105	-0.075629	-0.005524	-0.138164	-0.136801	0.001363
10	0.85925	0.027347	0.026429	0.000452	0.028632	0.030372	0.001739

****
TEST CONDS-VF=11 KPS, ALPHA=5.0 DEGREE, VI/VF=0.3, 10 PCT CHORD PRESS SIDE INJ. OF POLYOX
****

	VFI	VFA	CDI	CDW	CDW-CDI	CLI	CLW	CLW-CLI
AVG VALUE	11.0162	11.0152	0.0292947	0.0277290	-0.0015646	0.3904718	0.4009047	0.0104328
STAND DEV	0.0173	0.0242	0.0001515	0.0003657	0.0003979	0.0013297	0.0025631	0.0020407

PRESS TAP	X/C	CPPI	CPPA	CPPW-CPPI	CPSN	CPSW	CPSW-CPSN
1	0.18425	-0.245997	-0.245806	0.019290	-0.871286	-0.883836	-0.012550
2	0.23425	-0.317466	-0.294287	0.023180	-0.807695	-0.810552	-0.002856
3	0.28475	-0.350314	-0.326411	0.023903	-0.833485	-0.836978	-0.003493
4	0.33425	-0.396417	-0.383660	0.012759	-0.691999	-0.696020	-0.004021
5	0.38425	-0.373330	-0.374051	-0.000721	-0.739961	-0.744530	-0.004569
6	0.43425	-0.356141	-0.365230	-0.009090	-0.679113	-0.685110	-0.005997
7	0.53425	-0.297525	-0.298465	-0.000939	-0.529636	-0.532983	-0.003347
8	0.63425	-0.167547	-0.167533	0.000015	-0.302640	-0.310360	-0.007719
9	0.73425	-0.071198	-0.068756	0.002441	-0.138083	-0.144353	-0.006270
10	0.85925	0.027502	0.033302	0.005799	0.027559	0.019536	-0.008023

TEST CONDS-VF=11 KPS, ALPHA=5.0 DEGREE, VI/VF=0.1, 30 PCT CHORD SUCTN SIDE INJ. OF POLYOX

	VFN	VFW	CDN	CDW	CDW-CDN	CLN	CLW	CLW-CLN
AVG VALUE	11.0216	11.0242	0.0293482	0.0285053	-0.0008629	0.3916790	0.3967645	0.0050854
STAND DEV	0.0122	0.0116	0.0001132	0.0002333	0.0002622	0.0019412	0.0015780	0.0025114

PRESS TAP	X/C	CPPN	CPPW	CPPW-CPPN	CPSN	CPSW	CPSW-CPSN
1	0.18425	-0.263167	-0.264215	-0.001048	-0.871581	-0.873291	-0.001710
2	0.23425	-0.319273	-0.315977	0.003295	-0.810892	-0.808187	0.002705
3	0.28675	-0.349103	-0.348870	0.000233	-0.834359	-0.833893	0.000465
4	0.35925	-0.392701	-0.391208	0.001493	-0.695916	-0.777622	-0.081706
5	0.38425	-0.376190	-0.370115	0.006074	-0.739945	-0.754050	-0.014104
6	0.43425	-0.354368	-0.352267	0.002101	-0.679749	-0.685153	-0.005404
7	0.53425	-0.296831	-0.294768	0.002063	-0.532783	-0.539076	-0.006292
8	0.63425	-0.166923	-0.164478	0.002449	-0.303886	-0.311053	-0.007166
9	0.73425	-0.070379	-0.067071	0.003308	-0.139058	-0.147476	-0.008418
10	0.85925	0.027976	0.032854	0.004878	0.026892	0.019541	-0.007351

TEST CONDS-VF=11 KPS, ALPHA=5.0 DEGREE, VI/VF=0.3, 30 PCT CHORD SUCTN SIDE INJ. OF POLYOX

	VFN	VFW	CDN	CDW	CDW-CDN	CLN	CLW	CLW-CLN
AVG VALUE	11.0211	11.0177	0.0298328	0.0277508	-0.0015811	0.3897280	0.3710314	-0.0186967
STAND DEV	0.0162	0.0155	0.0001222	0.0001996	0.0003110	0.0012070	0.0014489	0.0021727

PRESS TAP	X/C	CPPN	CPPW	CPPW-CPPN	CPSN	CPSW	CPSW-CPSN
1	0.18425	-0.246357	-0.272251	-0.005894	-0.874171	-0.861139	0.013031
2	0.23425	-0.319898	-0.327056	-0.007158	-0.808819	-0.795112	0.013706
3	0.28675	-0.349622	-0.359249	-0.009426	-0.826095	-0.812010	0.014084
4	0.35925	-0.393517	-0.401594	-0.008076	-0.695862	-0.805890	-0.110027
5	0.38425	-0.376240	-0.378371	-0.002130	-0.741135	-0.773339	-0.032204
6	0.43425	-0.354752	-0.363250	-0.008497	-0.681105	-0.679025	0.002080
7	0.53425	-0.297562	-0.306147	-0.008584	-0.532437	-0.513082	0.019354
8	0.63425	-0.166767	-0.176930	-0.010163	-0.304415	-0.291995	0.012419
9	0.73425	-0.070460	-0.080722	-0.010262	-0.137970	-0.133289	0.004680
10	0.85925	0.027680	0.017828	-0.009860	0.027860	0.020786	-0.007074

TEST CONDS-VF=11 FPS, ALPHA=0.0 DEGREE, VI/VF=0.1, 10 PCT CHORD SUCTN SIDE INJ. OF PAM

	VFN	VFW	CDN	CDW	CDW-CDN	CLN	CLW	CLW-CLN
AVG VALUE	11.0171	11.0147	0.0117625	0.0105875	-0.0011749	0.0021390	0.0121556	0.0100166
STAND DEV	0.0156	0.0306	0.0000603	0.0000745	0.0000597	0.0005565	0.0009631	0.0009342

PRESS TAP	X/C	CPPN	CPPW	CPPW-CPPN	CPSN	CPSW	CPSW-CPSN
1	0.18425	-0.556697	-0.551584	0.005413	-0.605065	-0.596244	0.008821
2	0.23425	-0.561181	-0.555499	0.005681	-0.601086	-0.596449	0.004637
3	0.28675	-0.575482	-0.574460	0.004022	-0.628135	-0.624497	0.003638
4	0.33925	-0.552049	-0.552293	-0.000043	-0.587105	-0.601075	-0.013970
5	0.38425	-0.556722	-0.551126	0.005595	-0.555863	-0.577183	-0.021319
6	0.43425	-0.517496	-0.514754	0.003051	-0.516148	-0.537685	-0.021536
7	0.53425	-0.428563	-0.423830	0.004837	-0.406002	-0.419551	-0.013548
8	0.63425	-0.242997	-0.239509	0.003466	-0.234981	-0.242011	-0.007030
9	0.73425	-0.107607	-0.104158	0.003449	-0.106903	-0.116073	-0.009089
10	0.85925	0.032227	0.035557	0.003329	0.027926	0.024110	-0.003816

TEST CONDS-VF=11 FPS, ALPHA=0.0 DEGREE, VI/VF=0.3, 10 PCT CHORD SUCTN SIDE INJ. OF PAM

	VFN	VFW	CDN	CDW	CDW-CDN	CLN	CLW	CLW-CLN
AVG VALUE	11.0056	11.0114	0.0120715	0.0105940	-0.0014775	0.0020644	-0.0005881	-0.0026526
STAND DEV	0.0164	0.0228	0.0000660	0.0000570	0.0000792	0.0007815	0.0009364	0.0011420

PRESS TAP	X/C	CPPN	CPPW	CPPW-CPPN	CPSN	CPSW	CPSW-CPSN
1	0.18425	-0.553966	-0.560054	-0.006088	-0.604200	-0.592843	0.011357
2	0.23425	-0.562631	-0.564355	-0.001724	-0.604005	-0.590541	0.013463
3	0.28675	-0.581140	-0.583054	-0.001913	-0.630647	-0.615496	0.015350
4	0.33925	-0.566550	-0.565344	0.000793	-0.585774	-0.594115	-0.009340
5	0.38425	-0.556810	-0.556753	0.000743	-0.556976	-0.578880	-0.021904
6	0.43425	-0.519600	-0.520863	-0.001262	-0.515106	-0.531762	-0.016655
7	0.53425	-0.431166	-0.433495	-0.002328	-0.407924	-0.411082	-0.003157
8	0.63425	-0.245051	-0.247455	-0.002404	-0.235171	-0.237967	-0.002795
9	0.73425	-0.109472	-0.112626	-0.003154	-0.105881	-0.111488	-0.005606
10	0.85925	0.029908	0.023456	-0.006451	0.027798	0.028245	0.000446

****

TEST CONDS-VF=11 KPS, ALPHA=0.0 DEGREE, VI/VF=0.1, 30 PCT CHORD PRESS SIDE INJ. OF PAM

****

	VFN	VFW	CDN	CDW	CDW-CDN	CLN	CLW	CLW-CLN
AVG VALUE	11.0142	11.0184	0.0116090	0.0111291	-0.0007599	0.0023979	0.0012297	-0.0011682
STAND DEV	0.0258	0.0366	0.0000464	0.0000968	0.0000763	0.0005734	0.0006272	0.0007869

PRESS TAP	X/C	CPPN	CPPW	CPPW-CPPN	CPSN	CPSW	CPSW-CPSN
1	0.19425	-0.550636	-0.553512	0.001324	-0.603398	-0.603174	0.000223
2	0.23425	-0.561669	-0.561973	0.000295	-0.611184	-0.607904	0.003279
3	0.24675	-0.577677	-0.574332	0.003345	-0.635743	-0.632871	0.002871
4	0.35925	-0.555216	-0.612106	-0.056890	-0.581726	-0.583608	-0.001882
5	0.42425	-0.553651	-0.591702	-0.037850	-0.556406	-0.555947	0.000458
6	0.43425	-0.517221	-0.521973	-0.004751	-0.516648	-0.516128	0.000519
7	0.53425	-0.428861	-0.432991	-0.004130	-0.406145	-0.406005	0.000139
8	0.63425	-0.242965	-0.246188	-0.003223	-0.234986	-0.234012	0.000973
9	0.73425	-0.107618	-0.113209	-0.005590	-0.106992	-0.106951	0.000041
10	0.85925	0.031176	0.028976	-0.002200	0.027993	0.028293	0.000299

****

TEST CONDS-VF=11 KPS, ALPHA=0.0 DEGREE, VI/VF=0.3, 30 PCT CHORD PRESS SIDE INJ. OF PAM

****

	VFN	VFW	CDN	CDW	CDW-CDN	CLN	CLW	CLW-CLN
AVG VALUE	11.0136	11.0115	0.0120276	0.0109276	-0.0011000	0.0025052	0.0188762	0.0163709
STAND DEV	0.0130	0.0191	0.0000364	0.0000711	0.0000588	0.0007054	0.0010928	0.0014251

PRESS TAP	X/C	CPPN	CPPW	CPPW-CPPN	CPSN	CPSW	CPSW-CPSN
1	0.19425	-0.554677	-0.548340	0.006337	-0.605390	-0.612701	-0.007311
2	0.23425	-0.561846	-0.550783	0.011062	-0.611280	-0.614974	-0.003693
3	0.24675	-0.578834	-0.567565	0.011269	-0.636557	-0.641721	-0.005164
4	0.35925	-0.553077	-0.600639	-0.047561	-0.583925	-0.590957	-0.007031
5	0.42425	-0.554931	-0.587933	-0.033002	-0.557954	-0.564022	-0.006067
6	0.43425	-0.516624	-0.518681	-0.002057	-0.516396	-0.523817	-0.007421
7	0.53425	-0.427973	-0.419822	0.008151	-0.406753	-0.415462	-0.008709
8	0.63425	-0.244102	-0.235442	0.008659	-0.235266	-0.244592	-0.009326
9	0.73425	-0.108672	-0.104266	0.004406	-0.105089	-0.116561	-0.011471
10	0.85925	0.030121	0.035165	0.005043	0.028301	0.017168	-0.011132

****

TEST CONDS-VF=11 KPS, ALPHA=2.5 DEGREE, VI/VF=0.1, 10 PCT CHORD SUCTN SIDE INJ. OF PAM

****

	VFN	VFW	CDN	CDW	CDW-CDN	CLN	CLW	CLW-CLN
AVG VALUE	11.0090	11.0129	0.0170641	0.0173363	-0.0007517	0.1855851	0.2064920	0.0209068
STAND DEV	0.0167	0.0181	0.0000630	0.0001219	0.0001472	0.0005114	0.0008783	0.0011475

PRESS TAP	X/C	CPPN	CPPW	CPPW-CPPN	CPSN	CPSW	CPSW-CPSN
1	0.18425	-0.395387	-0.384892	0.010495	-0.765525	-0.764207	0.001317
2	0.23425	-0.422771	-0.414385	0.008386	-0.737136	-0.748510	-0.011373
3	0.28675	-0.442574	-0.434274	0.008299	-0.758208	-0.771385	-0.013177
4	0.35925	-0.475420	-0.465106	0.010313	-0.680011	-0.703335	-0.023324
5	0.38425	-0.472917	-0.462348	0.010568	-0.646024	-0.674916	-0.028892
6	0.43425	-0.439876	-0.430907	0.008968	-0.590958	-0.624347	-0.033409
7	0.53425	-0.375275	-0.366330	0.008945	-0.452693	-0.473050	-0.020357
8	0.63425	-0.213535	-0.203306	0.010229	-0.261087	-0.276308	-0.015220
9	0.73425	-0.095820	-0.083508	0.012312	-0.119023	-0.135920	-0.016897
10	0.85925	0.027258	0.040197	0.012938	0.031627	0.021333	-0.010293

****

TEST CONDS-VF=11 KPS, ALPHA=2.5 DEGREE, VI/VF=0.3, 10 PCT CHORD SUCTN SIDE INJ. OF PAM

****

	VFN	VFW	CDN	CDW	CDW-CDN	CLN	CLW	CLW-CLN
AVG VALUE	11.0106	11.0147	0.0170891	0.0164680	-0.0014210	0.1856171	0.1937379	0.0081208
STAND DEV	0.0284	0.0316	0.0000457	0.0000785	0.0001340	0.0006523	0.0011472	0.0011618

PRESS TAP	X/C	CPPN	CPPW	CPPW-CPPN	CPSN	CPSW	CPSW-CPSN
1	0.18425	-0.390921	-0.390443	0.000477	-0.764825	-0.755363	0.009461
2	0.23425	-0.422690	-0.417923	0.004766	-0.738654	-0.731568	0.007085
3	0.28675	-0.441743	-0.436191	0.005552	-0.761853	-0.757595	0.004258
4	0.35925	-0.476294	-0.469531	0.006763	-0.680585	-0.691112	-0.010526
5	0.38425	-0.473053	-0.473054	0.000054	-0.645219	-0.667664	-0.022444
6	0.43425	-0.437781	-0.435172	0.002608	-0.590639	-0.608129	-0.017489
7	0.53425	-0.374515	-0.371143	0.003371	-0.453330	-0.459023	-0.005693
8	0.63425	-0.213990	-0.210379	0.003610	-0.262767	-0.273519	-0.010751
9	0.73425	-0.096137	-0.091018	0.005119	-0.119678	-0.133513	-0.013834
10	0.85925	0.026295	0.028495	0.002200	0.029507	0.022080	-0.007427

TEST CONDS-VF=11 KPS, ALPHA=2.5 DEGREE, VI/VF=0.1, 30 PCT CHORD PRESS SIDE INJ. OF PAN

	VFI	VFX	CDI	CDW	CDW-CDI	CLI	CLW	CLW-CLI
AVG VALUE	11.0155	11.0172	0.0179245	0.0172767	-0.0006477	0.1856633	0.1882021	0.0025387
STAND DEV	0.0150	0.0172	0.0001482	0.0001234	0.0002150	0.0007826	0.0009629	0.0013305

PRESS TAP	X/C	CPPI	CPPW	CPPW-CPPI	CPSI	CPSW	CPSW-CPSI
1	0.18625	-0.393412	-0.392000	0.001412	-0.762760	-0.762302	0.000457
2	0.23625	-0.423130	-0.419107	0.004022	-0.738772	-0.743805	-0.005032
3	0.24675	-0.443493	-0.439725	0.003774	-0.763299	-0.762444	0.000855
4	0.35925	-0.474450	-0.507246	-0.032587	-0.678750	-0.681625	-0.002874
5	0.23625	-0.473023	-0.498768	-0.025745	-0.642870	-0.644354	-0.001483
6	0.43625	-0.440527	-0.441139	-0.000612	-0.591360	-0.592120	-0.000759
7	0.53625	-0.376136	-0.379383	-0.003247	-0.454090	-0.453876	0.000213
8	0.63625	-0.214593	-0.214060	0.000533	-0.262578	-0.264297	-0.001719
9	0.73625	-0.095514	-0.097388	-0.001873	-0.119793	-0.122277	-0.002484
10	0.85925	0.028013	0.027574	-0.000438	0.030397	0.028937	-0.001459

TEST CONDS-VF=11 KPS, ALPHA=2.5 DEGREE, VI/VF=0.3, 30 PCT CHORD PRESS SIDE INJ. OF PAN

	VFI	VFX	CDI	CDW	CDW-CDI	CLI	CLW	CLW-CLI
AVG VALUE	11.0127	11.0197	0.0179397	0.0174413	-0.0004974	0.1861455	0.2046142	0.0184687
STAND DEV	0.0237	0.0330	0.0000863	0.0001038	0.0001397	0.0007963	0.0008612	0.0013920

PRESS TAP	X/C	CPPI	CPPW	CPPW-CPPI	CPSI	CPSW	CPSW-CPSI
1	0.18625	-0.394164	-0.388540	0.005624	-0.768586	-0.774683	-0.006096
2	0.23625	-0.421461	-0.408260	0.013203	-0.743469	-0.749087	-0.005618
3	0.24675	-0.443556	-0.429062	0.014494	-0.766644	-0.771866	-0.005222
4	0.35925	-0.474772	-0.503234	-0.028461	-0.681022	-0.687793	-0.006771
5	0.23625	-0.475204	-0.497514	-0.022310	-0.645392	-0.653685	-0.008292
6	0.43625	-0.441243	-0.443770	-0.002721	-0.593053	-0.600267	-0.007213
7	0.53625	-0.375630	-0.366953	0.008677	-0.453784	-0.462365	-0.008581
8	0.63625	-0.214596	-0.203128	0.011468	-0.262535	-0.273208	-0.010673
9	0.73625	-0.096205	-0.089333	0.006871	-0.120017	-0.131337	-0.011319
10	0.85925	0.027865	0.033129	0.006066	0.030755	0.018190	-0.012564

TEST CONDS-VF=11 FPS, ALPHA=5.0 DEGREE, VT/VF=0.1, 10 PCT CHORD SUCTN SIDE INJ. OF PAM

	VFN	VFW	CDN	CDW	CDW-CDN	CLN	CLW	CLW-CLN
AVG VALUE	11.0169	11.0235	0.0306389	0.0304073	-0.0002865	0.3753949	0.4101722	0.0347772
STAND DEV	0.0212	0.0335	0.0001459	0.0000832	0.0001388	0.0008988	0.0010734	0.0015043

PRESS TAP	X/C	CPPN	CPPW	CPPW-CPPN	CPSN	CPSW	CPSW-CPSN
1	0.19425	-0.225534	-0.210358	0.015181	-0.923453	-0.937343	-0.013890
2	0.23425	-0.275409	-0.261170	0.014761	-0.869449	-0.895320	-0.025871
3	0.24675	-0.297579	-0.284302	0.013276	-0.892552	-0.918793	-0.026260
4	0.35025	-0.378077	-0.357591	0.020486	-0.766525	-0.800582	-0.034057
5	0.39425	-0.375220	-0.364112	0.010116	-0.728212	-0.773077	-0.044865
6	0.43425	-0.355610	-0.339984	0.015125	-0.658427	-0.698690	-0.040263
7	0.53425	-0.316134	-0.301179	0.014956	-0.493866	-0.522690	-0.028824
8	0.63425	-0.178122	-0.162015	0.016107	-0.283006	-0.309273	-0.026266
9	0.73425	-0.076508	-0.059230	0.017077	-0.129466	-0.158858	-0.029392
10	0.85925	0.026780	0.049039	0.022258	0.030707	0.015531	-0.015176

TEST CONDS-VF=11 FPS, ALPHA=5.0 DEGREE, VT/VF=0.3, 10 PCT CHORD SUCTN SIDE INJ. OF PAM

	VFN	VFW	CDN	CDW	CDW-CDN	CLN	CLW	CLW-CLN
AVG VALUE	11.0175	11.0018	0.0305733	0.0297027	-0.0008711	0.3747977	0.4040199	0.0292222
STAND DEV	0.0239	0.0374	0.0001057	0.0001462	0.0001654	0.0010485	0.0017089	0.0015410

PRESS TAP	X/C	CPPN	CPPW	CPPW-CPPN	CPSN	CPSW	CPSW-CPSN
1	0.19425	-0.225053	-0.215397	0.009656	-0.922100	-0.935405	-0.013304
2	0.23425	-0.274235	-0.263290	0.010944	-0.867833	-0.886263	-0.018429
3	0.24675	-0.295849	-0.283131	0.012699	-0.893849	-0.906690	-0.012841
4	0.35025	-0.379430	-0.367193	0.012136	-0.768315	-0.792626	-0.024310
5	0.39425	-0.376091	-0.369618	0.006463	-0.725785	-0.758004	-0.032218
6	0.43425	-0.355721	-0.345614	0.010107	-0.659615	-0.686897	-0.027282
7	0.53425	-0.316331	-0.304391	0.011939	-0.495245	-0.513591	-0.018345
8	0.63425	-0.174149	-0.163562	0.010627	-0.284619	-0.311146	-0.026526
9	0.73425	-0.077157	-0.065079	0.012078	-0.130378	-0.159784	-0.029406
10	0.85925	0.026035	0.041305	0.015269	0.030265	0.015371	-0.014913

****

TEST CONDS-VF=11 RPS, ALPHA=5.0 DEGREE, VT/VF=0.1, 30 PCT CHORD PRESS SIDE INJ. OF FAN

****

	VFS	VFW	CDS	CDW	CDW-CDS	CLS	CLW	CLW-CLS
AVG VALUE	11.0017	11.3214	0.0377344	0.0293668	-0.0083676	0.3752020	0.3792521	0.0040501
STAND DEV	0.0099	0.0156	0.0001534	0.0002601	0.0002190	0.0010066	0.0011246	0.0013319

PRESS TAP	X/C	CPPS	CPPW	CPPW-CPPS	CPSN	CPSW	CPSW-CPSN
1	0.13625	-0.[illegible]7	-0.222629	0.013458	-0.921346	-0.922270	-0.000924
2	0.23625	-0.[illegible]21	-0.[illegible]72	0.001450	-0.867230	-0.871098	-0.003868
3	0.24675	-0.[illegible]79	-0.[illegible]65	0.003305	-0.893568	-0.[illegible]34	-0.003366
4	0.35625	-0.[illegible]5	-0.[illegible]58	-0.021073	-0.767153	-0.[illegible]06	-0.000168
5	0.[illegible]625	-0.[illegible]06	-0.[illegible]81	-0.020175	-0.728548	-0.729672	-0.001124
6	0.46625	-0.[illegible]82	-0.[illegible]34	-0.001272	-0.659694	-0.661318	-0.001624
7	0.53625	-0.[illegible]56	-0.317329	-0.000471	-0.496664	-0.497140	-0.002475
8	0.61625	-0.[illegible]93	-0.175220	0.003372	-0.282355	-0.286683	-0.004327
9	0.71625	-0.076173	-0.[illegible]20	-0.001047	-0.128229	-0.132190	-0.003960
10	0.85625	0.026158	0.027510	0.001372	0.029949	0.027283	-0.002665

****

TEST CONDS-VF=11 RPS, ALPHA=5.0 DEGREE, VT/VF=0.3, 30 PCT CHORD PRESS SIDE INJ. OF FAN

****

	VFS	VFW	CDS	CDW	CDW-CDS	CLS	CLW	CLW-CLS
AVG VALUE	11.0175	11.3226	0.0377603	0.0297626	-0.0079777	0.3753979	0.3907522	0.0153552
STAND DEV	0.0138	0.0158	0.0001306	0.0001783	0.0002151	0.0007677	0.0013953	0.0011547

PRESS TAP	X/C	CPPS	CPPW	CPPW-CPPS	CPSN	CPSW	CPSW-CPSN
1	0.13625	-0.[illegible]41	-0.217158	0.012172	-0.921568	-0.930510	-0.008941
2	0.23625	-0.[illegible]34	-0.[illegible]12	0.007682	-0.871349	-0.877756	-0.006406
3	0.24675	-0.[illegible]75	-0.[illegible]75	0.010599	-0.894312	-0.900058	-0.005745
4	0.35625	-0.[illegible]57	-0.[illegible]22	-0.025325	-0.765556	-0.774131	-0.008595
5	0.[illegible]625	-0.[illegible]29	-0.[illegible]54	-0.015235	-0.727185	-0.734243	-0.007057
6	0.46625	-0.[illegible]37	-0.[illegible]86	-0.005978	-0.658870	-0.666104	-0.007234
7	0.53625	-0.[illegible]94	-0.[illegible]53	0.006841	-0.493873	-0.500472	-0.006599
8	0.61625	-0.[illegible]49	-0.[illegible]89	0.009460	-0.293464	-0.292987	-0.009582
9	0.71625	-0.076696	-0.[illegible]18	0.003677	-0.128876	-0.139356	-0.010479
10	0.85625	0.024163	0.026958	0.002797	0.028940	0.017961	-0.010978

****

TEST CONDS-VF=11 FPS, ALPHA=5.25 DEGREE, VI/VF=0.1, 10 PCT CHORD PRESS SIDE INJ. OF PAM

****

	VFI	VFW	CDI	CDW	CDW-CDI	CLI	CLW	CLW-CLI
AVG VALUE	11.0151	11.0055	0.0217734	0.0203989	-0.0013745	0.2590412	0.2499014	-0.0091397
STAND DEV	0.0203	0.0367	0.0000406	0.0003651	0.0003694	0.0008970	0.0011415	0.0017714

PRESS TAP	X/C	CPPI	CPPW	CPPW-CPPI	CPSI	CPSW	CPSW-CPSI
1	0.10425	-0.376964	-0.372570	0.004394	-0.772711	-0.771473	0.001238
2	0.23425	-0.412773	-0.405501	-0.007272	-0.740540	-0.734105	0.006435
3	0.24675	-0.442144	-0.433130	0.009014	-0.759673	-0.757721	0.001951
4	0.35925	-0.445151	-0.431467	-0.013684	-0.645095	-0.643208	0.001886
5	0.38425	-0.430091	-0.409745	-0.020346	-0.677978	-0.675428	0.002550
6	0.43425	-0.406401	-0.385542	-0.020859	-0.631043	-0.627907	0.003135
7	0.53425	-0.371469	-0.342954	-0.028515	-0.502023	-0.497295	0.004727
8	0.63425	-0.190123	-0.193348	-0.003225	-0.288157	-0.283251	0.004906
9	0.73425	-0.080821	-0.090979	-0.010158	-0.132468	-0.127412	0.005055
10	0.85925	0.031586	0.028894	-0.002692	0.025922	0.031059	0.005137

****

TEST CONDS-VF=11 FPS, ALPHA=5.25 DEGREE, VI/VF=0.3, 10 PCT CHORD PRESS SIDE INJ. OF PAM

****

	VFI	VFW	CDI	CDW	CDW-CDI	CLI	CLW	CLW-CLI
AVG VALUE	11.0137	11.0127	0.0218033	0.0202188	-0.0015845	0.2578622	0.2639825	0.0061204
STAND DEV	0.0139	0.0147	0.0000529	0.0000430	0.0000729	0.0009455	0.0014872	0.0014901

PRESS TAP	X/C	CPPI	CPPW	CPPW-CPPI	CPSI	CPSW	CPSW-CPSI
1	0.10425	-0.376534	-0.367601	0.008933	-0.769620	-0.769163	0.000457
2	0.23425	-0.406479	-0.406011	0.000468	-0.735891	-0.743010	-0.007118
3	0.24675	-0.442091	-0.429814	0.012276	-0.751454	-0.756272	-0.004817
4	0.35925	-0.446697	-0.432362	0.014334	-0.641780	-0.648504	-0.006723
5	0.38425	-0.433265	-0.430727	0.002538	-0.670524	-0.674044	-0.003519
6	0.43425	-0.405249	-0.425266	-0.020017	-0.629790	-0.635179	-0.005389
7	0.53425	-0.371549	-0.337471	0.034078	-0.501055	-0.504909	-0.003873
8	0.63425	-0.190413	-0.190549	-0.000136	-0.287768	-0.292455	-0.004747
9	0.73425	-0.081396	-0.084829	-0.003432	-0.132532	-0.134667	-0.002135
10	0.85925	0.031732	0.035922	0.004190	0.025615	0.021532	-0.004082

****
TEST CONDS-VF=11 MPS, ALPH=3.25 DEGREE, VI/VF=0.1, 30 PCT CHORD SUCTN SIDE INJ. OF PAM
****

	VFN	VFW	CDN	CDW	CDW-CDN	CLN	CLW	CLW-CLN
AVG VALUE	11.0178	11.0194	0.0217741	0.0212890	-0.0004850	0.2587355	0.2682169	0.0094813
STAND DEV	0.0226	0.0281	0.0000357	0.0000696	0.0000717	0.0005725	0.0016836	0.0015352

PRESS TAP	X/C	CPPN	CPPW	CPPW-CPPN	CPSN	CPSW	CPSW-CPSN
1	0.18425	-0.377624	-0.376758	0.000866	-0.771426	-0.778077	-0.006651
2	0.23425	-0.402593	-0.399955	0.002638	-0.735757	-0.739691	-0.003933
3	0.28675	-0.442045	-0.443726	-0.001681	-0.757919	-0.759332	-0.001412
4	0.35925	-0.443965	-0.441453	0.002511	-0.649033	-0.720875	-0.071841
5	0.38425	-0.431036	-0.421876	0.009159	-0.675971	-0.697829	-0.021857
6	0.43425	-0.405845	-0.401938	0.003908	-0.630343	-0.637081	-0.006738
7	0.53425	-0.332769	-0.328162	0.004598	-0.502869	-0.516202	-0.013333
8	0.63425	-0.189995	-0.185736	0.004259	-0.288231	-0.301296	-0.013065
9	0.73425	-0.080142	-0.075201	0.004940	-0.131330	-0.142086	-0.010756
10	0.85925	0.032510	0.040259	0.007748	0.026781	0.021462	-0.005318

****
TEST CONDS-VF=11 MPS, ALPH=3.25 DEGREE, VI/VF=0.3, 30 PCT CHORD SUCTN SIDE INJ. OF PAM
****

	VFN	VFW	CDN	CDW	CDW-CDN	CLN	CLW	CLW-CLN
AVG VALUE	11.0098	11.0089	0.0217664	0.0205878	-0.0011785	0.2587069	0.2487643	-0.0099426
STAND DEV	0.0254	0.0418	0.0000430	0.0000611	0.0000633	0.0008239	0.0014704	0.0017432

PRESS TAP	X/C	CPPN	CPPW	CPPW-CPPN	CPSN	CPSW	CPSW-CPSN
1	0.18425	-0.377179	-0.383991	-0.006811	-0.771803	-0.765885	0.005917
2	0.23425	-0.403551	-0.406903	-0.003351	-0.737565	-0.725468	0.012066
3	0.28675	-0.449938	-0.451286	-0.001347	-0.755665	-0.747427	0.008207
4	0.35925	-0.443551	-0.448532	-0.004980	-0.649170	-0.739092	-0.089922
5	0.38425	-0.428964	-0.440177	-0.011212	-0.677892	-0.704602	-0.026709
6	0.43425	-0.406177	-0.410627	-0.004450	-0.630369	-0.637344	-0.006975
7	0.53425	-0.332823	-0.336299	-0.003471	-0.502966	-0.498602	0.004363
8	0.63425	-0.189158	-0.193586	-0.004427	-0.288244	-0.290562	-0.002317
9	0.73425	-0.080123	-0.082057	-0.001933	-0.131591	-0.136642	-0.005050
10	0.85925	0.032285	0.032753	0.000468	0.025213	0.019265	-0.005947

TEST CONDS-VF=11 FPS, ALPHA=5.0 DEGREE, VI/VF=0.1, 10 PCT CHORD PRESS SIDE INJ. OF PAM

	VFI	VFW	CDI	CDW	CDW-CDI	CLN	CLW	CLW-CLN
AVG VALUE	11.0098	11.0078	0.0307049	0.0285907	-0.0021142	0.3937323	0.3890922	-0.0046400
STAND DEV	0.0196	0.0209	0.0001136	0.0002393	0.0002765	0.0014828	0.0010516	0.0013488

PRESS TAP	X/C	CPPI	CPPW	CPPW-CPPI	CPSI	CPSW	CPSW-CPSN
1	0.18425	-0.259709	-0.249454	0.010246	-0.877017	-0.875944	0.001072
2	0.23425	-0.301063	-0.301019	0.000044	-0.817815	-0.816722	0.001092
3	0.28675	-0.345284	-0.330699	0.014585	-0.843759	-0.843370	0.000388
4	0.35925	-0.374516	-0.397654	-0.023138	-0.700616	-0.698392	0.002223
5	0.38425	-0.391584	-0.378375	-0.013790	-0.741602	-0.740869	0.000733
6	0.43425	-0.369721	-0.366635	-0.003086	-0.681485	-0.679731	0.001754
7	0.53425	-0.293031	-0.303520	-0.010489	-0.534346	-0.532955	0.001390
8	0.63425	-0.164653	-0.167288	-0.002635	-0.304508	-0.301457	0.003050
9	0.73425	-0.066176	-0.074038	-0.007861	-0.136997	-0.134666	0.002331
10	0.85925	0.031495	0.039802	-0.000693	0.028767	0.032617	0.003849

TEST CONDS-VF=11 FPS, ALPHA=5.0 DEGREE, VI/VF=0.3, 10 PCT CHORD PRESS SIDE INJ. OF PAM

	VFI	VFW	CDI	CDW	CDW-CDI	CLN	CLW	CLW-CLN
AVG VALUE	11.0036	11.0167	0.0307094	0.0286526	-0.0020572	0.3927235	0.3986701	0.0059465
STAND DEV	0.0252	0.0237	0.0001999	0.0002760	0.0002526	0.0012341	0.0012448	0.0018442

PRESS TAP	X/C	CPPI	CPPW	CPPW-CPPI	CPSI	CPSW	CPSW-CPSN
1	0.18425	-0.257292	-0.248667	0.008624	-0.871893	-0.875824	-0.003931
2	0.23425	-0.300429	-0.299005	0.001422	-0.810966	-0.817782	-0.006845
3	0.28675	-0.339575	-0.333993	0.005582	-0.839068	-0.836861	0.002176
4	0.35925	-0.374101	-0.391926	-0.017824	-0.699238	-0.702726	-0.003488
5	0.38425	-0.357184	-0.370118	-0.012934	-0.737649	-0.741186	-0.003536
6	0.43425	-0.347739	-0.368313	-0.020577	-0.681257	-0.684639	-0.003381
7	0.53425	-0.291740	-0.296061	-0.004321	-0.531422	-0.536435	-0.005013
8	0.63425	-0.164184	-0.164001	0.000183	-0.302491	-0.306021	-0.003530
9	0.73425	-0.065570	-0.068685	-0.003115	-0.135528	-0.138489	-0.002961
10	0.85925	0.031387	0.034814	0.003426	0.029178	0.026069	-0.003108

TEST CONDS-VF=11 FPS, ALPHA=5.0 DEGREE, VI/VF=0.1, 30 PCT CHORD SUCTN SIDE INJ. OF PAN

	VFN	VFW	CDN	CDW	CDW-CDN	CLN	CLW	CLW-CLN
AVG VALUE	11.0185	11.0199	0.0306048	0.0305028	-0.0001019	0.3935906	0.4067041	0.0131134
STAND DEV	0.0211	0.0298	0.0001483	0.0002365	0.0002551	0.0013690	0.0018360	0.0012447

PRESS TAP	X/C	CPPN	CPPW	CPPW-CPPN	CPSN	CPSW	CPSW-CPSN
1	0.18425	-0.256436	-0.255637	0.002799	-0.874567	-0.883708	-0.009140
2	0.23425	-0.300707	-0.297427	0.003279	-0.811579	-0.815217	-0.003638
3	0.24675	-0.343519	-0.339919	0.003599	-0.842788	-0.850061	-0.007272
4	0.35925	-0.373719	-0.369285	0.004434	-0.701120	-0.781556	-0.080436
5	0.38425	-0.362389	-0.354135	0.004244	-0.741722	-0.764407	-0.022685
6	0.43425	-0.348452	-0.344231	0.004220	-0.681744	-0.691212	-0.009467
7	0.53425	-0.292456	-0.286515	0.005940	-0.534178	-0.543553	-0.009374
8	0.63425	-0.164543	-0.159158	0.005384	-0.304432	-0.319137	-0.014705
9	0.73425	-0.067039	-0.060535	0.006495	-0.138098	-0.149492	-0.011394
10	0.85925	0.030484	0.040567	0.010082	0.027339	0.020314	-0.007024

TEST CONDS-VF=11 FPS, ALPHA=5.0 DEGREE, VI/VF=0.3, 30 PCT CHORD SUCTN SIDE INJ. OF PAN

	VFN	VFW	CDN	CDW	CDW-CDN	CLN	CLW	CLW-CLN
AVG VALUE	11.0133	11.0213	0.0307499	0.0297295	-0.0010204	0.3935838	0.3907810	-0.0028029
STAND DEV	0.0156	0.0240	0.0001791	0.0001693	0.0002360	0.0014983	0.0018468	0.0023591

PRESS TAP	X/C	CPPN	CPPW	CPPW-CPPN	CPSN	CPSW	CPSW-CPSN
1	0.18425	-0.259009	-0.260623	-0.002613	-0.875187	-0.861360	0.013826
2	0.23425	-0.299316	-0.298246	0.001069	-0.812583	-0.801291	0.011292
3	0.24675	-0.344243	-0.342612	0.001630	-0.840493	-0.829314	0.011178
4	0.35925	-0.372957	-0.374058	-0.001101	-0.703464	-0.800386	-0.097421
5	0.38425	-0.355067	-0.357448	-0.002380	-0.742381	-0.766604	-0.024222
6	0.43425	-0.348757	-0.350347	-0.001590	-0.681226	-0.688520	-0.007293
7	0.53425	-0.291674	-0.292901	-0.001026	-0.532611	-0.529360	0.003250
8	0.63425	-0.164132	-0.163937	0.000194	-0.304978	-0.311640	-0.006662
9	0.73425	-0.066909	-0.064958	0.001950	-0.138082	-0.148134	-0.010051
10	0.85925	0.030654	0.035663	0.005008	0.027452	0.017347	-0.010104

****

TEST CONDS-VF=11 KPS, ALPHA=0.0 DEGREE, VI/VF=0.1, 10 PCT CHORD SUCTN SIDE INJ. OF JAGUAR

****

	VFN	VFW	CDN	CDW	CDW-CDN	CLN	CLW	CLW-CLN
AVG VALUE	11.0067	10.9970	0.0121907	0.0115754	-0.0006152	-0.0008743	0.0053993	0.0062736
STAND DEV	0.0149	0.0156	0.0000279	0.0000596	0.0000713	0.0007098	0.0012602	0.0017901

PRESS TAP	X/C	CPPN	CPPW	CPPW-CPPN	CPSN	CPSW	CPSW-CPSN
1	0.18425	-0.557557	-0.555040	0.002517	-0.590705	-0.598730	-0.008025
2	0.23425	-0.562197	-0.558436	0.003760	-0.592259	-0.585765	0.006494
3	0.24675	-0.580374	-0.576472	0.003901	-0.616595	-0.612102	0.004492
4	0.35925	-0.542575	-0.536335	0.006240	-0.569396	-0.577344	-0.007948
5	0.38425	-0.545472	-0.545396	-0.000024	-0.537466	-0.569890	-0.032423
6	0.43425	-0.512576	-0.510897	0.001679	-0.504491	-0.510327	-0.005835
7	0.53425	-0.423785	-0.421623	0.002162	-0.396756	-0.402590	-0.005834
8	0.63425	-0.241571	-0.239346	0.002224	-0.227841	-0.231778	-0.003937
9	0.73425	-0.108047	-0.104701	0.003345	-0.097962	-0.101179	-0.003217
10	0.85925	0.026664	0.030271	0.003607	0.035115	0.033013	-0.002101

****

TEST CONDS-VF=11 KPS, ALPHA=0.0 DEGREE, VI/VF=0.3, 10 PCT CHORD SUCTN SIDE INJ. OF JAGUAR

****

	VFN	VFW	CDN	CDW	CDW-CDN	CLN	CLW	CLW-CLN
AVG VALUE	11.0153	11.0150	0.0121599	0.0108130	-0.0013469	-0.0009560	0.0111430	0.0120990
STAND DEV	0.0150	0.0191	0.0000321	0.0000576	0.0000669	0.0005841	0.0010072	0.0010765

PRESS TAP	X/C	CPPN	CPPW	CPPW-CPPN	CPSN	CPSW	CPSW-CPSN
1	0.18425	-0.556422	-0.547976	0.008446	-0.592032	-0.601257	-0.009224
2	0.23425	-0.559184	-0.556365	0.002819	-0.589891	-0.608356	-0.018465
3	0.24675	-0.579279	-0.574268	0.005110	-0.619873	-0.631066	-0.011193
4	0.35925	-0.541147	-0.534378	0.006769	-0.571246	-0.580750	-0.009504
5	0.38425	-0.543220	-0.538795	0.004425	-0.537940	-0.586100	-0.048170
6	0.43425	-0.513571	-0.508512	0.005058	-0.505727	-0.526132	-0.020404
7	0.53425	-0.424956	-0.418912	0.006043	-0.398294	-0.404507	-0.006213
8	0.63425	-0.242230	-0.236829	0.005401	-0.228927	-0.237511	-0.008584
9	0.73425	-0.108061	-0.102077	0.005984	-0.097774	-0.104576	-0.006801
10	0.85925	0.027396	0.033943	0.006547	0.035542	0.031437	-0.004104

10	0.85925	0.027396	0.033943	0.006547	0.035542	0.031437	-0.004104

****

TEST CONDS-VF=11 MPS, ALPHA=0.0 DEGREE, VI/VF=0.1, 30 PCT CHORD PRESS SIDE INJ. OF JAGUAR

****

	VFN	VFW	CDN	CDW	CDW-CDN	CLN	CLW	CLW-CLN
AVG VALUE	11.0052	11.0033	0.0121020	0.0116658	-0.0005222	-0.0006111	-0.0066364	-0.0060252
STAND DEV	0.0209	0.0213	0.0000334	0.0000546	0.0000727	0.0010552	0.0011166	0.0017300

PRESS TAP	X/C	CPPN	CPPW	CPPW-CPPN	CPSN	CPSW	CPSW-CPSN
1	0.12425	-0.555673	-0.557907	-0.002228	-0.590362	-0.587689	0.002673
2	0.23425	-0.560871	-0.563605	-0.002733	-0.593976	-0.590999	0.002976
3	0.24675	-0.581195	-0.581748	-0.000553	-0.627988	-0.624643	0.003345
4	0.35925	-0.573576	-0.593573	-0.019997	-0.570478	-0.567578	0.002900
5	0.37425	-0.539955	-0.574252	-0.034296	-0.540070	-0.537514	0.002555
6	0.48425	-0.513091	-0.534970	-0.021079	-0.506233	-0.503625	0.002608
7	0.53425	-0.424569	-0.431525	-0.006956	-0.398168	-0.396445	0.001723
8	0.63425	-0.242962	-0.248651	-0.005688	-0.229307	-0.226226	0.003080
9	0.73425	-0.108246	-0.110575	-0.002329	-0.098865	-0.095314	0.003550
10	0.85925	0.027298	0.025500	-0.001787	0.035951	0.037968	0.002017

****

TEST CONDS-VF=11 MPS, ALPHA=0.0 DEGREE, VI/VF=0.3, 30 PCT CHORD PRESS SIDE INJ.OF JAGUAR

****

	VFN	VFW	CDN	CDW	CDW-CDN	CLN	CLW	CLW-CLN
AVG VALUE	11.0167	11.0146	0.0121650	0.0113158	-0.0008491	-0.0005627	-0.0043175	-0.0037547
STAND DEV	0.0190	0.0203	0.0000305	0.0000595	0.0000671	0.0006513	0.0010583	0.0012100

PRESS TAP	X/C	CPPN	CPPW	CPPW-CPPN	CPSN	CPSW	CPSW-CPSN
1	0.12425	-0.556097	-0.556583	-0.000575	-0.590144	-0.590295	-0.000151
2	0.23425	-0.563003	-0.558466	0.004542	-0.592060	-0.588482	0.003578
3	0.24675	-0.579754	-0.575144	0.004610	-0.625205	-0.624268	0.000937
4	0.35925	-0.537311	-0.593986	-0.056674	-0.570722	-0.568758	0.001963
5	0.37425	-0.546755	-0.575155	-0.031400	-0.539663	-0.537761	0.001902
6	0.48425	-0.513747	-0.536540	-0.023193	-0.505528	-0.503715	0.001813
7	0.53425	-0.423677	-0.433456	-0.009778	-0.397182	-0.396332	0.000849
8	0.63425	-0.241792	-0.253329	-0.011546	-0.228428	-0.226703	0.001724
9	0.73425	-0.103497	-0.105605	-0.002107	-0.069971	-0.067697	0.002274
10	0.85925	0.029060	0.028125	-0.000934	0.062949	0.065328	0.002379

****

TEST CONDS-VF=11 FPS, ALPHA=2.5 DEGREE, VI/VF=0.1, 10 PCT CHORD SUCTN SIDE INJ. OF JAGUAR

****

	VFN	VFW	CDN	CDW	CDW-CDN	CLN	CLW	CLW-CLN
AVG VALUE	11.0228	11.0257	0.0182026	0.0178195	-0.0003831	0.1832787	0.1952637	0.0119849
STAND DEV	0.0148	0.0136	0.0000749	0.0001557	0.0001677	0.0004745	0.0024870	0.0023304

PRESS TAP	X/C	CPPN	CPPW	CPPW-CPPN	CPSN	CPSW	CPSW-CPSN
1	0.18425	-0.394133	-0.383218	0.010914	-0.747938	-0.764056	-0.016118
2	0.23425	-0.421689	-0.414247	0.007442	-0.724781	-0.724757	0.000024
3	0.24675	-0.442381	-0.437047	0.005333	-0.755602	-0.756222	-0.000619
4	0.35925	-0.463143	-0.456499	0.006644	-0.664653	-0.675419	-0.010766
5	0.38425	-0.458742	-0.454690	0.004052	-0.628554	-0.674486	-0.045932
6	0.43425	-0.432500	-0.427813	0.004687	-0.579957	-0.585908	-0.005951
7	0.53425	-0.369610	-0.365619	0.003990	-0.444804	-0.451215	-0.006410
8	0.63425	-0.210244	-0.206153	0.004090	-0.255605	-0.261497	-0.005892
9	0.73425	-0.092523	-0.087311	0.005216	-0.112603	-0.117341	-0.004737
10	0.85925	0.025481	0.032533	0.007052	0.036712	0.032988	-0.003723

****

TEST CONDS-VF=11 FPS, ALPHA=2.5 DEGREE, VI/VF=0.3, 10 PCT CHORD SUCTN SIDE INJ. OF JAGUAR

****

	VFN	VFW	CDN	CDW	CDW-CDN	CLN	CLW	CLW-CLN
AVG VALUE	11.0039	11.0058	0.0180443	0.0172341	-0.0008101	0.1823869	0.2032394	0.0208523
STAND DEV	0.0131	0.0131	0.0000767	0.0001060	0.0001485	0.0003707	0.0009577	0.0010476

PRESS TAP	X/C	CPPN	CPPW	CPPW-CPPN	CPSN	CPSW	CPSW-CPSN
1	0.18425	-0.393495	-0.383997	0.009498	-0.746264	-0.762164	-0.015900
2	0.23425	-0.421170	-0.410857	0.010312	-0.722927	-0.737222	-0.014294
3	0.24675	-0.444462	-0.434965	0.009496	-0.746420	-0.759112	-0.012691
4	0.35925	-0.452670	-0.446506	0.006164	-0.663985	-0.675475	-0.011490
5	0.38425	-0.458644	-0.449950	0.008693	-0.627125	-0.677299	-0.050173
6	0.43425	-0.434218	-0.425743	0.008475	-0.579663	-0.616918	-0.037255
7	0.53425	-0.371210	-0.362976	0.008234	-0.445055	-0.459301	-0.014245
8	0.63425	-0.211032	-0.201257	0.009774	-0.255191	-0.267533	-0.012342
9	0.73425	-0.093093	-0.081346	0.011746	-0.113147	-0.123808	-0.010660
10	0.85925	0.024853	0.038803	0.013950	0.036479	0.028043	-0.008436

****
TEST CONDS-VF=11 FPS, ALPHA=2.5 DEGREE, VI/VF=0.1, 30 PCT CHORD PRESS SIDE INJ. OF JAGUAR
****

	VFN	VFW	CDN	CDW	CDW-CDN	CLN	CLW	CLW-CLN
AVG VALUE	11.0172	11.0166	0.0181053	0.0175016	-0.0006036	0.1822075	0.1802420	-0.0019655
STAND DEV	0.0194	0.0165	0.0000549	0.0002157	0.0002421	0.0007414	0.0005146	0.0003914

PRESS TAP	X/C	CPPN	CPPW	CPPW-CPPN	CPSN	CPSW	CPSW-CPSN
1	0.18425	-0.392829	-0.394102	-0.001273	-0.745567	-0.744787	0.000780
2	0.23425	-0.421386	-0.421351	0.000034	-0.722324	-0.723445	-0.001120
3	0.24675	-0.442984	-0.443667	-0.000683	-0.748670	-0.746526	0.002143
4	0.35925	-0.459238	-0.475079	-0.015841	-0.663341	-0.664579	-0.001238
5	0.38425	-0.486645	-0.487159	-0.000513	-0.628417	-0.628111	0.000306
6	0.43425	-0.434751	-0.451745	-0.016993	-0.578970	-0.578589	0.000381
7	0.53425	-0.371102	-0.374979	-0.003876	-0.444187	-0.444787	-0.000600
8	0.63425	-0.212053	-0.212454	-0.000400	-0.256474	-0.255143	0.001330
9	0.73425	-0.093639	-0.094213	-0.000575	-0.112259	-0.112013	0.000245
10	0.85925	0.024869	0.024852	-0.000016	0.036992	0.037964	0.000971

****
TEST CONDS-VF=11 FPS, ALPHA=2.5 DEGREE, VI/VF=0.3, 30 PCT CHORD PRESS SIDE INJ. OF JAGUAR
****

	VFN	VFW	CDN	CDW	CDW-CDN	CLN	CLW	CLW-CLN
AVG VALUE	11.0137	11.0131	0.0180395	0.0172025	-0.0008370	0.1823665	0.1825474	0.0001808
STAND DEV	0.0139	0.0166	0.0000827	0.0001819	0.0002106	0.0005768	0.0007763	0.0009433

PRESS TAP	X/C	CPPN	CPPW	CPPW-CPPN	CPSN	CPSW	CPSW-CPSN
1	0.18425	-0.390356	-0.392654	-0.001697	-0.745645	-0.743789	0.001856
2	0.23425	-0.419476	-0.415756	0.003720	-0.722593	-0.723096	-0.000503
3	0.24675	-0.443468	-0.439601	0.003867	-0.754104	-0.748759	0.005344
4	0.35925	-0.460531	-0.496403	-0.035872	-0.663478	-0.665105	-0.001626
5	0.38425	-0.457792	-0.477250	-0.019457	-0.627395	-0.628232	-0.000837
6	0.43425	-0.434259	-0.454606	-0.020355	-0.580557	-0.579805	0.000751
7	0.53425	-0.370631	-0.379899	-0.009268	-0.443647	-0.444346	-0.000698
8	0.63425	-0.210856	-0.220656	-0.009800	-0.254807	-0.256174	-0.001366
9	0.73425	-0.092885	-0.094140	-0.001254	-0.112577	-0.112496	0.000080
10	0.85925	0.024923	0.025036	0.000112	0.037243	0.037955	0.000711

TEST CONDS-VF=11 FPS, ALPHA=5.0 DEGREE, VI/VF=0.1, 10 PCT CHORD SUCTN SIDE INJ. OF JAGUAR

	VFN	VFA	CDN	CDW	CDW-CDN	CLN	CLA	CLW-CLN
AVG VALUE	11.0459	11.0438	0.0306209	0.0305601	-0.0000606	0.3702830	0.3891530	0.0188699
STAND DEV	0.0093	0.0102	0.0001264	0.0001330	0.0001395	0.0010066	0.0032501	0.0036714

PRESS TAP	X/C	CPN	CPA	CPA-CPN	CPSN	CPSW	CPSW-CPSN
1	0.13425	-0.207917	-0.215645	0.012158	-0.910377	-0.941568	-0.031191
2	0.23425	-0.277254	-0.269260	0.007997	-0.853175	-0.868245	-0.015069
3	0.34425	-0.345475	-0.338734	0.006740	-0.877644	-0.911507	-0.033863
4	0.45425	-0.366227	-0.361298	0.004998	-0.753256	-0.764985	-0.011748
5	0.54425	-0.364781	-0.364702	0.000079	-0.713934	-0.741737	-0.027803
6	0.64425	-0.359716	-0.344639	0.015077	-0.651257	-0.667686	-0.016429
7	0.53425	-0.314406	-0.306938	0.007467	-0.489446	-0.498121	-0.008675
8	0.83425	-0.175469	-0.168462	0.007117	-0.277900	-0.288544	-0.010644
9	0.73425	-0.072349	-0.064803	0.007546	-0.123157	-0.135237	-0.012079
10	0.85925	0.025114	0.038695	0.013981	0.033067	0.026540	-0.006526

TEST CONDS-VF=11 FPS, ALPHA=5.0 DEGREE, VI/VF=0.3, 10 PCT CHORD SUCTN SIDE INJ. OF JAGUAR

	VFN	VFA	CDN	CDW	CDW-CDN	CLN	CLW	CLW-CLN
AVG VALUE	11.0476	11.0449	0.0305699	0.0301108	-0.0004591	0.3708324	0.4005618	0.0297293
STAND DEV	0.0226	0.0283	0.0001469	0.0001245	0.0001549	0.0009171	0.0019683	0.0022476

PRESS TAP	X/C	CPN	CPA	CPA-CPN	CPSN	CPSW	CPSW-CPSN
1	0.13425	-0.225578	-0.214592	0.011295	-0.911137	-0.931064	-0.019927
2	0.23425	-0.275759	-0.266258	0.009450	-0.857386	-0.889816	-0.032430
3	0.34425	-0.301446	-0.288791	0.012655	-0.877147	-0.897135	-0.020987
4	0.45425	-0.364541	-0.353060	0.011481	-0.753408	-0.792049	-0.038641
5	0.54425	-0.366193	-0.361672	0.005521	-0.713534	-0.731149	-0.017615
6	0.64425	-0.352846	-0.341218	0.011727	-0.651041	-0.676777	-0.025735
7	0.53425	-0.315058	-0.304460	0.010597	-0.488677	-0.509850	-0.020972
8	0.83425	-0.174663	-0.160953	0.013714	-0.280228	-0.299611	-0.019382
9	0.73425	-0.072486	-0.057716	0.014770	-0.124516	-0.151450	-0.026933
10	0.85925	0.026216	0.046012	0.019795	0.032049	0.021139	-0.010910

15 [illegible]

****

TEST CONDS-VF=11 FPS, ALPHA=5.0 DEGREE, VI/VF=0.1, 30 PCT CHORD PRESS SIDE INJ. OF JAGUAR

****

	VFL	VFA	CDL	CDA	CDA-CDL	CLN	CLA	CLA-CLN
AVG VALUE	11.0230	11.0254	0.0306588	0.0300640	-0.0005948	0.3697043	0.3703000	0.0005957
STAND DEV	0.0128	0.0112	0.0001423	0.0001746	0.0001495	0.0008727	0.0014351	0.0019820

PRESS TAP	X/C	CPPL	CPPA	CPPA-CPPL	CPSL	CPSA	CPSA-CPSN
1	0.10425	-0.227519	-0.226356	0.001162	-0.908215	-0.913860	-0.005645
2	0.23425	-0.277153	-0.275860	0.001292	-0.852383	-0.855426	-0.003043
3	0.24675	-0.301674	-0.300167	0.001507	-0.875777	-0.875172	0.000604
4	0.25925	-0.369114	-0.366778	0.002336	-0.753547	-0.752093	0.001454
5	0.38425	-0.374010	-0.374355	-0.000345	-0.714686	-0.715899	-0.001211
6	0.43425	-0.352058	-0.353060	-0.001002	-0.650440	-0.650039	0.000400
7	0.53425	-0.315493	-0.314694	0.000798	-0.486695	-0.488365	-0.001669
8	0.63425	-0.174867	-0.177539	-0.002672	-0.277588	-0.278418	-0.000830
9	0.73425	-0.071035	-0.071977	-0.000941	-0.123668	-0.122977	0.000691
10	0.85925	0.025892	0.025749	-0.000142	0.033484	0.032897	-0.000587

****

TEST CONDS-VF=11 FPS, ALPHA=5.0 DEGREE, VI/VF=0.3, 30 PCT CHORD PRESS SIDE INJ. OF JAGUAR

****

	VFL	VFA	CDL	CDA	CDA-CDL	CLN	CLA	CLA-CLN
AVG VALUE	11.0137	11.0145	0.0301194	0.0295945	-0.0011239	0.3702532	0.3730849	0.0028317
STAND DEV	0.0122	0.0119	0.0001154	0.0001391	0.0001249	0.0008496	0.0010548	0.0013580

PRESS TAP	X/C	CPPL	CPPA	CPPA-CPPL	CPSN	CPSA	CPSA-CPSN
1	0.10425	-0.225194	-0.223243	0.001951	-0.910394	-0.911881	-0.001487
2	0.23425	-0.274454	-0.271523	0.002931	-0.853908	-0.858811	-0.004902
3	0.24675	-0.301151	-0.296558	0.004592	-0.877656	-0.879212	-0.001555
4	0.35925	-0.363746	-0.399927	-0.036181	-0.752519	-0.755043	-0.002523
5	0.38425	-0.370224	-0.381026	-0.010802	-0.711227	-0.714628	-0.003401
6	0.43425	-0.354108	-0.377518	-0.023409	-0.650498	-0.650866	-0.000368
7	0.53425	-0.314861	-0.322916	-0.008055	-0.486952	-0.489203	-0.002271
8	0.63425	-0.175582	-0.182487	-0.006905	-0.279313	-0.280774	-0.001460
9	0.73425	-0.071981	-0.072180	-0.000199	-0.123495	-0.123731	-0.000236
10	0.85925	0.025645	0.027327	0.001682	0.032616	0.031313	-0.001303

****
TEST CONDS-VF=11 KPS, ALPH=3.25 DEGREE, VI/VF=0.1, 10 PCT CHORD PRESS SIDE INJ. OF JAGUAR
****

	VFN	VFW	CDN	CDW	CDW-CDN	CLN	CLW	CLW-CLN
AVG VALUE	11.0103	11.0224	0.0213467	0.0209152	-0.0004705	0.2584671	0.2556219	-0.0028452
STAND DEV	0.0150	0.0185	0.0000575	0.0002158	0.0002452	0.0006062	0.0026589	0.0025322

PRESS TAP	X/C	CPPN	CPPW	CPPW-CPPN	CPSN	CPSW	CPSW-CPSN
1	0.18425	-0.360365	-0.375600	0.004765	-0.764619	-0.759266	0.005353
2	0.23425	-0.406122	-0.391382	0.014740	-0.735121	-0.730926	0.004195
3	0.28675	-0.442663	-0.434313	0.008350	-0.753955	-0.756407	-0.002451
4	0.33925	-0.440233	-0.443313	-0.003080	-0.642205	-0.644577	-0.002372
5	0.38425	-0.433307	-0.441073	-0.007766	-0.671739	-0.673629	-0.001890
6	0.43425	-0.400406	-0.405768	-0.005362	-0.625544	-0.623109	0.002434
7	0.53425	-0.328367	-0.329736	-0.001368	-0.495381	-0.494926	0.000455
8	0.63425	-0.187935	-0.188841	-0.001005	-0.285693	-0.284835	0.000857
9	0.73425	-0.078556	-0.078870	-0.000314	-0.129153	-0.128258	0.000894
10	0.85925	0.033490	0.032159	-0.001330	0.027838	0.029318	0.001480

****
TEST CONDS-VF=11 KPS, ALPH=3.25 DEGREE, VI/VF=0.3, 10 PCT CHORD PRESS SIDE INJ. OF JAGUAR
****

	VFN	VFW	CDN	CDW	CDW-CDN	CLN	CLW	CLW-CLN
AVG VALUE	11.0216	11.0291	0.0213742	0.0201252	-0.0012489	0.2581016	0.2528927	-0.0052087
STAND DEV	0.0309	0.0251	0.0000558	0.0000810	0.0000769	0.0008689	0.0012488	0.0017467

PRESS TAP	X/C	CPPN	CPPW	CPPW-CPPN	CPSN	CPSW	CPSW-CPSN
1	0.18425	-0.350953	-0.374851	0.005191	-0.762066	-0.758897	0.003169
2	0.23425	-0.404752	-0.399449	0.003962	-0.725374	-0.725057	0.000316
3	0.28675	-0.442521	-0.425746	0.016775	-0.750673	-0.747820	0.002852
4	0.33925	-0.440477	-0.470552	-0.029675	-0.645684	-0.644622	0.001062
5	0.38425	-0.428784	-0.442928	-0.014143	-0.674243	-0.671525	0.002717
6	0.43425	-0.402267	-0.411477	-0.009209	-0.626354	-0.624395	0.001959
7	0.53425	-0.328912	-0.340616	-0.011704	-0.495294	-0.492811	0.002483
8	0.63425	-0.188865	-0.191848	-0.003782	-0.284375	-0.282126	0.002249
9	0.73425	-0.079425	-0.084346	-0.004921	-0.131275	-0.127973	0.003302
10	0.85925	0.033074	0.031579	-0.001495	0.025348	0.029641	0.004292

10	0.85925	0.033674	0.031579	-0.001495	0.025348	0.029641	0.004292

****

TEST CONDS-VF=11 MPS, ALPH=3.25 DEGREE, VI/VF=0.1, 30 PCT CHORD SUCTN SIDE INJ. OF JAGUAR

****

	VFN	VFW	CDN	CDW	CDW-CDN	CLN	CLW	CLW-CLN
AVG VALUE	11.0180	11.0235	0.0212576	0.0210769	-0.0001806	0.2569491	0.2639904	0.0070413
STAND DEV	0.0211	0.0282	0.0000475	0.0000597	0.0000687	0.0012395	0.0019909	0.0021057

PRESS TAP	X/C	CPPN	CPPW	CPPW-CPPN	CPSN	CPSW	CPSW-CPSN
1	0.18425	-0.377474	-0.374202	0.003272	-0.766237	-0.770965	-0.004727
2	0.23425	-0.400555	-0.401499	0.000944	-0.733160	-0.734749	-0.001588
3	0.28675	-0.445494	-0.442548	0.002946	-0.752525	-0.752636	-0.000110
4	0.35925	-0.441088	-0.438155	0.002932	-0.642789	-0.719740	-0.076951
5	0.38425	-0.449767	-0.447071	0.002696	-0.671454	-0.699157	-0.027703
6	0.43425	-0.401448	-0.397359	0.004089	-0.625542	-0.648733	-0.023191
7	0.53425	-0.327522	-0.325142	0.002379	-0.497257	-0.507266	-0.010009
8	0.63425	-0.187092	-0.184637	0.002454	-0.283682	-0.288907	-0.005225
9	0.73425	-0.075176	-0.072457	0.002718	-0.129295	-0.131144	-0.001849
10	0.85925	0.034929	0.037286	0.002356	0.027387	0.026551	-0.000835

****

TEST CONDS-VF=11 MPS, ALPH=3.25 DEGREE, VI/VF=0.3, 30 PCT CHORD SUCTN SIDE INJ. OF JAGUAR

****

	VFN	VFW	CDN	CDW	CDW-CDN	CLN	CLW	CLW-CLN
AVG VALUE	11.0154	11.0107	0.0212815	0.0208009	-0.0004804	0.2570908	0.2649589	0.0078680
STAND DEV	0.0229	0.0378	0.0000454	0.0000566	0.0000456	0.0010196	0.0011904	0.0017832

PRESS TAP	X/C	CPPN	CPPW	CPPW-CPPN	CPSN	CPSW	CPSW-CPSN
1	0.18425	-0.377268	-0.374455	0.002812	-0.764562	-0.763352	0.001209
2	0.23425	-0.400180	-0.401555	0.001375	-0.727160	-0.729578	-0.002418
3	0.28675	-0.443765	-0.441071	0.002694	-0.739842	-0.743621	-0.003778
4	0.35925	-0.440955	-0.439442	0.001512	-0.651457	-0.742309	-0.090852
5	0.38425	-0.433744	-0.430386	0.003358	-0.672418	-0.694537	-0.022119
6	0.43425	-0.401154	-0.398779	0.002375	-0.625307	-0.645098	-0.019790
7	0.53425	-0.330169	-0.326205	0.003963	-0.496177	-0.503893	-0.007716
8	0.63425	-0.188694	-0.184915	0.003778	-0.285793	-0.294737	-0.008943
9	0.73425	-0.078717	-0.074380	0.004336	-0.129565	-0.135484	-0.005919
10	0.85925	0.034241	0.040197	0.005956	0.027426	0.024840	-0.002586

10	0.85925	0.034241	0.040197	0.005956	0.027426	0.024840	-0.002586

****

TEST CONDS-VF=11 FPS, ALPHA=5.0 DEGREE, VT/VF=0.1, 10 PCT CHORD PRESS SIDE INJ. OF JAGUAR

****

	VFN	VFW	CDN	CDW	CDW-CDN	CLN	CLW	CLW-CLN
AVG VALUE	11.0074	11.0157	0.0303599	0.0295185	-0.0008413	0.3900975	0.3880284	-0.0020691
STAND DEV	0.0190	0.0242	0.0001569	0.0001611	0.0002740	0.0012893	0.0019783	0.0019719

PRESS TAP	X/C	CPPN	CPPW	CPPW-CPPN	CPSN	CPSW	CPSW-CPSN
1	0.18425	-0.261960	-0.262026	-0.000146	-0.868659	-0.864101	0.004558
2	0.23425	-0.302601	-0.297890	0.004710	-0.804435	-0.802266	0.002168
3	0.24675	-0.345910	-0.333800	0.012110	-0.834589	-0.837148	-0.002558
4	0.35925	-0.373762	-0.377526	-0.003764	-0.702257	-0.701211	0.001026
5	0.38425	-0.376898	-0.382734	-0.005843	-0.736365	-0.734094	0.002270
6	0.43425	-0.349759	-0.350234	-0.000484	-0.675684	-0.675883	-0.000254
7	0.54425	-0.291373	-0.293551	-0.002177	-0.526689	-0.525076	0.001613
8	0.64425	-0.164202	-0.165969	-0.001766	-0.299461	-0.299058	0.000403
9	0.73425	-0.066679	-0.066669	-0.000589	-0.135234	-0.134291	0.000942
10	0.85925	0.032968	0.032960	-0.000828	0.030152	0.031604	0.001451

****

TEST CONDS-VF=11 FPS, ALPHA=5.0 DEGREE, VT/VF=0.3, 10 PCT CHORD PRESS SIDE INJ. OF JAGUAR

****

	VFN	VFW	CDN	CDW	CDW-CDN	CLN	CLW	CLW-CLN
AVG VALUE	11.0218	11.0185	0.0313145	0.0297433	-0.0015711	0.3866664	0.3838570	-0.0028094
STAND DEV	0.0218	0.0211	0.0002624	0.0003035	0.0002169	0.0021897	0.0016757	0.0024889

PRESS TAP	X/C	CPPN	CPPW	CPPW-CPPN	CPSN	CPSW	CPSW-CPSN
1	0.18425	-0.265512	-0.263326	0.002186	-0.844738	-0.848797	-0.004059
2	0.23425	-0.305537	-0.306872	-0.001335	-0.781700	-0.787133	-0.005432
3	0.24675	-0.345980	-0.331939	0.014041	-0.818811	-0.815576	0.003234
4	0.35925	-0.375248	-0.390484	-0.015196	-0.713211	-0.708088	0.005122
5	0.38425	-0.381956	-0.379540	0.002416	-0.733678	-0.729476	0.004202
6	0.43425	-0.349981	-0.369046	-0.019066	-0.671425	-0.672289	-0.000863
7	0.54425	-0.294743	-0.303654	-0.008910	-0.520272	-0.520843	-0.000571
8	0.64425	-0.166956	-0.169752	-0.002765	-0.307276	-0.305456	0.001820
9	0.73425	-0.056527	-0.061388	0.005138	-0.135137	-0.140330	-0.005193
10	0.85925	0.032911	0.034103	0.005591	0.030749	0.027297	-0.003452

TEST CONDS-VF=11 KPS, ALPHA=5.0 DEGREE, VI/VF=0.1, 30 PCT CHORD SUCTN SIDE INJ. OF JAGUAR

	VFN	VFW	CDN	CDW	CDW-CDN	CLN	CLW	CLW-CLN
AVG VALUE	11.0225	11.0240	0.0302912	0.0301093	-0.0001818	0.3894212	0.3973108	0.0078896
STAND DEV	0.0207	0.0255	0.0001941	0.0002446	0.0002489	0.0010548	0.0016112	0.0012926

PRESS TAP	X/C	CPPN	CPPW	CPPW-CPPN	CPSN	CPSW	CPSW-CPSN
1	0.10425	-0.243725	-0.238664	0.005060	-0.860005	-0.864051	-0.004046
2	0.23425	-0.383614	-0.404280	-0.020666	-0.797185	-0.800811	-0.003625
3	0.29425	-0.345964	-0.343027	0.002937	-0.825218	-0.826779	-0.001560
4	0.35425	-0.375326	-0.371394	0.003932	-0.709685	-0.784787	-0.075101
5	0.39425	-0.374983	-0.367734	0.007248	-0.734256	-0.759489	-0.025232
6	0.43425	-0.345344	-0.341601	0.003743	-0.673305	-0.695644	-0.022338
7	0.53425	-0.291049	-0.287859	0.003189	-0.526093	-0.533247	-0.007153
8	0.63425	-0.161544	-0.159552	0.001992	-0.298706	-0.303498	-0.004792
9	0.73425	-0.064492	-0.061391	0.003101	-0.134684	-0.138685	-0.004000
10	0.85925	0.032925	0.037152	0.004226	0.029741	0.028630	-0.001110

TEST CONDS-VF=11 KPS, ALPHA=5.0 DEGREE, VI/VF=0.3, 30 PCT CHORD SUCTN SIDE INJ. OF JAGUAR

	VFN	VFW	CDN	CDW	CDW-CDN	CLN	CLW	CLW-CLN
AVG VALUE	11.0259	11.0231	0.0304549	0.0299733	-0.0004815	0.3882487	0.3981539	0.0099050
STAND DEV	0.0196	0.0162	0.0001136	0.0002147	0.0002895	0.0013641	0.0020619	0.0016992

PRESS TAP	X/C	CPPN	CPPW	CPPW-CPPN	CPSN	CPSW	CPSW-CPSN
1	0.10425	-0.243612	-0.241488	0.002123	-0.854897	-0.857733	-0.002835
2	0.23425	-0.382159	-0.399721	-0.017562	-0.794314	-0.789001	0.005313
3	0.29425	-0.345341	-0.341283	0.004058	-0.818060	-0.817586	0.000473
4	0.35425	-0.374621	-0.370125	0.004495	-0.710325	-0.803599	-0.093274
5	0.39425	-0.375791	-0.371905	0.003885	-0.728695	-0.747203	-0.018507
6	0.43425	-0.345151	-0.341676	0.003474	-0.676015	-0.701981	-0.025966
7	0.53425	-0.292468	-0.288613	0.003855	-0.525643	-0.535535	-0.009902
8	0.63425	-0.165030	-0.160800	0.004230	-0.299142	-0.310664	-0.011521
9	0.73425	-0.060299	-0.061157	0.005141	-0.134674	-0.139803	-0.005129
10	0.85925	0.032310	0.037939	0.005628	0.030559	0.027179	-0.003380

T.R. 7603-1
Mailed 1/7/77

HYDRONAUTICS, Incorporated

DISTRIBUTION LIST
Contract No. N00014-77-C-0070
NR 062-325

Defense Documentation Center
Cameron Station
Alexandria, VA 22314 12

Technical Library
David W. Taylor Naval Ship
Research and Development
Center
Annapolis Laboratory
Annapolis, MD 21402 1

Professor Bruce Johnson
Engineering Department
Naval Academy
Annapolis, MD 21402 1

Library
Naval Academy
Annapolis, MD 21402 1

Professor R. B. Couch
Dept. of Naval Architecture
and Marine Engineering
University of Michigan
Ann Arbor, MI 48105 1

Professor W. P. Graebel
Dept. of Engr. Mechanics
University of Michigan
Ann Arbor, MI 48105 1

Professor T. Francis Ogilvie
Dept. of Naval Architecture
and Marine Engineering
University of Michigan
Ann Arbor, MI 48105 1

Professor C. S. Yih
Dept. of Engr. Mechanics
University of Michigan
Ann Arbor, MI 48105 1

Professor O. M. Phillips
Dept. of Earth & Planetary Sci.
The Johns Hopkins University
Charles and 34th Streets
Baltimore, MD 21218 1

NASA Scientific and Technical
Information Facility
P. O. Box 8757
BWI Airport, MD 21240 1

Librarian
Dept. of Naval Architecture
University of California
Berkeley, CA 94720 1

Professor P. Lieber
Dept. of Mechanical Engr.
University of California
Berkeley, CA 94720 1

Professor J. R. Paulling
Dept. of Naval Architecture
University of California
Berkeley, CA 94720 1

Professor W. C. Webster
Dept. of Naval Architecture
University of California
Berkeley, CA 94720 1

Professor J. V. Wehausen
Dept. of Naval Architecture
University of California
Berkeley, CA 94720 1

Director
Office of Naval Research
Branch Office
495 Summer Street
Boston, MA 02210 1

Commander
Puget Sound Naval Shipyard
Bremerton, WA 98314 1

Professor G. Birkhoff
Dept. of Mathematics
Harvard University
Cambridge, MA 02138 1

Professor G. F. Carrier
Div. of Engr. and Applied Physics
Pierce Hall, Harvard Univ.
Cambridge, MA 02138 1

Professor M. A. Abkowitz
Dept. of Ocean Engr.
Mass. Inst. of Technology
Cambridge, MA 02139 1

Commanding Officer
NROTC Naval Admin. Unit
Mass. Inst. of Technology
Cambridge, MA 02139 1

Professor J. Kerwin
Dept. of Ocean Engineering
Mass. Inst. of Technology
Cambridge, MA 02139 1

Professor P. Leehey
Dept. of Ocean Engineering
Mass. Inst. of Technology
Cambridge, MA 02139 1

Professor Phillip Mandel
Dept. of Ocean Engineering
Mass. Inst. of Technology
Cambridge, MA 02139 1

Professor C. C. Mei
Dept. of Civil Engineering
Mass. Inst. of Technology
Cambridge, MA 02139 1

Professor E. W. Merrill
Dept. of Chemical Engineering
Mass. Inst. of Technology
Cambridge, MA 02139 1

Professor E. Mollo-Christensen
Dept. of Meteorology
Room 54-1722
Mass. Inst. of Technology
Cambridge, MA 02139 1

Professor J. Nicholas Newman
Dept. of Ocean Engineering
Room 5-324A
Mass. Inst. of Technology
Cambridge, MA 02139 1

Dr. S. Orszag
Flow Research, Inc.
1 Broadway
Cambridge, MA 02142 1

Director
Office of Naval Research
Branch Office
536 South Clark Street
Chicago, IL 60605 1

Library
Naval Weapons Center
China Lake, CA 93555 1

Professor E. Reshotko
Div. of Chemical Engr. Science
Case Western Reserve Univ.
Cleveland, OH 44106 1

Commander
Charleston Naval Shipyard
Naval Base
Charleston, SC 29408 1

Professor J. M. Burgers
Inst. of Fluid Dynamics and
Applied Mathematics
University of Maryland
College Park, MD 20740 1

Professor Pai
Inst. for Fluid Dynamics and
Applied Mathematics
University of Maryland
College Park, MD 20740 1

Technical Library
Naval Weapons Surface Center
Dahlgren Laboratory
Dahlgren, VA 22418 1

Computation & Analyses Lab.
Naval Weapons Surface Center
Dahlgren Laboratory
Dahlgren, VA 22418 1

Dr. C. S. Wells, Jr.
Advanced Tech. Center, Inc.
P. O. Box 6144
Dallas, TX 75222 1

Professor A. McKillop
Dept. of Mechanical Engr.
Univ. of California
Davis, CA 95616 1

Dr. J. A. Young
JAYCOR
11401 Camino Del Mar
Del Mar, CA 92014 1

Dr. F. H. Kraichnan
Dublin, NH 03444 1

Dr. Martin H. Bloom
Dir. of Gas Dynamics Research
Polytechnic Inst. of New York
Long Island Center
Farmingdale, NY 11735 1

Technical Documents Center
Building 315
Army Mobility Equipment
Research Center
Fort Belvoir, VA 22060 1

Professor E. R. Lindgren
Dept. of Engr. Sciences
University of Florida
231 Aerospace Engr. Building
Gainesville, FL 32611 1

Professor D. Shepphard
Coastal and Oceanographic
Engineering Department
University of Florida
Gainesville, FL 32601 1

Technical Library
Webb Inst. of Naval Architecture
Glen Cove, NY 11542 1

Professor E. V. Lewis
Webb Inst. of Naval Architecture
Glen Cove, NY 11542 1

Dr. M. Poreh
Technion-Israel Inst. of Tech.
Dept. of Civil Engineering
Haifa, Israel 1

Dr. J. P. Breslin
Davidson Laboratory
Stevens Inst. of Technology
Castle Point Station
Hoboken, NJ 07030 1

Dr. D. Savitsky
Davidson Laboratory
Stevens Inst. of Technology
Castle Point Station
Hoboken, NJ 07030 1

Dr. J. P. Craven
University of Hawaii
1801 University Avenue
Honolulu, HI 96822 1

Professor F. Hussain
Dept. of Mech. Engineering
Cullen College of Engr.
University of Houston
Houston, TX 77004 1

Professor J. F. Kennedy, Dir.
Inst. of Hydraulic Research
University of Iowa
Iowa City, IA 52242 1

Professor L. Landweber
Inst. of Hydraulic Research
University of Iowa
Iowa City, IA 52242 1

Dr. D. E. Ordway
Sage Action, Inc.
P. O. Box 416
Ithaca, NY 14850 1

Dr. D.R.S. Ko
Flow Research Inc.
1819 S. Central Avenue
Kent, WA 98031 1

Professor V. W. Goldschmidt
School of Mech. Engineering
Purdue University
Lafayette, IN 47907 1

Professor J. W. Miles
Inst. of Geophysics and
Planetary Physics, A-025
Univ. of Calif., San Diego
La Jolla, CA 92093 1

Flow Research, Inc.
Los Angeles Division
9841 Airport Blvd., Suite 1004
Los Angeles, CA 90045 1

Professor A. T. Ellis
Dept. of Applied Mathematics
and Engineering Sciences
Univ. of Calif., San Diego
La Jolla, CA 90237 1

Director
Scipps Inst. of Oceanography
University of California
La Jolla, CA 92037 1

Professor W. Lindberg
Dept. of Mechanical Engineering
University of Wyoming
Laramie, WY 82070 1

Mr. Virgil Johnson, President
Hydronautics, Incorporated
7210 Pindell School Road
Laurel, MD 20810 1

Mr. M. P. Tulin
Hydronautics, Incorporated
7210 Pindell School Road
Laurel, MD 20810 1

Commander
Long Beach Naval Shipyard
Long Beach, CA 90801 1

Dr. C. W. Hirt
University of California
Los Alamos Scientific Lab.
P. O. Box 1663
Los Alamos, NM 87544 1

Professor John Laufer
Dept. of Aerospace Engineering
Univ. of S. California
University Park
Los Angeles, CA 90007 1

Professor J. M. Killen
St. Anthony Falls Hydraulic Lab
University of Minnesota
Minneapolis, MN 55414 1

Lorenz G. Straub Library
St. Anthony Falls Hydraulic Lab
University of Minnesota
Minneapolis, MN 55414 1

Professor J. Ripkin
St. Anthony Falls Hydraulic Lab
University of Minnesota
Minneapolis, MN 55414 1

Dr. F. Silberman
St. Anthony Falls Hydraulic Lab
University of Minnesota
Minneapolis, MN 55414 1

Professor Paul F. Pucci
Mechanical Engr. Department
Naval Postgraduate School
Monterey, CA 93940 1

Library
Naval Postgraduate School
Monterey, CA 93940 1

Professor J. Wu
College of Marine Studies
University of Delaware
Newark, DE 19711 1

Professor A. B. Metzner
Dept. of Chemical Engr.
University of Delaware
Newark, DE 19711 1

Technical Library
Naval Underwater Systems Center
Newport, RI 02840 1

Office of Naval Research
New York Area Office
715 Broadway - Fifth Floor
New York, NY 10003 1

Professor D. D. Fuller
Dept. of Mechanical Engr.
Columbia University
New York, NY 10027 1

Professor H. G. Elrod
Dept. of Mechanical Engr.
Columbia University
New York, NY 10027 1

Engineering Societies Library
345 East 47th Street
New York, NY 10017 1

Society of Naval Architects
and Marine Engineers
74 Trinity Place
New York, NY 10006 1

Technical Library
Naval Coastal System Laboratory
Panama City, FL 32401 1

Professor A. J. Acosta
Dept. of Mechanical Engineering
Calif. Inst. of Technology
Pasadena, CA 91109 1

Professor H. W. Liepmann
Graduate Aeronautical Labs.
California Inst. of Technology
Pasadena, CA 91109 1

Professor M. S. Plesset
Engineering Science Dept.
California Inst. of Tech.
Pasadena, CA 91109 1

Professor A. Roshko
Graduate Aeronautical Labs.
California Inst. of Tech.
Pasadena, CA 91109 1

Professor T. Y. Wu
Engr. Science Department
California Inst. of Tech.
Pasadena, CA 91109 1

Director
Office of Naval Research
Branch Office
1030 E. Green Street
Pasadena, CA 91101 1

Mr. R. Wade
Tetra Tech., Inc.
Marine & Environmental
Engineering Division
630 N. Rosemead Blvd.
Pasadena, CA 91107 1

Professor K. M. Agrawal
Va. State College
Dept. of Mathematics
Petersburg, VA 23803 1

Technical Library
Naval Ship Engineering Center
Philadelphia Division
Philadelphia, PA 19112 1

Technical Library
Philadelphia Naval Shipyard
Philadelphia, PA 19112 1

Dr. Paul Kaplan
Oceanics, Inc.
Technical Industrial Park
Plainview, NY 11803 1

Technical Library
Naval Missile Center
Point Mugu, CA 93041 1

Commander
Portsmouth Naval Shipyard
Portsmouth, NH 03801 1

Commander
Norfold Naval Shipyard
Portsmouth, VA 23709 1

Professor F. Hama
Dept. of Aerospace and
Mechanical Science
Princeton University
Princeton, NJ 08540 1

Army Research Office
P. O. Box 12211
Research Triangle Park,
NC 27709 1

Professor G. Patterson
Dept. of Chemical Engineering
University of Missouri-Rolla
Rolla, Missouri 65401 1

Dr. H. Norman Abramson
Southwest Research Inst.
8500 Culebra Road
San Antonio, TX 78228 1

ONR Scientific Liaison Group
American Embassy - Room A-407
APO San Francisco 96503 1

Editor
Applied Mechanics Review
Southwest Research Inst.
8500 Culebra Road
San Antonio, TX 78206 1

Dr. J. W. Hoyt
Code 2501
Naval Undersea Center
San Diego, CA 92132 1

Technical Library
Naval Undersea Center
San Diego, CA 92132 1

Dr. Andrew Fabula
Code 4007
Naval Undersea Center
San Diego, CA 92132 1

Office of Naval Research
San Francisco Area Office
760 Market Street, Room 447
San Francisco, CA 94102 1

Library
Pearl Harbor Naval Shipyard
Box 400
FPO San Francisco 96610 1

Technical Library
Hunters Point Naval Shipyard
San Francisco, CA 94135 1

Professor Bruce H. Adee
Dept. of Mechanical Engr.
University of Washington
Seattle, WA 98195 1

Professor C. E. Pearson
Aerospace Research Laboratory
University of Washington
Seattle, WA 98105 1

Dr. Steven Crow, President
Poseidon Research
11777 San Vicente Blvd.
Suite 641
Los Angeles, CA 90049 1

Mr. J. Enig (Room 3-252)
Naval Surface Weapons Center
White Oak Laboratory
Silver Spring, MD 20910 1

Librarian
Naval Surface Weapons Center
White Oak Laboratory
Silver Spring, MD 20910 1

Mr. J. Rogers
Naval Surface Weapons Center
White Oak Laboratory
Silver Spring, MD 20910 1

Fenton Kennedy Document Library
The Johns Hopkins University
Applied Physics Laboratory
Johns Hopkins Road
Laurel, MD 20810 1

Professor E. Y. Hsu
Dept. of Civil Engineering
Stanford University
Stanford, CA 94305 1

Dr. Byrne Perry
Dept. of Civil Engineering
Stanford University
Stanford, CA 94305 1

Dr. R. L. Street
Dept. of Civil Engineering
Stanford University
Stanford, CA 94305 1

Professor Milton Van Dyke
Dept. of Aeronautical Engr.
Stanford University
Stanford, CA 94305 1

Professor J. Thompson
Dept. of Aerophysics and
Aerospace Engineering
Mississippi State Univ.
State College, MS 39762 1

Professor R. DiPrima
Dept. of Mathematics
Rensselaer Polytechnic Inst.
Troy, NY 12181 1

Professor J. L. Lumley
Dept. of Aerospace Engr.
Pennsylvania State Univ.
University Park, PA 16802 1

Dr. J. M. Robertson
Dept. of Theoretical and
Applied Mechanics
University of Illinois
Urbana, IL 61803 1

Technical Library
Mare Island Naval Shipyard
Vallejo, CA 94592 1

Office of Naval Research
800 N. Quincy Street
Arlington, VA 22217
Attn: Code 438 3
Code 200 1
Code 211 1
Code 212 1
Code 221 1
Code 473 1
Code 481 1
Code 1021P (ONRL) 6

Naval Research Laboratory
Washington DC 20375
Attn: Code 2627 6
Code 4000 1
Code 6170(Dr. D.Hunston) 1
Code 6170(R.C. Little) 1
Code 7706 1
Code 8441(R.J. Hansen) 1

Naval Sea Systems Command
Washington, DC 20362
Attn: L. Benen (Code 0322) 1
J. Schuler (Code 032) 1
Code 03B 1
T. Peirce (Code 03512) 1
Library (Code 0908) 1

Naval Ship Engineering Center
Center Building
Prince George's Center
Hyattsville, MD 20782
Attn: Code 6034 1
Code 6101E 1
Code 6110 1
Code 6114 1
Code 6136 1
Code 6140 1

David W. Taylor Naval Ship
Research & Development Center
Bethesda, MD 20084
Attn:
Dr. A. Powell (Code 01) 1
W. M. Ellsworth (Code 11) 1
Dr. W.E. Cummins (Code 15) 1
G. H. Gleissner (Code 18) 1
R. Wermter (Code 152) 1
Dr. W.B. Morgan (Code 154) 1
Dr. P.C. Pien (Code 1521) 1
P. S. Granville (Code 1541) 1
J. H. McCarthy, Jr. (Code 1552) 1
Dr. N. Salvesen (Code 1552) 1
Mrs. J. Schot (Code 1843) 1
Library (Code 5641) 1

Naval Air Systems Command
Washington, DC 20361
Attn: Code 03 — 1
Code 03B — 1
Code 310 — 1
Code 5301 — 1

Strategic Systems Projects Office
Department of the Navy
Washington, DC 20376 — 1

Mr. Norman Nilsen (SP 2022)
Strategic Systems Projects Office
Department of the Navy
Washington, DC 20376 — 1

Commander
Naval Oceanographic Office
Washington, DC 20373 — 1

Dr. A. L. Slafkosky
Scientific Advisor
Commandant of the Marine Corps (Code AX)
Washington, DC 20380 — 1

Librarian Station 5-2
Coast Guard Headquarters
NASSIF Building
400 Seventh Street, SW
Washington, DC 20591 — 1

Office of Research and Development
Maritime Administration
441 G Street, NW
Washington, DC 20235 — 1

Division of Ship Design
Maritime Administration
441 G Street, NW
Washington, DC 20235 — 1

Air Force Office of Scientific Research/NA
Building 410
Bolling AFB
Washington, DC 20332 — 1

Chief of Research and Development
Office of Chief of Staff
Department of the Army
Washington, DC 20310 — 1

Dr. G. Kulin
Fluid Mechanics Section
National Bureau of Standards
Washington, DC 20234 — 1

National Science Foundation
Engineering Division
1800 G Street, NW
Washington, DC 20550 — 1

Science and Technology Division
Library of Congress
Washington, DC 20540 — 1

Professor T. W. Kao
Dept. of Aerospace and Atmospheric Sciences
Catholic Univ. of America
Washington, DC 20017 — 1

Professor H. P. Pao
Dept. of Aerospace and Atmospheric Sciences
Catholic University of America
Washington, DC 20017 — 1

Professor J. V. Foa
School of Engr. and Applied Sci.
George Washington Univ.
Washington, DC 20006 — 1

Defense Research and
Development Attache
Australian Embassy
1601 Massachusetts Ave., NW
Washington, DC 20036 1

Dr. A. Thirubengadam
Daedalean Associates, Inc.
Springlake Research Center
15110 Frederick Road
Woodbine, MD 21797 1

Dr. A. S. Iberall, President
General Technical Services, Inc.
451 Penn Street
Yeadon, PA 19050 1

Mr. Dennis Bushell
NASA Langley Research Center
Langley Station
Hampton, VA 23365 1